Master Thesis

Rational design and characterization of recombinant *Botrytis aclada* laccase for use in biofuel cells

conducted at the

Institute of Food Biotechnology
University of Natural Resources and Life Sciences, Vienna

by

Christoph Gonaus

Vienna, May 2011

Acknowledgement

I would like to express my sincere gratitude to those who supported me during my work on this master thesis, especially to Dr. Dietmar Haltrich, Dr. Roman Kittl and Dr. Roland Ludwig at BOKU Vienna, Institute of Food Biotechnology for their scientific support and supervision. I would also like to extend my thanks to Dr. Wolfgang Schuhmann, Yvonne Beyl (M.Sc.) and Sascha Pöller (Dipl. Chem.) at the Ruhruniversität Bochum (Analytische Chemie - Elektroanalytik & Sensorik) who made my stay in Bochum possible and gave me the opportunity to experience a truly interdisciplinary research environment.

This work and my whole studies would not have been possible if not for my family and I take this chance to express my sincere thanks for their support.

Abstract

Fungal laccases are blue multicopper oxidases reducing O_2 to water while oxidizing aromatic substrates. They are studied among others for application in miniature biofuel cells. A novel recombinant laccase derived from the ascomycete *Botrytis aclada* was heterologously expressed in *Pichia pastoris,* purified and characterized. It exhibited a high Cl^- tolerance and could be efficiently produced in this established expression system. The inhibition characteristics of Cl^- and F^- were investigated in depth and a novel complex mixed type inhibition was suggested for Cl^-. One of the major drawbacks of laccases for the use in miniature biofuel cells is their low pH optimum. Site directed mutagenesis was employed to create mutants of the T1 site which were screened for higher pH optimum. L513M was a promising candidate for further research with 40% remaining activity at pH 7. Heterologously expressed, purified and concentrated *Ba*Lac L513M with a specific activity of 88 U mg^{-1} was produced. *Botrytis aclada* laccase was finally tested for immobilization in Os-modified polymer on GC electrodes. Os-modified anodic polymers were found to be not suitable and an alternative in form of covalently cross linked Os-modified non-charged backbone polymers was considered.

Contents

1 INTRODUCTION 1

1.1 Fungal laccases 1

1.2 Kinetics of fungal laccases 2

1.3 Designer laccases 4

1.4 Reversible laccase inhibition 5

1.5 Application of laccases in miniature biofuel cells 6

2 EXPERIMENTAL PROCEDURES 8

2.1 Material 8
2.1.1 Media 8
2.1.2 Strains 11
2.1.3 Plasmids 11
2.1.4 Primers 11
2.1.5 Chemicals 12
2.1.6 Os-modified polymers 13
2.1.7 Electrodes 13

2.2 Site directed mutagenesis of *Ba*Lac cDNA and preparations for expression in *Pichia pastoris* 14
2.2.1 Site directed mutagenesis 15
2.2.2 PCR 15
2.2.3 Agarose Gel Electrophoresis 17
2.2.4 DNA gel extraction / DNA purification 17
2.2.5 Template degradation, DNA restriction and ligation 17
2.2.6 Proliferation of plasmid in *E. coli* 18
2.2.7 Extraction of plasmid from *E. coli* 18
2.2.8 Sequencing of plasmid to confirm correct mutation 18
2.2.9 Electroporation of *Pichia pastoris* 19

2.3 Heterologous expression and purification of *Ba*Lac 19
2.3.1 Methanol induced enzyme expression by *Pichia pastoris* in shaking flasks 19
2.3.2 Methanol induced enzyme expression by *Pichia pastoris* in 0.5 L Multifors bioreactor 20
2.3.3 Purification 20
2.3.4 Concentrating samples and exchanging buffer 21

2.4 Characterization of *Ba*Lac 22
2.4.1 Photometric activity tests 22
2.4.2 High throughput screening 24

2.5 96-well fermentation and enzyme activity screening 25

2.6 Electrochemistry 25
2.6.1 Preparation of laccase-Os-complex-modified electrodes 25
2.6.2 Circular Voltammetry 26

3 RESULTS 27

3.1 Site directed mutagenesis of *Ba*Lac cDNA and preparations for expression in *Pichia pastoris* 27

3.2 High throughput enzyme activity screening 28

3.3 Heterologous expression and purification of *Ba*Lac 33

3.4 Characterization of *Ba*Lac 36
3.4.1 General *Ba*Lac kinetics 36
3.4.2 Temperature dependency of *Ba*Lac activity 39
3.4.3 *Ba*Lac stability 39
3.4.4 NaCl tolerance *Ba*Lac mutants 43
3.4.5 NaCl / NaF inhibition assays 43

3.5 Application of laccases on glassy carbon electrodes 49

4 DISCUSSION 52

4.1 Creation and screening of single point *Ba*Lac mutants 52

4.2 Heterologous expression and purification of *Ba*Lac 54

4.3 Characterization of *Ba*Lac 55
4.3.1 *General Ba*Lac kinetics 55
4.3.2 *Ba*Lac stability 56
4.3.3 NaCl tolerance *Ba*Lac mutants 58
4.3.4 NaCl / NaF inhibition assays 59

4.4 Application of laccases on glassy carbon electrodes 62

5 CONCLUSION 64

A. APPENDIX 66

B. ABBREVIATIONS 80

C. BIBLIOGRAPHY 81

List of Figures

Figure 1.1: Melanocarpus albomyces laccase crystal structure; visualization with PyMOL(TM) Molecular Graphics System, Version 1.3. (Schrodinger, USA) based on the work of Hakulinen et al. (2002). N-terminus (N), C-terminus (C), T1 copper site (T1), trinuclear copper cluster (T2/T3) and the 3 enzyme domains (1-3) are marked. 1

Figure 1.2: Catalytic cycle of laccase with phenolic substrates (Baldrian, 2006) 2

Figure 1.3: Reaction equation of partial non-competitive enzyme inhibition (Bisswanger, 2000, 85) 5

Figure 1.4: Reaction speed for partial non-competitive inhibition at steady state kinetics (Bisswanger 2000, 86) 5

Figure 1.5: Cellobiose dehydrogenase (anode) / laccase (cathode) based biofuel cell based on Os-complex mediated electron transfer (Stoica et al., 2009) 7

Figure 1.6: Cyclic voltammogram of Os-modified anodidc polymer on glassy carbon electrode with entrapped Trametes hirsuta laccase exposing catalytic current due to O_2 reduction. (argon: dotted lines, air: solid lines, saturated oxygen: bold solid lines; phosphate citrate buffer (100 mM) pH 4.0, scan rate 0.005 V s^{-1}) (Ackermann et al., 2010) 7

Figure 2.1: Site directed mutagenesis of BaLac cDNA using four primers method (A) and DpnI method (B) and subsequent creation of mutant laccase expressing Pichia pastoris 14

Figure 3.1: BaLac wt structure model visualized with PyMOL(TM) Molecular Graphics System, Version 1.3. (Schrodinger, USA) with targeted amino acids for mutation being marked (red: salt tolerance mutation, yellow and cyan: T1 copper redox potential mutations, grey: direct electron transfer pathway mutations). 31

Figure 3.2: BaLac wt structure model details visualized with PyMOL(TM) Molecular Graphics System, Version 1.3. (Schrodinger, USA) with targeted amino acids for mutation being marked (red: salt tolerance mutation, yellow and cyan: T1 copper redox potential mutations, grey: direct electron transfer pathway mutations) 31

Figure 3.3: Results of BaLac mutants high throughput activity assays in 96 well plates at standard conditions (with 0.5 mM ABTS, 1 mM 2,6-DMP) using pipetting robot and plate reader 32

Figure 3.4: Results of BaLac 505 mutants high throughput activity assays in 96 well plates at standard conditions (with 0.5 mM ABTS, 1 mM 2,6-DMP, 1 mM guaiacol, 10 mM catechol) using pipetting robot and plate reader. 32

Figure 3.5: BaLac wt compared to mutants in standard high throughput assays with 0.5 mM ABTS (■) and 0.2 mM 2,6-DMP (♦) in citrate buffer (pH 4-5.5, 100 mM) and citrate-phosphate buffer (pH 6-7.5, 100 mM). BaLac I505D with 2,6-DMP was measured separately in a conventional standard pH profile assay. 33

Figure 3.6: (A) Monitoring of cell density in shaking flask fermentation. For BaLac R129H (♦), BaLac R129F (■) and BaLac L513M (●) OD600 was measured and for BaLac I505N (▲) the wet cell mass. (B) Development of volumetric activity during fermentation of BaLac R129H (♦), BaLac R129F (■), BaLac L513M (●) and BaLac I505N (▲). The BaLac I505N fermentation was harvested already after 6 days. 34

Figure 3.7: Progression of BaLac L513M expression in 6-force fermentor. Acquired data for wet cell mass (▲), volumetric activity (■) and specific activity (♦) are given. 36

Figure 3.8: Correlation between K_m (♦) respectively k_{cat} (■) and the pH value in kintec assays of BaLac wt with 2,6-DMP, ABTS and guaiacol. 37

Figure 3.9: Activity assay pH profile with 2,6-DMP (0.2 mM) with purified and concentrated enzymes from shaking flask fermentation (BaLac R129H (●), BaLac R129F (♦), BaLac L513M (▲) and BaLac I505N (○)). The pH profile of BaLac wild type (■) with 2,6-DMP is shown as reference. 38

Figure 3.10: BaLac wt temperature optimum 39

Figure 3.11: Enzyme stability with 100 mM citrate buffer at pH 4.5 (●), 5.5 (■), 100 mM citrate phosphate buffer at pH 6.5 (▼), 7.5 (▲) and storage temperatures of 4℃, 21℃ and 37℃. 40

Figure 3.12: Enzyme stability at pH 4.0 (100 mM citrate buffer) and storage temperatures of 45℃ (■), 55℃ (●) and 65℃ (▲)..... 40
Figure 3.13: Inactivation of BaLac wt stored in ethanol and methanol (0% (■), 10% (♦), 20% (▲), 30% (●), 40% (○), 50% (Δ)) at pH 5 (100 mM citrate buffer)..... 41
*Figure 3.14: Enzyme stability in solution with Os-modified anodic redox polymers at pH 4 (citrate buffer 100 mM) and room temperature. Reference was enzyme in buffer only (Δ) and all activities are in relation to its initial activity (**A**) Inactivation of BaLac wt by Os-modified anodic polymers p009-p91 (♦) and p405-p91 (■). (**B**) Inactivation of BaLac wt by Os-complex p91 alone (■), non modified polymer backbone of p405 (♦) and Os-modified polymer p405 (▲) **(C)** Inactivation of ThLac wt by Os-modified anodic polymers p009-p91 (♦) and p405 (■) 41*
Figure 3.15: BaLac wt stability in solution at pH 5 (citrate buffer 100 mM) with Os-modified cathodic redox polymers p002b-p91 (◊) and p004b-p91 (□) at room temperature with reference of BaLac wt in buffer only (Δ) 42
*Figure 3.16: **(A)** Comparing BaLac wt (▲)and ThLac wt (■) stability in solution at pH 4 (citrate buffer 100 mM) with Os-modified non-charged backbone redox polymers p011-p91. BaLac wt (Δ) respectively ThLac wt (□) with buffer only served as reference. **(B)** Effect of 2,2'-(Ethylenedioxy)diethanthiol (dithiol-crosslinker) on stability of BaLac wt at pH 4 (citrate buffer 100 mM). 0.36% (▲) and 0.009% dithiol-crosslinker (♦) were tested with BaLac wt (Δ) in buffer only as reference. 43*
Figure 3.17: Cl- inihibition of BaLac wt (Δ), BaLac R129H (■) and BaLac R129F (●) at pH 4 43
Figure 3.18: Conventional NaCl inhibition assay of BaLac wt with 2.6-DMP at pH 3 and pH 4.5 (citrate buffer 100 mM)..... 44
Figure 3.19: 96-well inhibition assay of BaLac wt with ABTS and inhibitor NaCl (0 mM (●), 3.9 mM (○), 7.8 mM (▼), 15.6 mM (▽), 31.3 mM (■), 62.5 mM (□), 125 mM (♦), 250 mM (◊), 500 mM (▲), 1 M (Δ), 2 M (●)) at pH 3, 4.5 and 6..... 44
Figure 3.20: 96-well inhibition assay of TpLac with ABTS and inhibitor NaCl (concentrations given in graph in µM) at pH 3, 4.5 and 6. 45
Figure 3.21: 96-well inhibition assay of BaLac with ABTS and inhibitor NaF (concentrations given in graph in µM) at pH 3, 4.5 and 6. 46
Figure 3.22: 96-well inhibition assay of BaLac wt with 2,6-DMP and inhibitor NaCl (0 mM (●), 3.9 mM (○), 7.8 mM (▼), 15.6 mM (▽), 31.3 mM (■), 62.5 mM (□), 125 mM (♦), 250 mM (◊), 500 mM (▲), 1 M (Δ), 2 M (●)) at pH 3, 4.5 and 6. 46
Figure 3.23: 96-well inhibition assay of BaLac wt with guaiacol and inhibitor NaCl (0 mM (●), 3.9 mM (○), 7.8 mM (▼), 15.6 mM (▽), 31.3 mM (■), 62.5 mM (□), 125 mM (♦), 250 mM (◊), 500 mM (▲), 1 M (Δ), 2 M (●)) at pH 3, 4.5 and 6. 47
Figure 3.24: 96-well inhibition assay of TpLac with 2,6-DMP and inhibitor NaCl (concentrations given in graph in µM) at pH 3, 4.5 and 6..... 48
Figure 3.25: 96-well inhibition assay of BaLac with 2,6-DMP and inhibitor NaF (concentrations given in graph in µM) at pH 3, 4.5 and 6..... 48
Figure 3.26: 96-well inhibition assay of BaLac wt with guaiacol and inhibitor NaF (concentrations given in graph in µM) at pH 3, 4.5 and 6..... 49
Figure 3.27: Circular Voltammetry of glassy carbon electrode modified with Botrytis aclada laccase wt and Os-modified polymer p009-p91, conducted at standard conditions in argon and oxygen (100 mM citrate buffer: pH 4, reference electrode: Ag/AgCl (3 M), scan rate: 0.005 $V*s^{-1}$) 50
Figure 3.28: Circular Voltammetry of glassy carbon electrode modified with Trametes hirsuta laccase wt and Os-modified polymer p011-p91, conducted at standard conditions in argon and oxygen (100 mM citrate buffer: pH 4, reference electrode: Ag/AgCl (3 M), scan rate: 0.005 $V*s^{-1}$) 51
Figure 4.1: Suggested locations of inhibition at Botrytis aclada laccase 61
Figure A.1: Nucleotide sequence of BaLac wt cDNA. 67
Figure A.2: Amino acid sequence derived from BaLac wt cDNA. The positions of the salt tolerance mutants (green) and T1 copper redox potential mutants (yellow) created in this work are marked. Single point mutations of other mutants used in this work are highlighted in blue (T1 copper redox potential mutants) and in grey (direct electron pathway mutants)..... 68

Figure A.3: pH profiles of BaLac 273, 373, 429 mutants and wild type. Standard high throughput assays with 0.5 mM ABTS (■) and 0.2 mM 2,6-DMP (♦) in citrate buffer (pH 4-5.5, 100 mM) respectively citrate-phosphate buffer (pH 6-7.5, 100 mM). 69
Figure A.4: pH profiles of BaLac 430 and 505 mutants. Standard high throughput assays with 0.5 mM ABTS (■) and 0.2 mM 2,6-DMP (♦) in citrate buffer (pH 4-5.5, 100 mM) respectively citrate-phosphate buffer (pH 6-7.5, 100 mM). BaLac I505D with 2,6-DMP was measured in a conventional standard pH profile assay. 70
Figure A.5: pH profiles of BaLac 455, 513 and 534 mutants. Standard high throughput assays with 0.5 mM ABTS (■) and 0.2 mM 2,6-DMP (♦) in citrate buffer (pH 4-5.5, 100 mM) respectively citrate-phosphate buffer (pH 6-7.5, 100 mM). 71
Figure A.6: Alternative scheme for creating Os-modified polymers 80

List of Tables

Table 1.1: Reversible enzyme inhibition types and their characteristics (Bisswanger, 2000, 87) 5
Table 3.1: Site directed mutagenesis, DpnI method 27
Table 3.2: Site directed mutagenesis, four primer method 28
Table 3.3: In Pichia pastoris expressed NaCl tolerance BaLac mutants 28
Table 3.4: In Pichia pastoris expressed T1 copper redox-potential BaLac mutants 28
Table 3.5: BaLac mutations (including those newly created in this work) screened in high throughput activity screening. 30
Table 3.6: Purification scheme of harvested Pichia pastoris supernatant of BaLac R129H, BaLac R129F, BaLac L513M and BaLac I505N shaking flask fermentations. 35
Table 3.7: Final enzyme specifications after downstream processing of Pichia pastoris supernatant from shaking flask fermentation. 35
Table 3.8: Purification scheme of BaLac L513M from Pichia pastoris supernatant from 0.5 L Multifors bioreactor 36
Table 3.9: K_m-value assay of BaLac wt with 2,6-DMP, ABTS and guaiacol at pH 3-6 (100 mM citrate buffer pH 3-5, 100 mM citrate-phosphate buffer pH 6) and catechol at pH 4. 37
Table 3.10: K_m-values of BaLac mutants with 2,6-DMP, ABTS, guaiacol and catechol at pH 4 (100 mM citrate buffer) 38
Table 3.11: Apparent K_m values determined by Michaelis-Mendten regression of individual data sets from 96-well inhibition assay of BaLac wt with NaCl and ABTS at pH 3 and 4.5. 45
Table 3.12: Apparent K_m values determined by Michaelis-Mendten regression of individual data sets from 96-well inhibition assay of TpLac with NaCl and ABTS at pH 3 and 4.5 45
Table 3.13: Apparent K_m values determined by Michaelis-Mendten regression of individual data sets from 96-well inhibition assay of BaLac wt with NaCl and 2,6-DMP at pH 3 and 4.5 47
Table 3.14: Apparent K_m values determined by Michaelis-Mendten regression of individual data sets from 96-well inhibition assay of BaLac wt with NaCl and guaiacol at pH 3 and 4.5. 47
Table 3.15: Apparent K_m values determined by Michaelis-Mendten regression of individual data sets from 96-well inhibition assay of TpLac with NaCl and 2,6-DMP at pH 3 and 4.5. 48
Table 3.16: Apparent K_m values determined by Michaelis-Mendten regression of individual data sets from 96-well inhibition assay of BaLac wt with NaF as inhibitor and guaiacol as substrate at pH 3 and 4.5. 49
Table A.1: 96-well inhibition assay of BaLac with ABTS and inhibitor NaCl at pH 3, 4.5 (citrate buffer, 100 mM) and pH 6 (citrate-phosphate buffer, 100 mM) 72
Table A.2 96-well inhibition assay of BaLac with ABTS and inhibitor NaF at pH 3, 4.5 (citrate buffer, 100 mM) and pH 6 (citrate-phosphate buffer, 100 mM) 73
Table A.3: 96-well inhibition assay of TpLac with ABTS and inhibitor NaCl at pH 3, 4.5 (citrate buffer, 100 mM) and pH 6 (citrate-phosphate buffer, 100 mM) 74
Table A.4: 96-well inhibition assay of BaLac with 2,6-DMP and inhibitor NaCl at pH 3, 4.5 (citrate buffer, 100 mM) and pH 6 (citrate-phosphate buffer, 100 mM) 75
Table A.5: 96-well inhibition assay of BaLac with 2,6-DMP and inhibitor NaF at pH 3, 4.5 (citrate buffer, 100 mM) and pH 6 (citrate-phosphate buffer, 100 mM) 76
Table A.6: 96-well inhibition assay of TpLac with 2,6-DMP and inhibitor NaCl at pH 3, 4.5 (citrate buffer, 100 mM) and pH 6 (citrate-phosphate buffer, 100 mM) 77
Table A.7: 96-well inhibition assay of BaLac with guaiacol and inhibitor NaCl at pH 3, 4.5 (citrate buffer, 100 mM) and pH 6 (citrate-phosphate buffer, 100 mM) 78
Table A.8: 96-well inhibition assay of BaLac with guaiacol and inhibitor NaF at pH 3, 4.5 (citrate buffer, 100 mM) and pH 6 (citrate-phosphate buffer, 100 mM) 79

1 Introduction

1.1 Fungal laccases

Laccases are enzymes which belong to the small group of blue copper oxidases. They are found in fungi, bacteria, plants and insects and were first described in the 19th century by Yoshida (1883) who studied the laccase from *Rhus vernificera*. In fungi they are found in many basidiomycetes and ascomycetes (Gianfreda et al., 1999). The function of laccase in fungi includes lignin degradation, morphogenesis, stress defense and pathogenic purposes (Giardina et al., 2010). Kudanga et al. (2011) reviewed the various possible applications of laccase and the progress made in the different areas. Among others laccases are of interest in environmental remediation in lignin modification and organic synthesis. Also applications in the textile, food and pharmaceutical industries are studied. Focus of this work was, however, the application of laccase in biofuel cells.

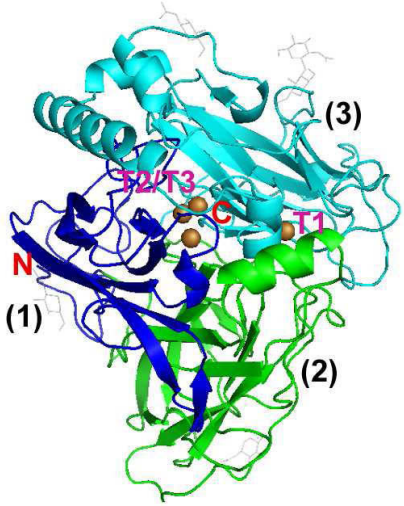

Figure 1.1: *Melanocarpus albomyces* laccase crystal structure; visualization with PyMOL(TM) Molecular Graphics System, Version 1.3. (Schrodinger, USA) based on the work of Hakulinen et al. (2002). N-terminus (N), C-terminus (C), T1 copper site (T1), trinuclear copper cluster (T2/T3) and the 3 enzyme domains (1-3) are marked.

According to Giardina et al. (2010) few laccase X-ray crystallography structures could be resolved so far. Of basidiomycete laccases the crystal structure of the intensely studied *Trametes versicolor* laccase (Antorini et al., 2002; Piontek et al., 2002) is available among others. Only one ascomycete laccase 3D structure was found in literature which is from *Melanocarpus albomyces* (Hakulinen et al., 2002; Hakulinen et al., 2008) and can be seen in Figure 1.1. This structure shows a monomer with 3 different domains. The T1 copper site and the trinuclear copper cluster are coordinated in between these domains with the C terminus of the enzyme being located directly at the trinuclear cluster.

Laccases oxidize mainly aromatic compounds while reducing O_2 to water which is something they share with only few other enzymes. For that purpose four single electrons from the substrate are transferred via four coppers to dioxygen which is reduced to water. Typically 4 copper atoms of 3 different types are involved at two sites, one T1 and T2 copper and two T3 coppers with T2 and T3 forming a trinuclear cluster (Solomon et al., 1996). Possible substrates are various phenols but also polyamines and aryl diamines. Also some inorganic substrates were reported (Giardina et al., 2010). Figure 1.2 summarizes the catalytic scheme of laccases.

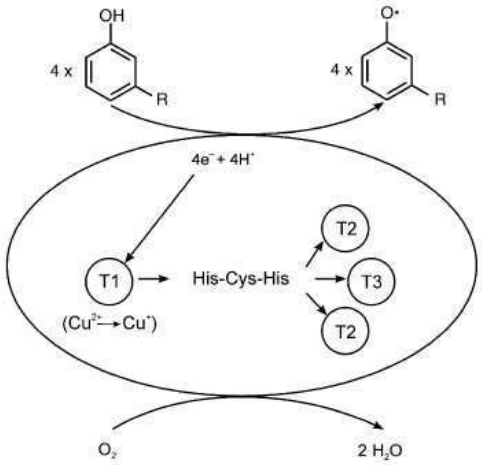

Figure 1.2: Catalytic cycle of laccase with phenolic substrates (Baldrian, 2006)

1.2 Kinetics of fungal laccases

Specificity (K_m) and turnover number (k_{cat}) of a wide range of substrates were reviewed by Baldrian (2006) for various fungal laccases. Generally high affinities exist towards the unnatural substrate ABTS. 2,6-DMP and guaiacol are other commonly tested substrates however with less affinity towards laccase in general.

While laccases from basidiomycetes like *Trametes* spp. are high redox potential laccases, other fungi like ascomycetes express low / middle redox potential laccases. That means the redox potential of the T1 copper is lower with 420 – 710 mV (vs. NHE) instead of 780 mV (vs. NHE) (Christenson et al., 2004). Ascomycete laccases tend to feature such lower redox potentials (Rodgers et al., 2010). Xu (1996) suggested that the catalytic efficiency (K_m/k_{cat}) of laccases depends on the electron transfer from substrate to the T1 copper. Furthermore this step is supposed to follow an “outer sphere” mechanism which means that its rate depends on the redox potential difference between substrate and T1 copper. A higher T1 redox potential would therefore enable higher catalytic efficiency which means *Trametes* laccases

have an advantage over Ascomycete laccases in this regard. But *Trametes* laccases are harder to genetically manipulate and scale up in industrial production is challenging. Furthermore heterologous expression is problematic as well (Rodgers et al., 2010).

Catalytic efficiency also depends on the reaction conditions. Optimal conditions vary from laccase to laccase and can also change with different substrates. pH optima for different substrates and temperature optima have been studied widely and were reviewed by Baldrian (2006). Almost all of the reviewed laccases have their pH optimum in the acidic pH range and the majority at pH 4 or below. This is the case for ascomycete and basidiomycete laccases alike. Xu (1997) suggested mechanisms explaining the nature of laccase pH profiles for the two common substrates ABTS and 2,6-DMP. According to them OH^- inhibits the laccase by acting on the T2/T3 cluster thereby slowing down electron transfer from the T1 site to the T2/T3 cluster. This affects the catalytic rate with both substrates. Phenolic substrates, however, might additionally influence the enzyme activity because their redox potential is decreasing at higher pH levels. Therefore pH profiles with ABTS are supposed to monotonously fall at rising pH while phenolic substrates like 2,6-DMP are expected to follow a bell shaped curve consisting of two phases. The first phase showing an increase in enzyme activity due to the decrease in redox potential of the phenolic substrate and the second one a decrease due to the OH^- inhibition.

The optimal temperatures for highest catalytic activity of reviewed laccases reach from 25 to 80℃. The median as well as the average temperature optimum is well in between these extremes at 55℃ (Baldrian, 2006). Studies of tempe rature inactivation of basidiomycete laccases (*Trametes hirsuta* and *Trametes ochracea* laccase) indicated that at rising temperatures initially conformational changes occur at the T1 and T2 copper sites. Then T2 copper is lost, leading to reduced interaction of the enzyme domains with each other and the inactivation of the enzyme. This happens well before the protein starts to unfold. Therefore critical loss of enzyme activity is taking already place when the protein structure is still largely intact (Koroleva et al., 2001).

Also inhibition by substances present in solution is a major issue. Reports on inhibition by a broad range of substances were reviewed by Baldrian (2006) as well. A focus of this work is inhibition by halides. Xu (1996) has done the most comprehensive study on this so far but there are no reviews published about it yet. His results showed that the tested ascomycete laccase of *Myceliophthora thermophila* had several times higher I_{50} than the basidiomycete laccases (*Trametes villosa, Rhizoctonia solani* and *Scytalidium thermophilum*). In case of Cl^- the former had an I_{50} of 600 mM while the latter had I_{50} of 50 mM or less. Furthermore the

highest tested Cl- tolerance for a *Trametes* laccase was for *Trametes trogii* with an I_{50} of 70 mM (Garzillo et al., 1998). Only one basidiomycete laccase with a higher Cl^- tolerance than the one expressed by *Myceliophthora thermophila* was found in literature, which was *Pycnoporus sanguineus laccase* with an I_{50} of 1000 mM (Garzillo et al., 1998). These results suggest that basidiomycetes but especially *Trametes* laccases are less tolerant than the tested ascomycete laccases. More conclusive studies would be needed for confirmation however.

1.3 Designer laccases

Creation of designer laccases is a possibility to combine the advantage of different laccases and/or evading disadvantages. There are three different approaches described in literature. The first is site directed mutagenesis which is a rational approach. The second one is directed evolution and the third, the semi rational approach, combines aspects of the former two. Site directed mutagenesis bases on X-ray crystallographic information which gives insights into the 3-dimensional coordination of amino acids (Rodgers et al., 2010). A challenge for ascomycete laccases is therefore that so far only one crystal structure has been published, the one of *Melanocarpus albomyces* laccase (Hakulinen et al., 2002). Molecular directed evolution is an alternative which does not require detailed spatial and structural information of the enzyme. It is simulating the principles of evolution by repeatedly testing a large number of random mutations for specific features and selecting those mutants in each cycle that fit best. A possible selection criterion could be for example a high pH activity optimum. In more sophisticated approaches selection is based on more than one criterion. Well established high throughput methods are needed however for conducting directed evolution approaches (Kunamneni et al., 2008). These were not yet available during this work which is why the focus was on rational site directed mutagenesis based on crystal structures described above (1.1).

Common targets of site directed mutations are amino acids of the active site and the substrate binding pocket. The intention is often to change the precise coordination of the T1 copper and possibly changing its redox potential by doing so (Rodgers et al., 2010). Furthermore modifications of amino acids in the binding pocket were reported to have raised the pH optimum, like in the case of *Trametes versicolor* laccase (Madzak et al., 2006).

1.4 Reversible laccase inhibition

Reversible enzyme inhibition comes in various forms. If the reduction of oxygen to water is not taken directly into account and only one inhibitor at a time is considered, the reversible inhibition model of laccases includes one substrate and its product, one inhibitor and the enzyme. Such a simplified model for steady state kinetics is described by Bisswanger (2000, Chapter 2.5) and shown in Figure 1.3 and Figure 1.4. The reaction equation for partial non-competitive inhibition is the basic form of which the equations of the other inhibition types are simplifications. The special characteristics of competitive, non-competitive and uncompetitive inhibition, respectively complete and partial inhibition which are used for these simplifications are listed in Table 1.1.

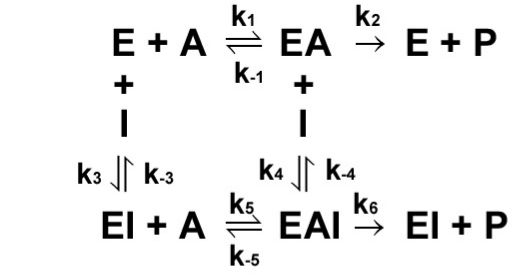

$$K_A = \frac{\kappa_{-1}}{\kappa_1} = \frac{[E][A]}{[EA]} \qquad K_{IC} = \frac{\kappa_{-3}}{\kappa_3} = \frac{[E][I]}{[EI]}$$

$$K_{AI} = \frac{\kappa_{-5}}{\kappa_5} = \frac{[EI][A]}{[EAI]} \qquad K_{IU} = \frac{\kappa_{-4}}{\kappa_4} = \frac{[EA][I]}{[EAI]}$$

Figure 1.3: Reaction equation of partial non-competitive enzyme inhibition (Bisswanger, 2000, 85)

$$v = \frac{\left(V_1 \frac{V_2[I]}{K_{iu}}\right)[A]}{\left(1+\frac{[I]}{K_{ic}}\right)+\left(1+\frac{[I]}{K_{iu}}\right)[A]} \qquad V_1 = k_2[E]_0 \qquad V_2 = k_6[E]_0$$

Figure 1.4: Reaction speed for partial non-competitive inhibition at steady state kinetics (Bisswanger 2000, 86)

Table 1.1: Reversible enzyme inhibition types and their characteristics (Bisswanger, 2000, 87)

Inhibition type			**Special case**
Competitive inhibition		$K_{iu} \rightarrow \infty$	Product inhibition (I = P)
Non-competitive inhibition	mixed type	$K_{ic} \neq K_{iu}$	
Non-competitive inhibition	pure	$K_{ic} = K_{iu}$	
Uncompetitive inhibition		$K_{ic} \rightarrow \infty$	Substrate inhibition (I = A)

Complete inhibition	$V_2 = 0$
Partial inhibition	$V_2 \neq 0$

The type of inhibition can be identified by determining the inhibitor dependency of apparent K_m and v_{max}. Non-competitive inhibition does not prevent the substrate from binding but inhibits its catalysis. Both factors are dependent on the inhibitor concentration when the inhibition follows that type. If however v_{max} is independent from it, the inhibition is competitive. In this case the inhibitor and the substrate prevent each other from binding. This can be because of both sharing the same binding site but can also be due to other reasons. The rare type of uncompetitive inhibition is indicated by both, v_{max} and k_m being independent from the inhibitor concentration. This rare type describes the inhibitor only binding to already bound substrate and inhibiting the enzyme that way. The inhibition is partial rather than complete, if bound inhibitor does not stop enzyme activity completely but only reduces the catalytic rate (Bisswanger, 2000, Chapter 2.5).

1.5 Application of laccases in miniature biofuel cells

Miniaturized biofuel cells are considered a potential power source for invasive medical devices. The goal is to create small, low power and biocompatible systems (Barrière, 2006). To achieve a strong miniaturization biofuel cells have to be single compartment systems as no separating membrane is needed (Chen et al., 2001). That means both electrodes share the same compartment and the anode and cathode reaction must not interfere with each other. Furthermore the enzymes from both electrodes have to be suitable for the same conditions like pH, ionic strength, electrolytes etc (Stoica et al., 2009).

The first single compartment biofuel cell was created by Katz et al. (1999). Chen et al. (2001) adopted that approach for the use of laccase-modified cathodes but tested it in Cl^- free solution. A glucose oxidase / *Trametes versicolor* laccase system was designed by Barrière et al. (2006) for use at physiological conditions. The low pH optimum of fungal laccases was identified as a major drawback. A low Cl^- tolerance reported for fungal laccases in solution could be improved by the used immobilization technique.

Figure 1.5 shows the design of Stoica et al. (2009) where also the basic concept of single compartment biofuel cells is illustrated. On the electrode a film of laccase-Os-modified polymers is deposited and attached. This way the electron mediator and the laccase are immobilized but electrons and oxygen respectively water are able to move. The life span of the enzyme is expected to be increased by its embedding into the polymer. Optimization can be achieved by fine tuning the length of the spacer between Os-complex and polymer backbone, the redox potential of the modified polymer and diffusion characteristics of the film (Stoica et al., 2009).

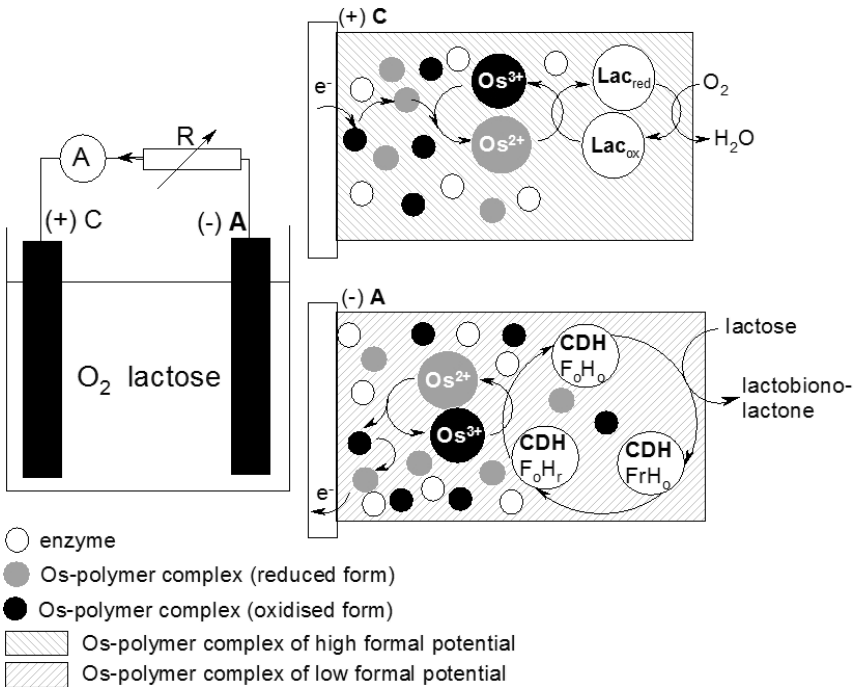

Figure 1.5: Cellobiose dehydrogenase (anode) / laccase (cathode) based biofuel cell based on Os-complex mediated electron transfer (Stoica et al., 2009)

An optimized *Trametes hirsuta* laccase based cathode was developed by Ackermann et al. (2010) for possible use in single compartment fuel cells like the one shown in Figure 1.5. pH deposited Os-modified anodic electrodeposition polymers were used with a redox potential 50 mV below the one of *Trametes hirsuta* laccase. Glassy carbon served as electrode. Figure 1.6 shows the achieved bioelectric catalytic current in cyclic voltammetry which was -325 µA cm^{-2} in saturated oxygen.

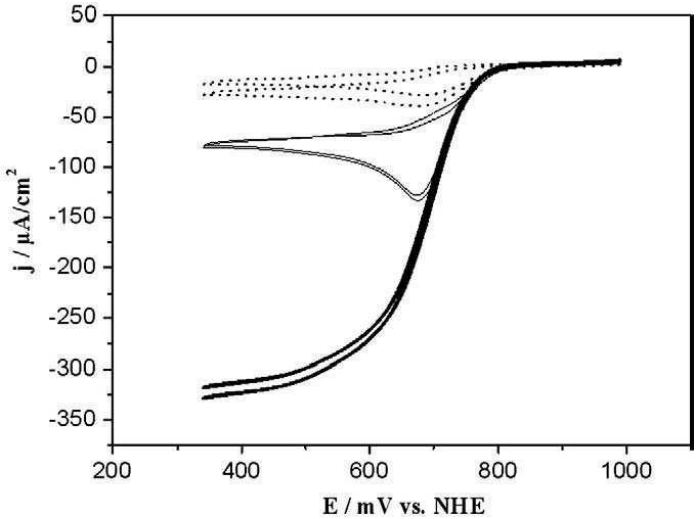

Figure 1.6: Cyclic voltammogram of Os-modified anodidc polymer on glassy carbon electrode with entrapped *Trametes hirsuta* laccase exposing catalytic current due to O_2 reduction. (argon: dotted lines, air: solid lines, saturated oxygen: bold solid lines; phosphate citrate buffer (100 mM) pH 4.0, scan rate 0.005 V s^{-1}) (Ackermann et al., 2010)

2 Experimental Procedures

2.1 Material

2.1.1 Media

SOC medium:

20 g/L tryptone

5 g/L yeast extract

0.5 g/L NaCl

0.186 g/L KCl

Adjusted to pH 7.0 with NaOH

autoclaved

10 ml/L sterile filtrated 1M $MgCl_2$

20 ml/L sterile filtrated 1 M glucose

LB zeo

LB stock:	10 g/L Tryptone
	5 g/L yeast extract
	5 g/L NaCl
LB agar stock	additionally 15 g/L agar agar

Add 0.25 µl Zeocin per ml stock to LB stock solution after autoclaving

YPD zeo:

YPD zeo medium:	20 g/L Tryptone
	5 g/L yeast extract
	0.4 g/L D-Glucose
YPD zeo agar:	additionally 15 g/L agar agar

Add 1 µl Zeocin per ml stock to YPD stock solution after autoclaving

BMM agar: (for 0.5 L)

339 ml RO-water

7.5 g Agar Agar

Autoclave and add the following sterile filtrated ingredients:

50 ml 1M Potassium phosphate buffer at ph 6: 59 g KH_2PO_4

46 g K_2HPO_4

Fill to 0.5 L marking with dH_20

Equilibrate with phosphoric acid

50 ml "10X YNB": 35 g/L YNB without amino acids and $(NH_4)_2SO_4$

+ 100 g/L $(NH_4)_2SO_4$

1 ml "500X Biotin": 10 mg Biotin + 50 ml RO-water

50 ml "10X methanol": 2.5 ml methanol + 47.5 ml RO-water

5 ml ABTS: 20 mM = 329 mg in 30 ml RO-water

5 ml $CuSO_4xH_2O$: 10 mM = 74.9 mg in 30 ml RO-water

BMMY Medium (+ $CuSO_4$): (for 0.5 L)

344 ml RO-water

5 g yeast extract

10 g peptone

Autoclave and add the following sterile filtrated ingredients:

50 ml 1M Potassium phosphate buffer at ph 6 (see BMM recipe)

50 ml "10X YNB": 35 g/L YNB without amino acids and $(NH_4)_2SO_4$

+ 100 g/L $(NH_4)_2SO_4$

1 ml "500X Biotin": 10 mg Biotin + 50 ml RO-water

50 ml "10X methanol": 2.5 ml methanol + 47.5 ml RO-water

5 ml $CuSO_4xH_2O$: 1 mM = 25 mg in 100 ml RO-water

BMGY (for 0.5 L)

349 ml RO-water

5 g yeast extract

10 g peptone

Autoclave and add the following sterile filtrated ingredients:

50 ml 1M Potassium phosphate buffer at ph 6 (see BMM recipe)

50 ml "10X YNB": 35 g/L YNB without amino acids and $(NH_4)_2SO_4$

+ 100 g/L $(NH_4)_2SO_4$

1 ml "500X Biotin": 10 mg Biotin + 50 ml RO-water

50 ml 10X Glycerol: (5 ml = 6.3 g Glycerol + 45 ml RO-water)

BMD1 (1% D-Glucose): (for 0.5 L)

299 ml RO-water

Autoclave and add the following sterile filtrated ingredients:

100 ml potassium phosphate buffer pH 6 (1 M) (see BMM recipe)

50 ml “10X YNB”: 35 g/L YNB without amino acids and $(NH_4)_2SO_4$ + 100 g/L $(NH_4)_2SO_4$

50 ml “10X D-Glucose”: 5 g D-glucose filled up to 50 ml with RO-water

1 ml “500X Biotin”: 10 mg Biotin + 50 ml RO-water

BMM2 (2% MeOH): (for 0.5 L)

339 ml RO-water

Autoclave and add the following sterile filtrated ingredients:

100 ml potassium phosphate buffer pH 6 (1 M) (see BMM recipe)

10ml methanol

50 ml “10X YNB”: 35 g/L YNB without amino acids and $(NH_4)_2SO_4$ + 100 g/L $(NH_4)_2SO_4$

1 ml “500X Biotin”: 10 mg Biotin + 50 ml RO-water

BMM10 (10% MeOH): (for 0.5 L)

299 ml RO-water

Autoclave and add the following sterile filtrated ingredients:

100 ml potassium phosphate buffer pH 6 (1 M) (see BMM recipe)

50 ml methanol

50 ml “10X YNB”: 35 g/L YNB without amino acids and $(NH_4)_2SO_4$ + 100 g/L $(NH_4)_2SO_4$

1 ml “500X Biotin”: 10 mg Biotin + 50 ml RO-water

Fermentation Basal Salts Medium: (for 1 L)

0.93 g $CaSO_4$

18.2 g K_2SO_4

14.9 g $MgSO_4x7H_2O$

4.13 g KOH

40 g glycerol

26.7 ml phosphoric acid (85%)

Fill up to 1 L with RO-water

2.1.2 Strains

NEB5-alpha competent *E. coli* (high efficiency) (New England Biolabs, Beverly, USA)

Genotype: *fhuA2Δ(argF-lacZ)U169 phoA glnV44 Φ80 Δ(lacZ)M15 gyrA96 recA1 relA1 endA1 thi-1 hsdR17*

Electrocompetent *Pichia pastoris* strain X33 (Invitrogen, Carlsbad, USA)

Genotype: wild type

2.1.3 Plasmids

pPICZ B (Invitrogen): 3328 bp

This plasmid can be selected and amplified in *Escherichia coli* but also has the ability of homologuous recombination into the *Pichia pastoris* genome at the AOX1 locus which is used for integration into this methanotrophic yeast where expression under methanol induction is possible. Successfully transformed *Escherichia coli* and *Pichia pastoris* can both be selected with Zeocin.

pBan2:

pPICZ B vector with *Ba*Lac cDNA insert between the restriction sites eco72I and XbaI

2.1.4 Primers

NaCl stability mutants (mutations marked):

5BaLR129H	5'-GGC ATG GAA TT**C** **AT**C AAC TAG-3'
3BaLR129H	5'-CCT AGT TG**A** **TG**A ATT CCA TGC-3'
5BaLR129L2	5'-TGG AAT T**CT** **T**CA ACT AGG AAG TCT CG-3'
	T_m (thermodynamic): 56.3℃
3BaLR129L2	5'-GTT G**AA** **G**AA TTC CAT GCC AGT G-3'
	T_m (thermodynamic): 53.7℃
5BaLR129F3	5'-TGG AAT T**TT** **T**CA ACT AGG AAG TCT CG-3'
	T_m (thermodynamic): 56.3℃
3BaLR129F2	5'-GTT G**AA** **A**AA TTC CAT GCC AGT G-3'
	T_m (thermodynamic): 53.7℃

T1 redox potential mutants (mutations marked):

5BaLD273N	"2A"	5'-ATT **AAC** AGT CAC TTC GAA TTC G-3'
		T_m (thermodynamic): 48.3℃
3BaLD273N	"2B"	5'-TGA CT**G** **TT**A ATT CCG ACA TTG ATC-3'
		T_m (thermodynamic): 52.6℃
5BaLD273A	"3A"	5'-ATT **GCC** AGT CAC TTC GAA TTC G-3'
		T_m (thermodynamic): 55.7℃
3BaLD273A	"3B"	5'-TGA CT**G** **GC**A ATT CCG ACA TTG ATC-3'
		T_m (thermodynamic): 59.7℃
5BaLD455N2	"N2A"	5'-CGT ATA TGT CAT CGA A**AA** **T**CT CAC CGG CTT C-3'
		T_m (thermodynamic): 65.7℃
3BaLD455N2	"N2B"	5'-GAT GAC ATA TAC CCA CTC TTC-3'
		T_m (thermodynamic): 51.2℃
5BaLD455A	"5A"	5'-CAT CGA A**GC** **T**CT CAC CGG C-3'
		T_m (thermodynamic): 55.5℃
3BaLD455A	"5B"	5'-GAG **AGC** TTC GAT GAC ATA TAC G-3'
		T_m (thermodynamic): 48.6℃
5BaLE534Q	"6A"	5'-CAT CT**C** **AG**G GGT TGG CAA TGC-3'
		T_m (thermodynamic): 58.9℃
3BaLE534Q	"6B"	5'-ACC C**CT** **G**AG ATG CGT GCC ATG-3'
		T_m (thermodynamic): 61.5℃
5BaLE534A	"8A"	5'-CAT CT**G** **CT**G GGT TGG CAA TGC-3'
		T_m (thermodynamic): 59.9℃
3BaLE534A	"8B"	5'-ACC C**AG** **C**AG ATG CGT GCC ATG-3'
		T_m (thermodynamic): 62.6℃

Sequencing primers:

5AOX1	5'-GAC TGG TTC CAA TTG ACA AGC-3'
3AOX1	5'-GCA AAT GGC ATT CTG ACA TCC-3'

2.1.5 Chemicals

2,2′-(Ethylenedioxy)bis(ethylamine): Mw: 148.21 $mg*mol^{-1}$, CAS number: 929-59-9

2,2′-(Ethylenedioxy)diethanthiol: Mw:182.31 $mg*mol^{-1}$, CAS number: 14970-87-7

4-(4 aminophenyl) butyric acid: Mw: 179.22$mg*mol^{-1}$, CAS number: 15118-60-2

2.1.6 Os-modified polymers

Os-modified anodic polymers:

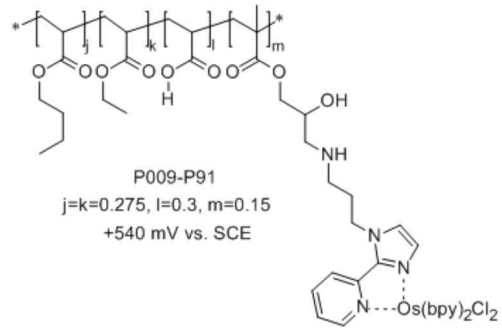

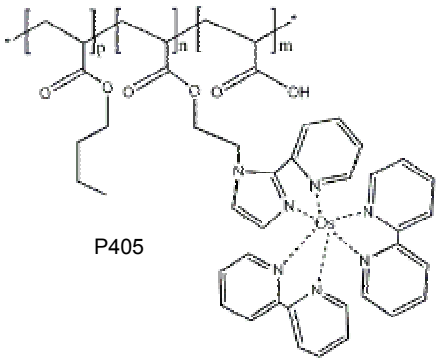

Os-modified cathodic polymers:

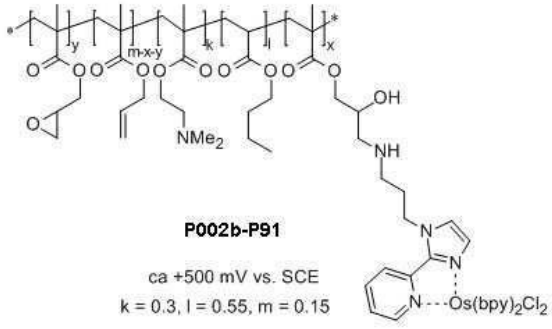

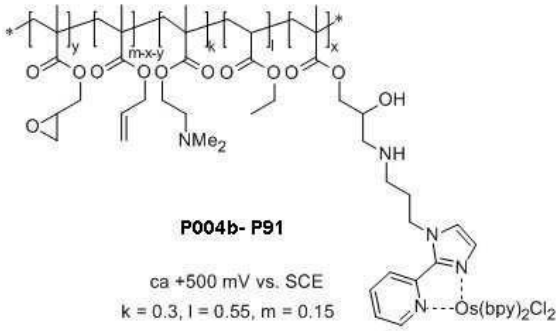

Os-modified uncharged backbone polymers:

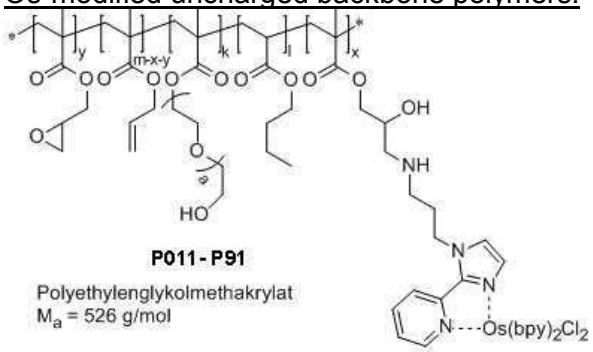

2.1.7 Electrodes

- Glassy carbon (r = 1.5 mm) in teflon housing (HTW Hochtemperatur-Werkstoffe GmbH, Germany)
- Ag/AgCl (3M) reference electrode
- Platinum wire

2.2 Site directed mutagenesis of BaLac cDNA and preparations for expression in Pichia pastoris

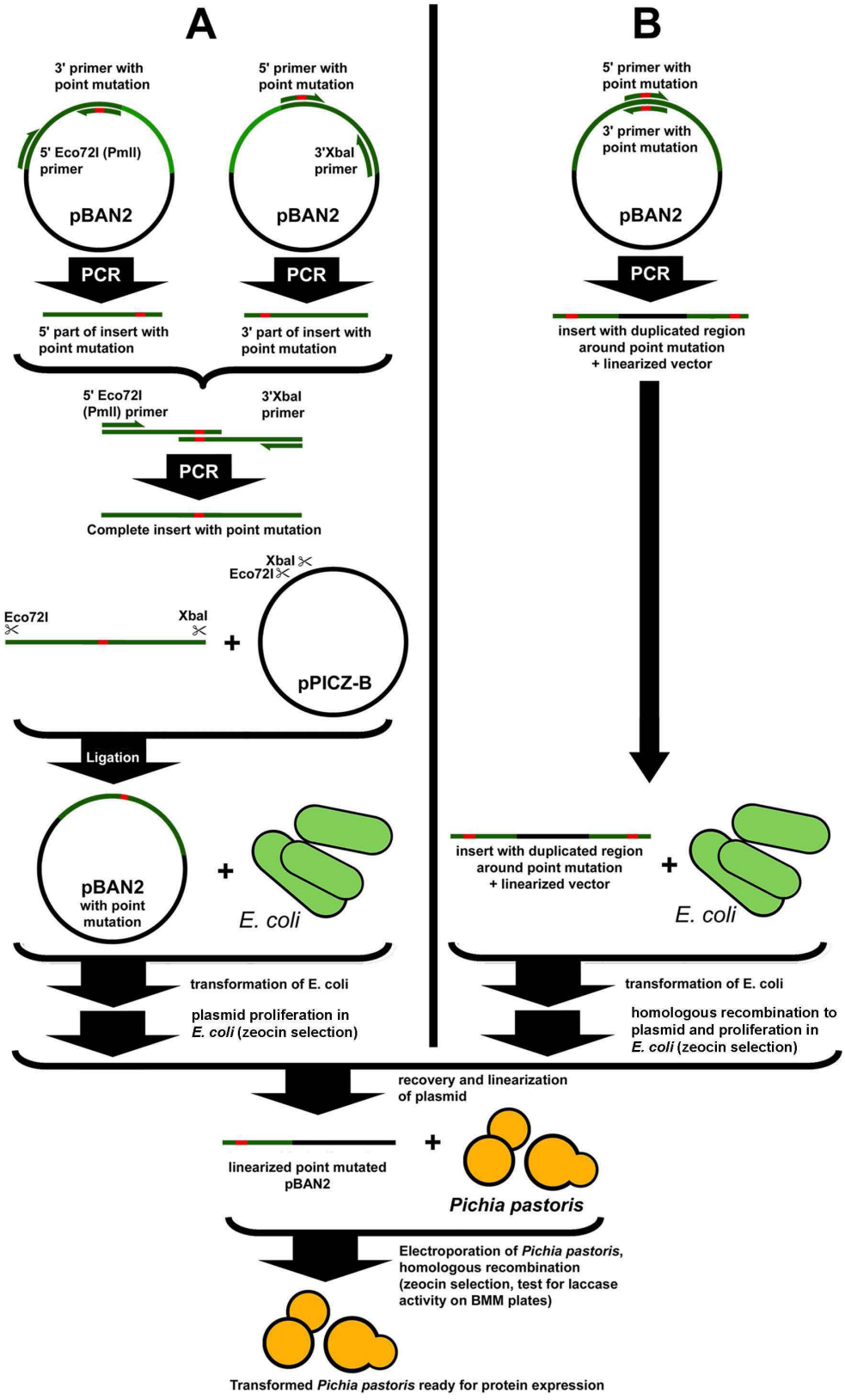

Figure 2.1: Site directed mutagenesis of *Ba*Lac cDNA using four primers method (A) and *Dpn*I method (B) and subsequent creation of mutant laccase expressing *Pichia pastoris*

2.2.1 Site directed mutagenesis

DpnI method

Phusion-PCRs with two primers featuring the same specific mutation were used to create linearized vectors with the point mutated laccase insert as shown in Figure 2.1 B. The recovered PCR product was incubated with *Dpn*I to degrade the non mutated template and used for chemical transformation of competent *E. coli*. The transformants were selected on LB Zeocin plates and the proliferated plasmids were recovered from *E. coli* again. The point mutations were confirmed by bar code sequencing of recovered plasmids.

Four primers method

Two initial Phusion-PCRs where used to create two halves of the insert between two restriction sites (*Eco72*I, *Xba*I) which had a short homologous sequence around the created point mutation (Figure 2.1 A). In both PCRs only one primer was point mutated and the other one was fitted to one of these restriction sites. In a second step both halves served together as template and the two restriction site primers as primers. By cutting the resulting PCR product as well as an empty pPICZ-B vector at these restriction sites and ligating them with each other a finished mutated insert carrying vector was created. That vector was proliferated in *E. coli* transformants on LB Zeocin selection plates and also sent to bar code sequencing after recovering it from the cells.

2.2.2 PCR

For the creation of specifically point mutated laccase cDNA Phusion PCR (New Biolabs, Beverly, USA) was conducted in a C1000 Thermal Cycler (BioRad, USA).

Preparing primers

The appropriate amount of sterile RO water was added to the lyophilized primer (VBC Biotech, Austria) as listed in the shipping documents in order to establish a concentration of 100 pg*µl^{-1}. An incubation at 65℃ and 700 rpm followed for at least 10 min until primer is fully in solution. The stock solution was homogenized and a 1:10 dilution in RO water established in order to get a solution with 10 pg*µl^{-1} primer.

Phusion PCR

Phusion Master Mix: 750 µl HF Buffer 6x
7.5 µl of each: dATP, dGTP, dCTP, dTTP (each 100 mM)
1057.5 µl sterile RO water
37.5 µl Phusion Polymerase
Homogenize and make aliquots of 150 µl in sterile tubes.

PCR set up in PCR tube: 12.5 µl Phusion Master Mix
1 µl Template (100 ng*µl^{-1})
2 µl forward primer (10 pg*µl^{-1})
2 µl reverse primer (10 pg*µl^{-1})

The PCR Tubes are put into the slots of the thermocycler after lid preheating and just before program starts.

Standard PCR program: 1x 2 min 98℃
30x 10 sec 98℃, 20 sec annealing temp., 20 sec p er kb at 72℃
1x for 5 min 72℃
1x for ever at 4℃

2nd step PCR program in 2 step procedure:

PCR mix without primers
1x 2 min 98℃
5x 10 sec 98℃, 20 sec annealing temp., 20 sec pe r kb at 72℃
Adding primers to the mix
30x 10 sec 98℃, 20 sec annealing temp., 20 sec p er kb at 72℃
1x for 5 min 72℃
1x for ever at 4℃

The PCR product was run on an Agarose Gel Electrophoresis, the chosen DNA band excised and the DNA recovered from gel by DNA extraction.

2.2.3 Agarose Gel Electrophoresis

In order to isolate PCR or other DNA constructs Agarose Gel Electrophoresis was used. An ethidium bromide agarose gel in 1x TAE buffer.was prepared and per gel 5 µl of DNA Ladder were loaded in one position as reference. The others were filled with samples which were prepared by adding 5 µl 6x loading dye per 25 µl sample solution. To conduct the electrophoresis voltage from 80 to 100 V was applied for about 30 min. UV light visualized the finished gel and DNA bands of interest were cut out and transferred to a sterile stube.

Stock solutions:

50x TAE Buffer: 24.2% Tris base, 5.72% acetic acid, 10% 0.5 M EDTA pH 8

Agarose Gel: 2 g per 250 ml TAE 1x Buffer, boil in microwave until agar is in solution then store bottle in water bath at 60℃, 2 drops of Eth idium Bromide are added per gel before use.

2.2.4 DNA gel extraction / DNA purification

With the Wizard SV Gel and PCR Clean-Up System (Promega, USA) DNA was extracted out of an agarose gel or purified from small DNA fragments and enzymes.. 1 µl membrane binding solution per mg gel was added to the tube in which the gel was stored and the mixture was incubated in the heating block for at least 10 min at 58℃ and 400 rpm until the gel was dissolved. Alternatively if DNA is in solution the same volume of membrane binding solution was added. For binding of DNA to the membrane the mixture was transferred to the minicolumn provided, incubated for 1 min at room temperature and subsequently centrifuged at 13000 rpm for 1 min. The flow-through was disposed. The first wash of the membrane was done with 700 µl membrane wash solution, by centrifugation at 13000 rpm for 1 min and the second wash with 500 µl membrane wash solution with centrifugation at 13000 rpm for 5 min. Both times the flow-through was disposed. The empty column was centrifuged with open lid at 13000 rpm for 1 min and then it was transferred from the collection tube to a sterile 1.5 mL tube. 50 µl sterile dH_2O were pippeted into the column, incubated at room temperature for 1 min and centrifuged at 13000 rpm for 1 min in order to elute the DNA. The DNA solution was stored at -20℃.

2.2.5 Template degradation, DNA restriction and ligation

The methylated template plasmid was degraded by mixing 1 µl *Dpn*I, 5 µl 10x Tango buffer (both from Fermentas, St. Leon-Rot, Germany) and 50 µl of extracted DNA solution,

homogenizing it and incubating it at 37℃ for sever al hours. For restriction of PCR product, or linearization of plasmid with *Mss*I, 20 µl DNA, 24 µl RO water, 5 µl 10x buffer and 1 µl of the respective restriction enzyme were mixed. Restricted DNA was purified from enzymes and short DNA fragments with the Wizard SV Gel Clean-Up System.

Used restriction enzymes:	*Dpn*I	10x Tango buffer	(Fermentas)
	*Eco72*I *(Pml*I)	10x Tango buffer	(Fermentas)
	*Xba*I	10x Tango buffer	(Fermentas)
	*Mss*I (*Pme*I)	10x Buffer B	(Fermentas)

The ligation of two DNA fragments was conducted with the Rapid DNA Ligation Kit (Roche Applied Science). 3 µl insert and 1 µl vector DNA were mixed with 2 µl T4 DNA rapid ligation buffer (5x), 1 µl T4 DNA ligase and 3 µl RO water and incubated at room temperature for one hour.

2.2.6 Proliferation of plasmid in *E. coli*

Chemically competent *E. coli* NEB5-alpha suspension was defrosted on ice and immediately afterwards portioned into 50 ml aliquots. 1-5 µl of DNA sample were added and after flicking gently the mixture was incubated on ice for 30 min. A 30 sec heat shock at 42℃ was applied and samples were put back on ice again for 5 min. Then 500 ml SOC medium were added and the suspension was incubated for 1 hour at 37℃ and 120 rpm. Cells were plated subsequently on appropriate selection plates (LB zeo agar plates for pPICZ-B plasmids) and incubated at 37℃ over night.

2.2.7 Extraction of plasmid from *E. coli*

Proliferated Plasmid was extracted from *E. coli* according to the "PureYield^{TM} Plasmid Miniprep System Quick Protocol" (Promega, USA). Step 1 was modified by centrifuging 1 ml cell culture at 12000 rpm for 30 sec, disposing the supernatant and resuspending the pellet in 600 µl added cell culture

2.2.8 Sequencing of plasmid to confirm correct mutation

Bar code sequencing of 10 µl mutated, proliferated and purified plasmid sample was conducted by LGC Genomics (Berlin, Germany) using the standard primers 5AOX1 and 3AOX1.

2.2.9 Electroporation of *Pichia pastoris*

Plasmid with the correct sequence was prepared for electroporation by linearizing it with *Mss*I. 50 µl electrocompetent *Pichia pastoris* cell suspension (freshly thawed on ice) and up to 4 µl linearized DNA (100 ng) were mixed in a chilled tube by pipetting up and done and subsequently transferred to a chilled 2 mm Cuvette. Electroporation was conducted at 1.5 kV and 125 ohm for 3 msec and immediately afterwards 500 µl of 1 M sorbitol and 500 µl of YPD medium were added. The suspension was pipetted up and down, transferred to a fresh tube and incubated at 30℃ for 3-4 hours at 120 rpm. Afterwards it was pelleted (1 min, 12000 rpm) and 700 µl supernatant were disposed. The resuspended pellet was plated on appropriate YPD selection plates (YPD zeo agar plates for pPICZ-B plasmids) and incubated for 2 days at 30℃.

Successful plasmid integration into the *Pichia pastoris* genome and sufficient activity of secreted laccase were assessed by transferring clones in parallel on BMM plates (containing ABTS) and YPD plates. If clone is positive a green halo appears around the colonies within 2-4 days at 30℃ and the same clone from the YPD plate can be used for further propagation.

*2.3 Heterologous expression and purification of Ba*Lac

2.3.1 Methanol induced enzyme expression by *Pichia pastoris* in shaking flasks

A preparatory culture of production *Pichia pastoris* strain in in shaking flasks with 50 ml YPD medium was incubated at 30℃ at 120 rpm over night. It was used to start the fermentation in 1 L shaking flasks with 200 ml BMMY medium once the cell density reached an OD_{600} of 1. All flasks were connected via peristaltic pumps to a feed of 50% methanol. The fermentation took place at 30℃ for 7 days whereas methanol induction was started on the second day (pump rotation at 105 rpm) and methanol influx was continued until the end. Samples were drawn each day to determine wet cell mass and specific enzyme activity (ABTS standard assay and Bradford assay). The cultivations were harvested by pooling flasks containing the same expressed enzyme and the supernatant was attained by centrifugation in 0.5 L centrifuge bottles at 3000 rpm for 10 min and stored at 4℃.

2.3.2 Methanol induced enzyme expression by *Pichia pastoris* in 0.5 L Multifors bioreactor

Methanol induced heterologous expression of *Ba*Lac in *Pichia pastoris* was conducted according to the Invitrogen "Pichia Fermentation Process Guidelines" (Version B 053002) in a 0.5 L Multifors bioreactor (Infors-ht, Bottmingen, Switzerland). Progress was monitored with daily sampling and testing for enzyme activity in ABTS standard assays, protein concentration according to Bradford as well as wet cell mass. After 70 hours methanol induction was started and after 5 days the supernatant was harvested and separated from the biomass in 0.5 L centrifuge bottles at 3000 rpm for 10 min.

2.3.3 Purification

$(NH_4)_2SO_4$ precipitation

The supernatant was 20% saturated with $(NH_4)_2SO_4$ by adding 100% saturated $(NH_4)_2SO_4$ solution. In a second step 123 $g*L^{-1}$ crystalline $(NH_4)_2SO_4$ were added slowly under constant agitation to increase the content to 40% saturation. The solution was then purified from remaining cells and insoluble components by ultracentrifugation at 25000 rpm for 30 min (4℃) with subsequent vacuum filtration with 45 µm nitrocellulose filters.

Hydrophobic Interaction Chromatography (HIC)

Solutions which are prepared as described above can be purified by HIC. ÄKTA purifier and ÄKTA explorer (GE Amersham Pharmacia, USA), respectively were used. A 20 ml Phenyl-Source and a 70 ml Phenyl-Sepharose column, respectively were used.

Buffers (filtrated and degassed):

- Washing buffer: 40% saturated $(NH_4)_2SO_4$ pH 5.5 citrate buffer (50 mM)
- Elution buffer: pH 5.5 citrate buffer (50 mM)

1 step Phenyl-Source HIC:

Äkta was prepared by inserting the Phenyl Source column between "sample valve 1" and dedector. Inlet A1 was used for washing buffer and B1 for elution buffer. The UV/VIS-detector was set to 280 nm and 615 nm and the alarm pressure to 0.7 mPa. After executing the option "pump wash purifier" the column was flushed at a rate of 3 $ml*min^{-1}$ (load: "injection valve", outlet: "waste", 0% B1) with washing buffer until measured conductivity remained constant, at which point the UV/Vis-dedector was set to autozero. By pausing the system, changing inlet A1 to the sample solution and resuming the flow the loading process

started. Maximum load for this column is 100 mg protein. Once the column was loaded it was flushed with washing buffer again. After the 280 nm measurement approached the base line a falling $(NH_4)_2SO_4$ gradient (from 0 to 100% B1 in 70 min, outlet: “fraction”) was started and the eluent was portioned by the autosampler. Laccase containing fractions were identified by testing for specific activity (ABTS standard activity assay and Bradford assay).

Alternative 2 step HIC:

For a higher degree of purification a 2 step procedure was employed. The first run was done with the Phenyl-Sepharose Column using the same protocol as above except that the flow rate was modified to 10 ml per minute and the gradient was run from 0 to 100% B1 in 20 min. The pooled fractions were prepared for the second run by adding 100% saturated $(NH_4)_2SO_4$ under stirring. The conductivity was measured and the salt solution was added until the same conductivity was reached as in the solution before the first run. In the following HIC with a Phenyl-Source column a gradient from 0 to 100% B1 in 20 min at a flow rate of 2.5 ml per minute was set. Otherwise the same procedure as described above was applied.

Äkta cleaning protocol:

The system was flushed with 100% elution buffer (100% B1) until most of the 280 nm signal had vanished, at which point both inlets were transferred into the elution buffer and flushing was continued with 50% B1. Then the column subsequently washed with 0.5 M NaOH, RO-water, 0.5 M acetic acid, RO-water again and finally a few column volumes of 20% ethanol before shutting down Äkta.

2.3.4 Concentrating samples and exchanging buffer

Purified laccase solutions were concentrated with Amicon Ultra-15 Centrifugal Filter Units (Millipore, USA). To do so the sample was centrifuged at 3500 rpm until the volume was reduced to 1 ml. Flow-through was discharged when necessary. Before use the centrifuge filter tubes had to be washed with RO water. After usage they were stored in 20% ethanol.

Using the same centrifuge filter tubes as above the sample buffer was exchanged by washing the 1 ml sample with 30 ml new buffer (for laccases 50 mM pH 5.5 citrate buffer with 50 mM $(NH_4)_2SO_4$). The centrifuge was used at 3500 rpm until volume was down to 1 ml again. The final enzyme solution was then transferred to tubes and stored at 4℃.

*2.4 Characterization of Ba*Lac

Wet Cell Mass (WCM)

2 ml of cell culture sample were centrifuged at 12000 rpm for 10 min and the supernatant was disposed. Remaining fluid was carefully removed with paper. Afterwards the pellet was weighed and WCM per ml calculated.

Protein concentration

Protein was quantified based on the rapid protein quantification method of Bradford (1976) using protein assay reagent from BioRad (Hercules, CA, USA) and bovine albumin serum for establishing the standard curve which was done according to the manufacturer's manual. The samples were incubated with the reagent solution for 15 minutes before measuring against a blank assay mixture.

2.4.1 Photometric activity tests

Standard laccase activity assay (with ABTS)

Laccase activity was measured with 2 mM 2,2'-azino-bis(3-ethylbenzthiazoline-6-sulphonic acid) (ABTS) in pH 4 citrate buffer (100 mM) at 30°C and 420 nm (ε_{420} = 36 $mM^{-1}*cm^{-1}$) (Bourbonnais et al., 1998). One unit was defined as 1 µmol substrate being oxidized per minute at these conditions.

Enzyme kinetics

Laccase activity was measured in citrate buffer (100 mM) at 30℃ to determine the K_m-value with substrates of interest: ABTS (ε_{420} = 36 $mM^{-1}*cm^{-1}$) (Bourbonnais et al., 1998), 2,6-DMP (ε_{468} = 49.6 $mM^{-1}*cm^{-1}$) (Wariishi et al., 1992), guaiacol (ε_{465} = 12.1 $mM^{-1}*cm^{-1}$) and catechol (ε_{392} = 1.46 $mM^{-1}cm^{-1}$) (Galhaup et al., 2002). For this purpose a substrate dilution row was established reaching from concentrations which were at least 5 times lower and higher than the K_m-value. To improve reproducibility, enzyme activity was always calculated from the entire 5 min lasting measurements. Kinetic curves based on the Michaelis-Menten equation were established and K_M- and k_{cat}-value determined with Sigma Plot 11.0 (Systat Software, Chicago, USA) employing nonlinear least squares regression (Mueangtoom et al., 2010).

pH activity profile

A pH row was prepared with citrate buffer (100 mM) and citrate phosphate buffer (100 mM) within a range from pH 2.5 to pH 8. Except for the buffers the assay with ABTS was

conducted like the standard activity assay. 2,6-Dimethoxyphenol (2,6-DMP, 10 mM, ε_{468} = 49.6 $mM^{-1}*cm^{-1}$) was used as an alternative substrate for laccases.

Temperature optimum and stability

To determine activity optima the ABTS standard activity assay was used at varying temperatures, from room temperature to 60℃ in 5℃ steps.

In order to test stability, the enzyme was stored at various temperatures and remaining activity was then determined in ABTS standard assays. For temperatures higher than 55℃ one cuvette sufficed and one standard assay could be used with an extended measurement time of 20-40 min. For that purpose the sample had to be diluted accordingly to feature a volumetric activity of around 0.1 $U*ml^{-1}$.

NaCl inhibition assay

Citrate buffers (pH 4, 100 mM) with NaCl concentrations from 0 to 4 M were used in the assay. For each NaCl containing buffer solution the pH was corrected if necessary and conductivity tested. ABTS (1 mM, ε_{420} = 36 $mM^{-1}*cm^{-1}$) (Bourbonnais et al., 1998) and 2,6-DMP (0.2 mM, ε_{468} = 49.6 $mM^{-1}*cm^{-1}$) (Wariishi et al., 1992) were used as substrate whereas ABTS could be used only up to 1 M NaCl as it precipitates at higher concentrations. The assay was conducted at 30℃.

Type 1:

Buffer and sample were mixed and incubated for 5 min at 30℃, the measurement was started after adding the substrate

Type 2:

A mixture of buffer and substrate was measured directly after sample was added.

Solvent enzyme inactivation assay

Solvent dilutions in pH 5 citrate buffer (100 mM) were created containing 0-50% ethanol respectively methanol in 10% steps. The tested laccase was diluted with the various ethanol/methanol buffers and the dilution was stored at 4℃. The activity was measured immediately and over time by standard ABTS activity assays.

Os-modified polymer / crosslinker enzyme inactivation assay

A stock mixture containing 2% (w/v) Os-modified-polymer (equilibrated beforehand at pH 4 with 100 mM citrate buffer) and 0.2% (w/v) laccase in pH 4 citrate buffer (100 mM) was established. The possible loss in activity was determined over time with appropriate dilutions from the stock mixture in standard ABTS activity assays. For testing the effect of crosslinkers different concentrations of it were added to the stock solution instead of Os-modified polymer. Stock solution with buffer and laccase only was used as reference.

Os-complex / polymer backbone enzyme inactivation assay

The stock solution contained 0.2% (w/v) laccase and 5% (w/v) polymer backbone or 0.07% (w/v) Os-complex.. Otherwise the assay was conducted like the Os-modified polymer inhibition assay.

2.4.2 High throughput screening

For high throughput 96-well plate activity screening, JANUS Automated Workstation (Perkin Elmer, USA) in combination with a “Sunrise” 96-well plate reader (Tecan, Switzerland) was used.

Activity and pH profile screening

Fermentation supernatant was taken from centrifuged (3500 rpm for 15 min) deep well plates. The plate was pipetted as shown by the following scheme and read in the plate reader at given wavelengths.

Pipetting scheme for each well:

160 µl buffer

20 µl substrate

20 µl supernatant from 96 deep well plate fermentation

Used stock solutions:

substrates: ABTS (5 mM, ε_{420} = 36 $mM^{-1}*cm^{-1}$) (Bourbonnais et al., 1998)

guaiacol (10 mM, ε_{465} = 12.1 $mM^{-1}*cm^{-1}$) (Galhaup et al., 2002)

2,6-DMP (10 mM, ε_{468} = 49.6 $mM^{-1}*cm^{-1}$) (Wariishi et al., 1992)

catechol (100 mM, ε_{392} = 1.46 $M^{-1}cm^{-1}$) (Galhaup et al., 2002)

buffers: pH 4 citrate buffer (100 mM) for activity screening

citrate buffer (pH 4-5.5, 100 mM) and citrate-phosphate buffer (pH 6-7.5, 100 mM) for pH profiles

NaCl inhibition of *Ba*Lac

Stock Solutions: (volumes needed per 96-well plate duplicate)

20 ml 4 M NaCl in RO-water

1.4 ml 80 mM ABTS respectively 2,6-DMP

20 ml enzyme dilution in appropriate citrate buffer (266 mM)

RO-water

Assay Scheme per well:

100µl NaCl solution

25µl Substrate solution

75µl Enzyme/Buffer solution

Dilution rows of inhibitor and substrate were established by the pipetting robot with 1:2 dilutions. The robot then prepared the assays in 96 well plates which were measured subsequently with plate reader at 420 nm (ABTS) or 468 nm (2,6 DMP).

2.5 96-well fermentation and enzyme activity screening

Autoclaved 96-deep well plates with 300 µl BMD1 medium were inoculated with toothpicks, sealed off with a gas permeable membrane and incubated at 25℃ and 300 rpm. After 60 hours when the stationary growth phase is reached 300 µl BMM2 were added. After 70 hours 70 µl BMM10 were added, a step which was repeated at hour 82 and 108. After 130 hours the deep well plate was centrifuged at 3500 rpm for 15 min and the supernatant transferred to a 96-well plate which was tested as described in section 2.4.2.

2.6 Electrochemistry

2.6.1 Preparation of laccase-Os-complex-modified electrodes

The used Os-modified polymers (2.1.6) were produced at the Ruhruniversität Bochum (Analytische Chemie - Elektroanalytik & Sensorik, Prof. Schuhmann) analogous to the

procedure described by (Ackermann et al., 2010) with the exception of Os-modification for p009-p91, p002B-p91, p004B-p91 and p011-p91, which was done as shown in the appendix in Figure A.6.

pH deposited modified polymers

A mixture of 0.2% (w/v) Laccase and 2% (w/v) Os-modified anodic polymer (equilibrated at pH 4 with 100 mM citrate buffer) was prepared and 5 µl were deposited on a polished glassy carbon electrode at pH 3 (100 mM citrate buffer). The modified electrode was then washed with pH 4 citrate buffer (100 mM).

Covalently bound modified polymers

For covalent binding Os-modified-polymers with a non-charged backbone were used. The polished glassy carbon electrodes were prepared by electrochemical reduction of in situ generated diazonium salts as described by Breton and Bélanger (2008). The method was modified using 4-(4 aminophenyl) butyric acid as amine and cyclic voltammetry between 200 and -800 mV over three cycles for reduction. In a second step a diamine linker (2,2'-(ethylenedioxy)bis(ethylamine)) with a Boc protection group on one side was covalently bound at the carboxylic groups. The electrode was incubated in Thionyl chloride and subsequently in 0.5 ml 0.1 M linker with a few µl of ethylamine. The covalently bound linker was then activated by 4 M HCl in Dioxan and washed in 5 M KOH and RO-water.

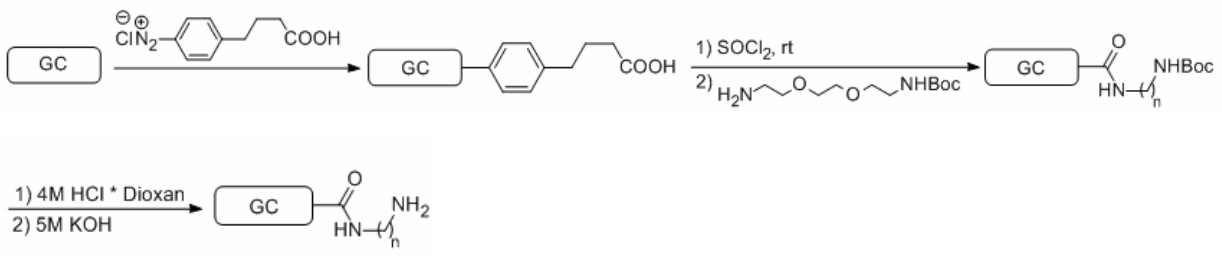

A mixture of 2% (w/v) Os-modified polymer, 0.2% (w/v) laccase and 0.2% (w/v) crosslinker (2,2′-(Ethylenedioxy)diethanthiol) was prepared and 10 µl used to incubate on the prepared glassy carbon electrode over night at room temperature.

2.6.2 Circular Voltammetry

For conducting circular voltammetry the modified glassy carbon electrode was used as working electrode, an Ag/AgCl (3M) electrode as reference and platinum as counter electrode in a cell with 100 mM citrate buffer solution at pH 4. A potentiostat (1030B Series Multi Potentiostat, CH Instruments, USA) applied potentials ranging from 800 mV to 0 mV at a scan rate of 0.005 $V*s^{-1}$.

3 Results

3.1 Site directed mutagenesis of BaLac cDNA and preparations for expression in Pichia pastoris

Additionally to already established *Ba*Lac mutants, 6 more T1 redox potential mutants were created by site directed mutagenesis of amino acids close to the T1 copper because similar amino acid alternations had shown the capability of changing the E°of the T1 copper site (Xu et al., 1999c). Moreover 3 NaCl tolerance mutants were created with alterations close to the T2 copper at which the structure of *Melanocarpus albomyces* laccase suggested the presence of a chloride ion (Hakulinen et al., 2002). An arginine which is found in *Ba*Lac in vicinity to that location was exchanged with less basic or non-polar amino acids (histidine, phenylalanine and leucine). Phenylalanine was chosen because the high potential *Trametes hirsuta* laccase (*Th*Lac) and *Trametes pubescens* laccase (*Tp*Lac) show it in the equivalent amino acid sequence position (Frasconi et al., 2010; Galhaup et al., 2002). The mutants were created to test if by reducing the positive charge of the environment the chloride ion could be influenced which might change the Cl^- inhibition.

Most of the site-directed mutagenesis of *Ba*Lac cDNA was conducted according to the *Dpn*I method (Table 3.1). In those cases where no correctly mutated PCR product could be obtained with that method or not sufficient amounts of it the more solid but also more complex four primer method was used (Table 3.2). The results of *Pichia pastoris* electroporation with the mutated *Ba*Lac cDNAs can be seen in Table 3.3 and Table 3.4. Colonies which showed a green halo after 2-4 days were considered positive. This was the case for all mutated enzymes except for *Ba*Lac R129L. An amino acid sequence of *Ba*Lac *wt* cDNA with all mutated positions is given in the appendix in Figure A.2.

Table 3.1: Site directed mutagenesis, *Dpn*I method

Mutant	Primers	Template	T_a [℃]
BaLR129H	5BaLR129H + 3BaLR129H	pBan2	67
BaLD273A	5BaLD273A + 3BaLD273A	pBan2	58
BaLD273N	5BaLD273N + 3BaLD273N	pBan2	54
BaLD455A	5BaLD455A + 3BaLD455A	pBan2	58
BaLD455N	5BaLD455N2 + 3BaLD455N2	pBan2	55
BaLE534A	5BaLE534A + 3BaLE534A	pBan2	67
BaLE534Q	5BaLE534Q + 3BaLE534Q	pBan2	58

Table 3.2: Site directed mutagenesis, four primer method

Mutant		Primers	Template	T_a [℃]
*Ba*Lac R129F	PCR1a	3BaLR129F2 + 5BPmlI	pBan2	50
	PCR1b	5BaLR129F3 + 3BAxbaI	pBan2	50
	PCR2	5BPmlI + 3BAxbaI	PCR products from PCR1a and PCR1b	58
*Ba*Lac R129L	PCR1a	3BaLR129L2 + 5BPmlI	pBan2	50
	PCR1b	5BaLR129L2 + 3BAxbaI	pBan2	50
	PCR2	5BPmlI + 3BAxbaI	PCR products from PCR1a and PCR1b	58

Table 3.3: In *Pichia pastoris* expressed NaCl tolerance *Ba*Lac mutants

Amino acid position	Replaced triplette	Mutant triplet	Mutant name	BMM test
129	CGT (Arginine)	CAT (Histidine)	*Ba*Lac R129H	Positive
		TTT (Phenylalanine)	*Ba*Lac R129F	Positive
		CTT (Leucine)	*Ba*Lac R129L	Very weak green halo started to develop after about 7 days

Table 3.4: In *Pichia pastoris* expressed T1 copper redox-potential *Ba*Lac mutants

Amino acid position	Replaced triplette	Mutant triplet	Mutant name	BMM test
273	GAC (Aspartic Acid)	GCC (Alanine)	BaLac D 273A	Positive
		AAC (Asparagine)	BaLac D 273N	Positive
455	GAT (Aspartic Acid)	GCT (Alanine)	BaLac D 455A	Positive
		AAT (Asparagine)	BaLac D 455N	Positive
534	GAG (Glutamic Acid)	GCT (Alanine)	BaLac D 534A	Positive
		CAG (Glutamine)	BaLac D 534Q	Positive

3.2 High throughput enzyme activity screening

Redoxtitration for determination of the T1 redox potential of *Ba*Lac *wt* and mutants could not be established within the timeframe of this work. Therefore *Ba*Lac *wt* and the site directed mutants listed in Table 3.5 were tested for enzymatic activity and pH activity optima in order to do a pre-selection of promising mutants. Figure 3.1 and Figure 3.2 show the position of those site directed mutations within the enzyme. Mutants with higher pH optima and/or higher enzymatic activities than the wild type *Ba*Lac were looked for. This was done by

heterologous expression with *Pichia Pastoris* in 96-deep well plates and subsequently testing the enzyme containing supernatants for activity with ABTS and 2,6-DMP in 96-well plate assays at standard conditions (Figure 3.3). A number of *Ba*Lac 505 mutant screenings were repeated and additionally tested with guaiacol and catechol as substrate (Figure 3.4) as their results showed excessive variations in the first screening. All mutant activities were set into relation to the determined wild type activities with the respective substrate.

While activities relative to the wild-type depended largely on the used enzyme and not so much on the substrate in these screenings some mutants of *Ba*Lac I505 showed also significant differences depending on the substrate. *Ba*Lac I505W exhibited the strongest change in substrate specificity with little activity left with all tested phenolic substrates compared to the wild type. Also *Ba*Lac I505M and S showed little activity with guaiacol and catechol but not with the phenolic substrate 2,6-DMP.

pH profiles with ABTS and 2,6-DMP from pH 4 - 7.5 were measured for all mutants except for some which had shown only very low activities compared to the *Ba*Lac wild type. To manage the high number of mutants standard 96-well plate high throughput assays were conducted. The aim was to identify *Ba*Lac mutants with a shifted pH optimum closer to neutral pH. Those that had their optimum with 2,6-DMP at pH 4.5 or higher are shown in Figure 3.5. A complete list of screened pH profiles can be found in the appendix (Figure A.3, Figure A.4 and Figure A.5). For *Ba*Lac L513F1 and *Ba*Lac I505W activity with 2,6-DMP was too low for measuring a pH profile. The same was the case for *Ba*Lac I505D which could be measured separately in a conventional standard assay however.

In the pH profile assays with 2,6-DMP as substrate *Ba*Lac I505S, I505D and I505N were identified as the mutants with the highest pH optimum which was at pH 6.5. Also *Ba*Lac L513M showed a strongly changed profile with 40% remaining relative activity at pH 7. ABTS on the other side lead to substantially different results than 2,6-DMP with no mutant having a higher pH optimum than the wild type *Botrytis aclada* laccase. Some like the I505 mutants even showed lower relative activities with ABTS than the wild type.

Table 3.5: *Ba*Lac mutations (including those newly created in this work) screened in high throughput activity screening.

T1 copper redox potential mutants				
Amino acid position	Exchanged amino acid	Mutant amino acid	Mutant name	Short name
273	Aspartic acid	Alanine	*Ba*Lac D273A	273A
		Asparagine	*Ba*Lac D273N	273N
455	Aspartic Acid	Alanine	*Ba*Lac D455A	455A
		Asparagine	*Ba*Lac D455N	455N
528	Isoleucine	Alanine	*Ba*Lac I505A	505A
		Cysteine	*Ba*Lac I505C	505C
		Aspartic acid	*Ba*Lac I505D	505D
		Phenylalanine	*Ba*Lac I505F	505F
		Histidine	*Ba*Lac I505H1	505H1
		Lysine	*Ba*Lac I505K	505K
		Leucine	*Ba*Lac I505L	505L
		Methionine	*Ba*Lac I505M	505M
		Asparagine	*Ba*Lac I505N	505N
		Serine	*Ba*Lac I505S	505S
		Valine	*Ba*Lac I505V	505V
		Tryptophan	*Ba*Lac I505W	505W
534	Glutamic acid	Alanine	*Ba*Lac E534A	534A
		Glutamine	*Ba*Lac E534Q	534Q
536	Leucine	Phenylalanine	*Ba*Lac L513F1	513F1
		Phenylalanine	*Ba*Lac L513F2	513F2
		Histidine	*Ba*Lac L513H1	513H1
		Methionine	*Ba*Lac L513M	513M

Direct Electron Transfer pathway mutants				
Amino acid position	Exchanged Amino acid	Mutant Amino acid	Mutant name	Short name
404	Tryptophan	Alanine	*Ba*Lac W373A	373A
		Phenylalanine	*Ba*Lac W373F1	373F1
		Histidine	*Ba*Lac W373H	373H
		Tyrosine	*Ba*Lac W373Y	373Y
459	Phenylalanine	Alanine	*Ba*Lac F427A	427A
		Cysteine	*Ba*Lac F427C	427C
461	Isoleucine	Alanine	*Ba*Lac I429A	429A
		Phenylalanine	*Ba*Lac I429F	429F
		Histidine	*Ba*Lac I429H	429H
		Glutamic acid	*Ba*Lac I429E	429E
		Glutamine	*Ba*Lac I429Q	429Q
462	Tryptophan	Alanine	*Ba*Lac W430A	430A
		Cysteine	*Ba*Lac W430C	430C

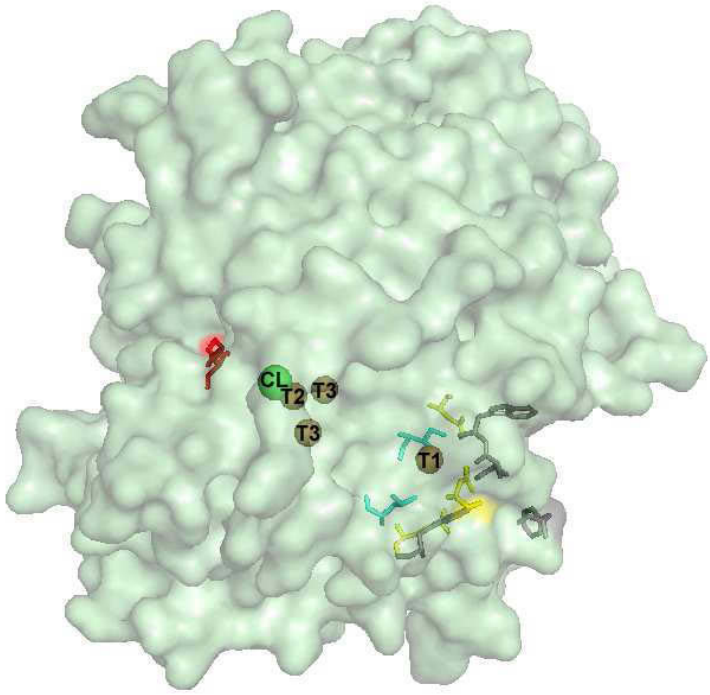

Figure 3.1: *Ba*Lac *wt* structure model visualized with PyMOL(TM) Molecular Graphics System, Version 1.3. (Schrodinger, USA) with targeted amino acids for mutation being marked (red: salt tolerance mutation, yellow and cyan: T1 copper redox potential mutations, grey: direct electron transfer pathway mutations).

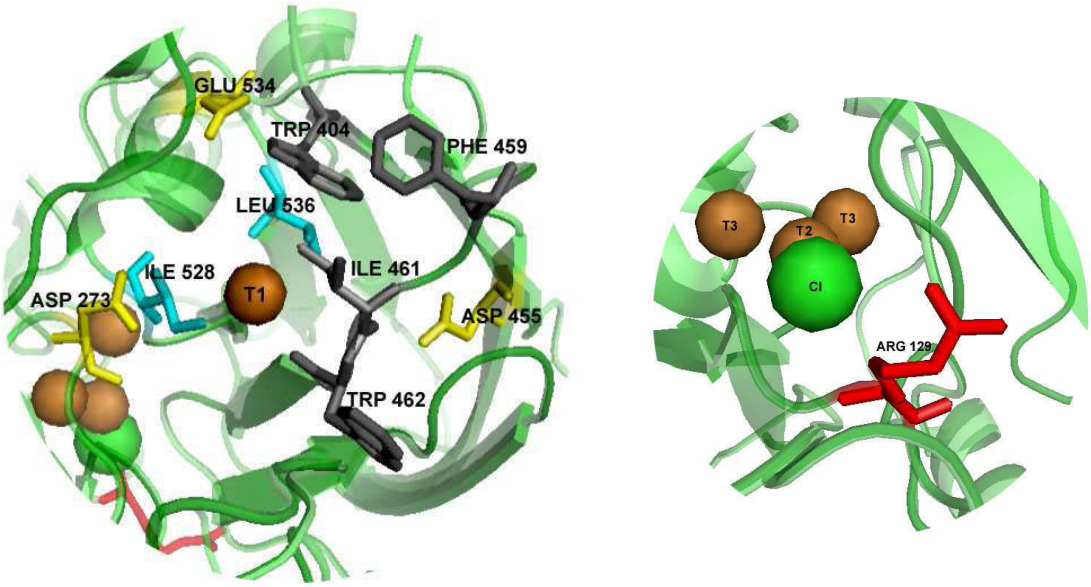

Figure 3.2: *Ba*Lac *wt* structure model details visualized with PyMOL(TM) Molecular Graphics System, Version 1.3. (Schrodinger, USA) with targeted amino acids for mutation being marked (red: salt tolerance mutation, yellow and cyan: T1 copper redox potential mutations, grey: direct electron transfer pathway mutations)

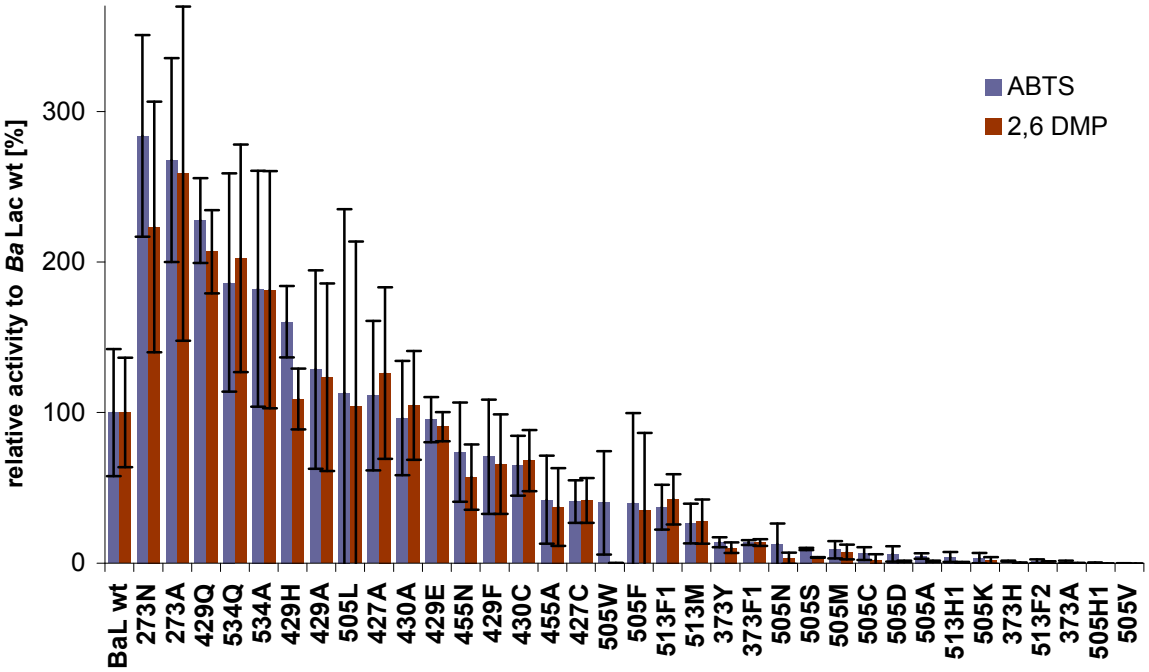

Figure 3.3: Results of *Ba*Lac mutants high throughput activity assays in 96 well plates at standard conditions (with 0.5 mM ABTS, 1 mM 2,6-DMP) using pipetting robot and plate reader

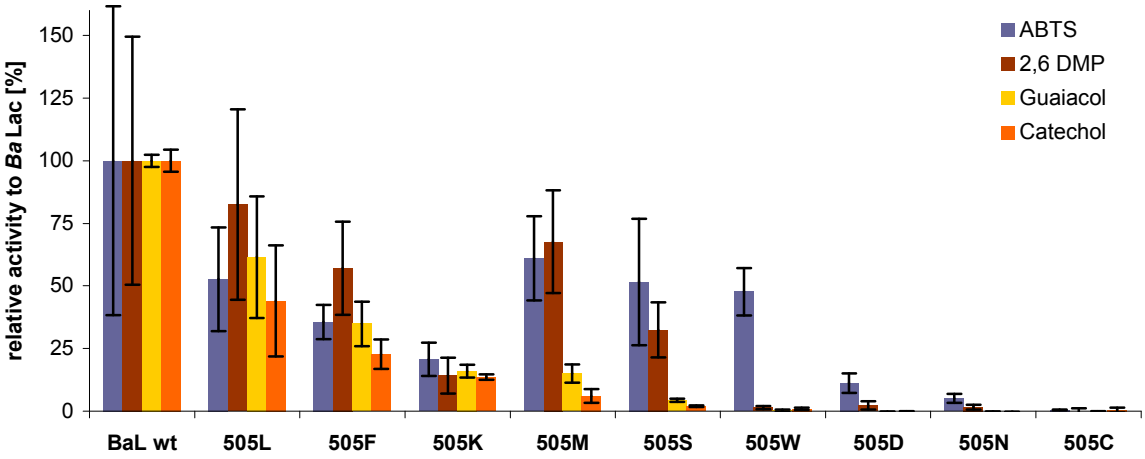

Figure 3.4: Results of *Ba*Lac 505 mutants high throughput activity assays in 96 well plates at standard conditions (with 0.5 mM ABTS, 1 mM 2,6-DMP, 1 mM guaiacol, 10 mM catechol) using pipetting robot and plate reader

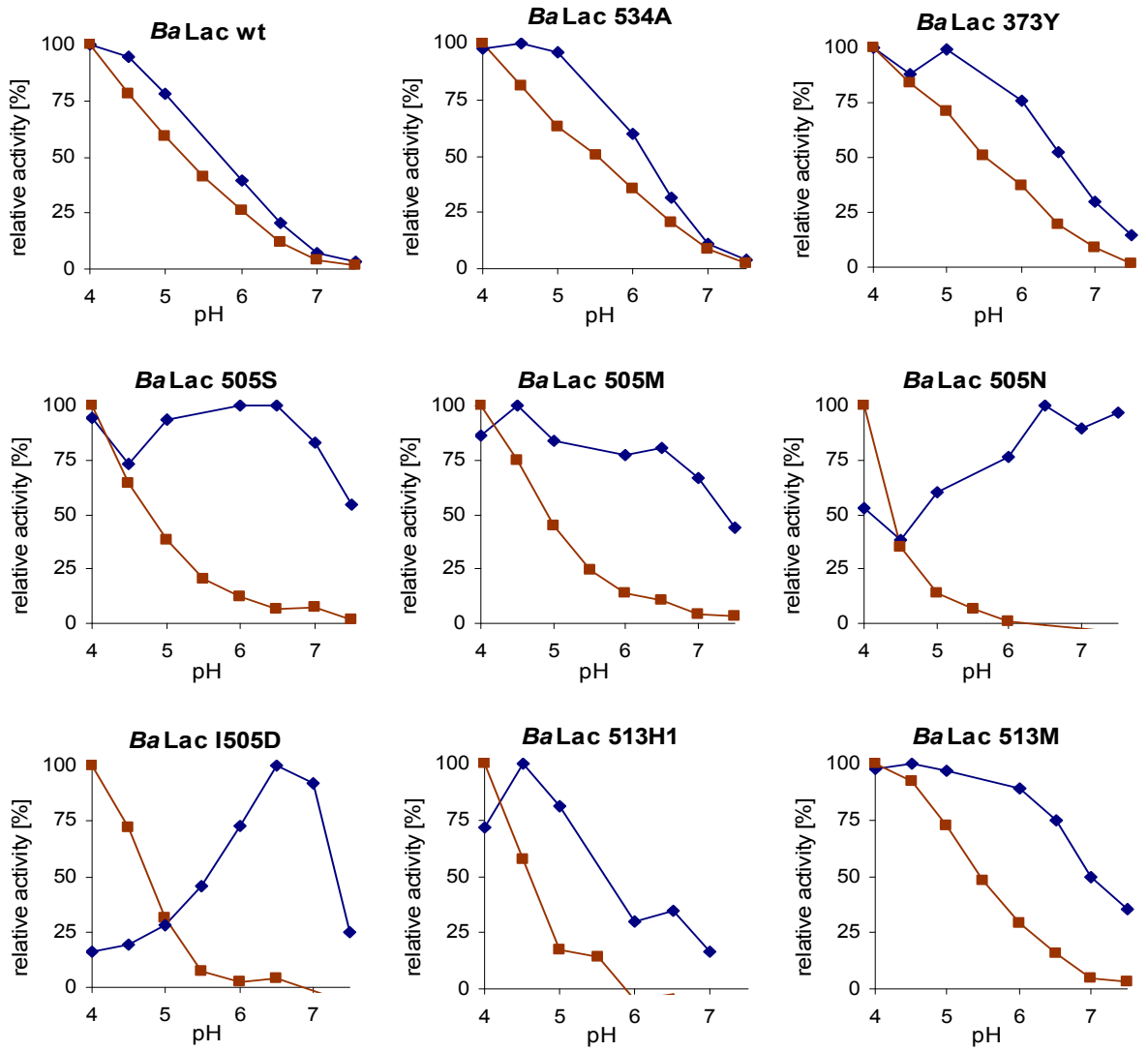

Figure 3.5: *Ba*Lac *wt* compared to mutants in standard high throughput assays with 0.5 mM ABTS (■) and 0.2 mM 2,6-DMP (♦) in citrate buffer (pH 4-5.5, 100 mM) and citrate-phosphate buffer (pH 6-7.5, 100 mM). *Ba*Lac I505D with 2,6-DMP was measured separately in a conventional standard pH profile assay.

3.3 Heterologous expression and purification of BaLac

Shaking flask fermentations

From the NaCl tolerance mutant laccases *Ba*Lac R129F and R129H and from the T1 redox potential mutants *Ba*Lac I505N and L513M were selected for small scale methanol induced heterologous expression in *Pichia pastoris* in shaking flasks. The fermentation was conducted for each mutant in duplicates as described in the method section. However except for *Ba*Lac I505N, OD_{600} was measured as cell density indicator instead of wet cell mass. Due to the low protein concentrations the Bradford assay did not deliver reliable results. Therefore specific activity could not be determined before the enzyme solution was concentrated. Instead the development of fermentation and downstream processing was monitored by

determining the volumetric activity. To reduce the risk of contamination during the first fermentation round only one of the duplicates was monitored. In case of *Ba*Lac R129F the monitored one was contaminated. Data from the non contaminated flask was collected from the 5th day onwards. In the *Ba*Lac 505N fermentation both flasks were monitored and average values were calculated. Figure 3.6 shows the progression of *Pichia pastoris* fermentation, mutant laccase expression and secretion into the supernatant. The biomass developed in all cases similar except for the *Ba*Lac I505N fermentation which showed about 50% higher biomass concentration than the others. Whereas the two salt tolerance mutants lead to similar results, BaL I505N had the lowest volumetric activities and *Ba*Lac L513M achieved more than 5 times higher volumetric activities than the other supernatants.

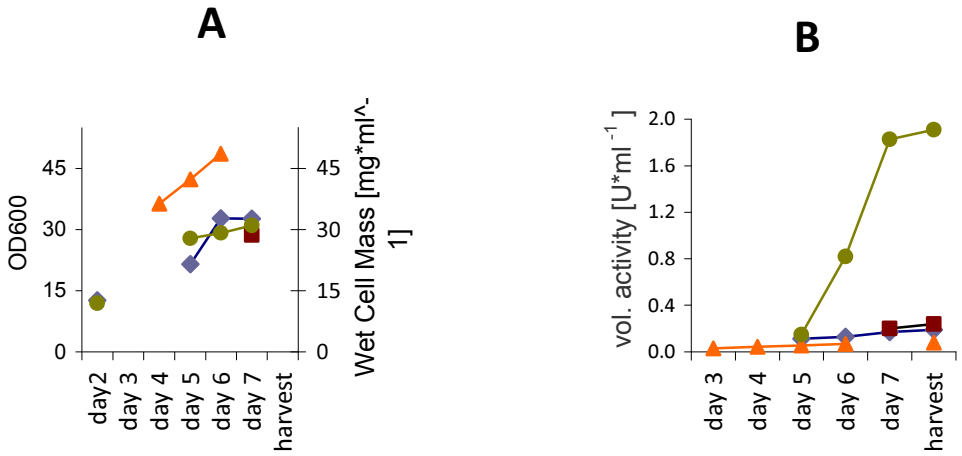

Figure 3.6: (A) Monitoring of cell density in shaking flask fermentation. For *Ba*Lac R129H (♦), *Ba*Lac R129F (■) and *Ba*Lac L513M (●) OD600 was measured and for *Ba*Lac I505N (▲) the wet cell mass. (B) Development of volumetric activity during fermentation of *Ba*Lac R129H (♦), *Ba*Lac R129F (■), *Ba*Lac L513M (●) and *Ba*Lac I505N (▲). The BaLac I505N fermentation was harvested already after 6 days.

The harvested supernatant was purified in a one step Hydrophobic Interaction Chromatography (Phenyl-Source column) and concentrated. A purification scheme is shown in Table 3.6. The specific activities of the final and concentrated enzyme solutions are given in Table 3.7. Only the final specific activities could be determined and not their development during purification. The purification of the two salt tolerance mutants led to very different outcomes. While the highest specific activity was achieved with *Ba*Lac R129F (58.84 U*mg^{-1}), the one of *Ba*Lac R129H was less than 1% of that. Also the total and volumetric activities of *Ba*Lac R129H were about 20 times lower. Most of the total activity of *Ba*Lac R129H was lost during the Hydrophobic Interaction Chromatography. *Ba*Lac I505N had a high remaining total activity after purification and higher total and volumetric activities than *Ba*Lac R129F but at the same time its final specific activity was 10 times lower (5.88 U*mg^{-1}). *Ba*Lac L513M had the largest total activity at harvest but lost more than 95%

of it mostly during Hydrophobic Interaction Chromatography. Final specific activity was with 31.65 U*mg^{-1} about half of what could be achieved with *Ba*Lac R129F.

Table 3.6: Purification scheme of harvested *Pichia pastoris* supernatant of *Ba*Lac R129H, *Ba*Lac R129F, *Ba*Lac L513M and *Ba*Lac I505N shaking flask fermentations.

	***Ba*Lac L513M**		***Ba*Lac I505N**		***Ba*Lac R129H**		***Ba*Lac R129F**	
	Total activity [U]	Vol. activity [U*ml^{-1}]	Total activity [U]	Vol. activity [U*ml^{-1}]	Total activity [U]	Vol. activity [U*ml^{-1}]	Total activity [U]	Vol. activity [U*ml^{-1}]
Harvest	1661.16	2.29	43.06	0.10	120.38	0.23	74.30	0.29
$(NH_4)_2SO_4$ precipitation	1309.12	1.44			110.88	0.17	65.79	0.20
HIC (phenyl-source)	155.93	3.90	41.08	0.37	2.52	0.08	23.10	0.92
Concentration	58.91	39.28	35.95	24.79	0.09	0.09	19.92	18.11

Table 3.7: Final enzyme specifications after downstream processing of *Pichia pastoris* supernatant from shaking flask fermentation.

Laccase mutant	Volumetric activity [U*ml^{-1}]	Protein concentration [mg*ml^{-1}]	**Specific activity [U*mg^{-1}]**	**Total activity [U]**
***Ba*Lac R129H**	0.09	0.27	**0.34**	**0.09**
***Ba*Lac R129F**	18.11	0.31	**58.84**	**19.92**
***Ba*Lac I505N**	24.80	4.22	**5.88**	**35.95**
***Ba*Lac L513M**	39.28	1.24	**31.65**	**58.91**

0.5 L Multifors bioreactor

*Ba*Lac L513M was produced in methanol induced *Pichia pastoris* fermentation in a 0.5 L fermenter (see 2.3.2). In Figure 3.7 the progression of the fermentation is shown. After induction at the 70th hour measured volumetric activity increased to a level of finally above 15 U*ml^{-1} at harvest.

The harvested supernatant was purified similarly to the shaking flask supernatants, a 2 step HIC procedure was used however. Table 3.8 shows the purification scheme. The purification of secreted *Ba*Lac L513M increased specific activity more than three fold. During concentrating and buffer changing activity was lost however leading approximately to an overall doubling of specific activity when comparing the final enzyme solution with the harvested supernatant. The final results of the production of *Ba*Lac L513M are also listed in Table 3.8. The achieved specific activity was about 50% higher than the best result of the

shaking flask fermentations with following purification and the overall output was about 20 times of the most productive shaking flask fermentation. Furthermore the loss in total activity during purification and concentration was considerably lower with about 25% remaining total activity.

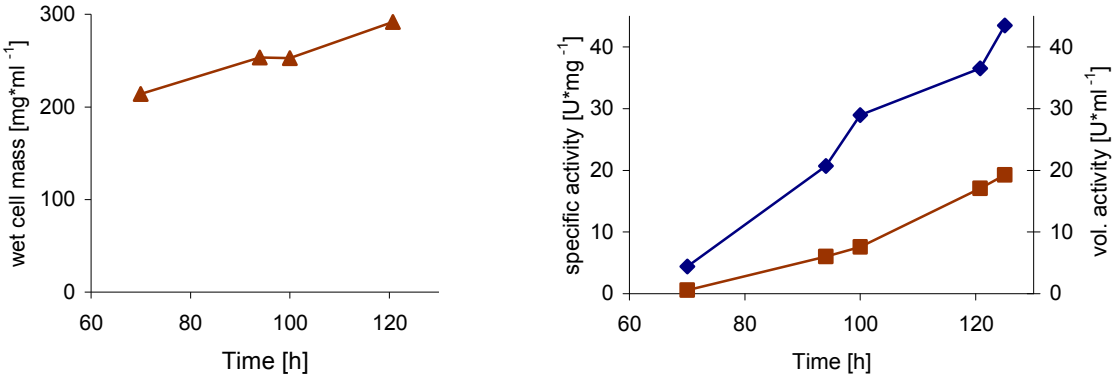

Figure 3.7: Progression of *Ba*Lac L513M expression in 6-force fermentor. Acquired data for wet cell mass (▲), volumetric activity (■) and specific activity (♦) are given.

Table 3.8: Purification scheme of *Ba*Lac L513M from *Pichia pastoris* supernatant from 0.5 L Multifors bioreactor

***Ba*Lac L513M**						
	Protein conc. [mg*ml^{-1}]	**Vol. activity [U*ml^{-1}]**	**Specific activity [U*mg^{-1}]**	**Total activity [U]**	**Yield [%]**	**Purification factor**
Culture supernatant	0.44	19.26	43.48	3371	100	1.0
$(NH_4)_2SO_4$ (to 40% sat.)	0.26	8.09	30.90	2550	76	0.7
1st HIC (Phenyl-Sepharose)	0.14	12.57	88.15			2.0
2nd HIC (Phenyl-Source)	1.25	176.44	141.66	1191	35	3.3
Concentration	**12.97**	**1146.24**	**88.37**	**802**	**24**	**2.0**

3.4 *Characterization of Ba*Lac

3.4.1 General *Ba*Lac kinetics

The produced *Ba*Lac mutants and *Ba*Lac *wt* were tested for substrate specificity at standard assay conditions. The wild type was also exposed to different acidic pH environments to observe possible pH dependency of the substrate specificity. k_{cat} values were calculated from all test rows. As can be seen in Table 3.9 *Ba*Lac *wt* exhibited catalytic turnover rates in the range of 2.3 - 26.5 s^{-1} and the substrate specificity was the highest for 2,6-DMP and ABTS.

Figure 3.8 shows that at rising pH K_m-values of *Ba*Lac *wt* decreased for 2,6-DMP and guaiacol whereas it increased for ABTS.

Table 3.9: K_m-value assay of *Ba*Lac *wt* with 2,6-DMP, ABTS and guaiacol at pH 3-6 (100 mM citrate buffer pH 3-5, 100 mM citrate-phosphate buffer pH 6) and catechol at pH 4.

BaLac wt	**ABTS**	**K_m [µM]**	**k_{cat} [s^{-1}]**	**k_{cat}/K_m [s^{-1} mM^-1]**
	pH 3	2.66	26.47	9949
	pH 4	3.55	18.92	5336
	pH 5	7.75	11.31	1460
	pH 6	7.19	8.86	1232
Ba*Lac *wt	**2,6-DMP**			
	pH 3	19.17	9.29	485
	pH 4	4.52	4.23	936
	pH 5	1.83	4.57	2501
	pH 6	1.94	3.71	1910
Ba*Lac *wt	**Catechol**			
	pH 4	219.74	23.22	106
Ba*Lac *wt	**Guaiacol**			
	pH 3	343.56	2.32	6.76
	pH 4	72.27	2.12	29.28
	pH 5	49.11	1.65	33.68
	pH 6	60.54	0.84	13.91

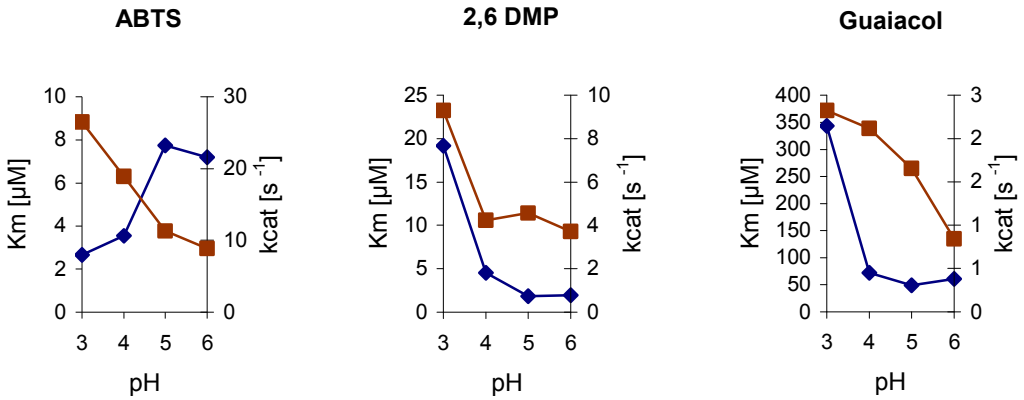

Figure 3.8: Correlation between K_m (♦) respectively k_{cat} (■) and the pH value in kintec assays of *Ba*Lac *wt* with 2,6-DMP, ABTS and guaiacol.

The gathered K_m values of the two produced T1 copper redox potential mutants and the two NaCl tolerance mutants differed largely from each other (Table 3.10). The NaCl tolerance mutants exhibited similar substrate specificity as the wild type. *Ba*Lac R129F also had comparable turnover rates but *Ba*Lac R129H was less active. On the other side the two T1 redox potential mutant laccases were 4 to 100 fold less specific and also less active with

tested substrates except for *Ba*Lac L513M with 2,6-DMP and ABTS where equal or higher turnover rates than the wild type were observed.

Table 3.10: K_m-values of *Ba*Lac mutants with 2,6-DMP, ABTS, guaiacol and catechol at pH 4 (100 mM citrate buffer)

pH 4	Substrate	K_m [µM]	k_{cat} [s^{-1}]	k_{cat}/K_m [s^{-1} $mM^{\wedge-1}$]
Ba*Lac *wt	2,6-DMP	4.52	4.23	936
	ABTS	3.55	18.92	5336
	Guaiacol	72.27	2.12	29.28
	Catechol	219.74	23.22	106
***Ba*Lac L513M**	2,6-DMP	94.10	4.68	49.76
	ABTS	18.42	34.58	1877.31
	Guaiacol	7512	3.18	0.42
	Catechol	5560	9.70	1.74
***Ba*Lac I505N**	2.6 DMP	2001	0.15	0.07
	ABTS	590	0.41	0.69
***Ba*Lac R129H**	2,6-DMP	4.0	1.11	276.61
	Guaiacol	106.6	1.20	11.26
***Ba*Lac R129F**	2,6-DMP	6.4	4.07	635.96
	Guaiacol	170.0	3.30	19.41

The produced *Ba*Lac mutants and the wild type were also tested in standard assays for pH dependency of enzyme activity with 2,6-DMP in a pH range from 2.5 to 8 (Figure 3.9). *Ba*Lac R129F and the wild type were almost identical in their behavior and showed an optimum below pH 4. *Ba*Lac R129H was even more sensitive to higher pH values than these two. Both other mutants that were selected for their deviant pH optimum confirmed the results of the screening experiments. *Ba*Lac L513M exhibited a bell activity curve with an optimum around pH 5 and a remaining activity of 40% at pH 7. *Ba*Lac I505N had its highest activity at a neutral pH before it rapidly declined in alkaline environments.

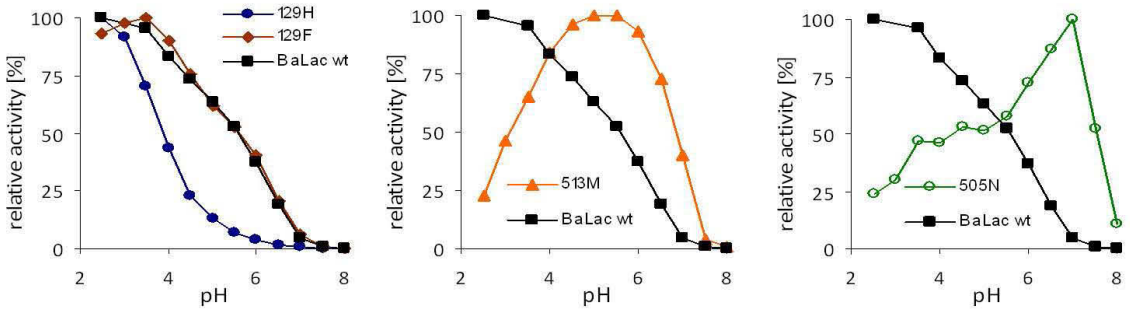

Figure 3.9: Activity assay pH profile with 2,6-DMP (0.2 mM) with purified and concentrated enzymes from shaking flask fermentation (*Ba*Lac R129H (●), *Ba*Lac R129F (♦), *Ba*Lac L513M (▲) and *Ba*Lac I505N (○)). The pH profile of *Ba*Lac wild type (■) with 2,6-DMP is shown as reference.

3.4.2 Temperature dependency of *Ba*Lac activity

For the *Botrytis aclada* laccase wild type a temperature profile with ABTS was established in assays which were apart from the temperature variations conducted at standard conditions (Figure 3.10). The curve was calculated with a third order polynomial function and the temperature optimum was found to be 43℃. At physio logic conditions of 37℃ 92% of the maximal activity could be achieved. Within the measured temperature range the relative activity was below 75% only at temperatures above 53℃.

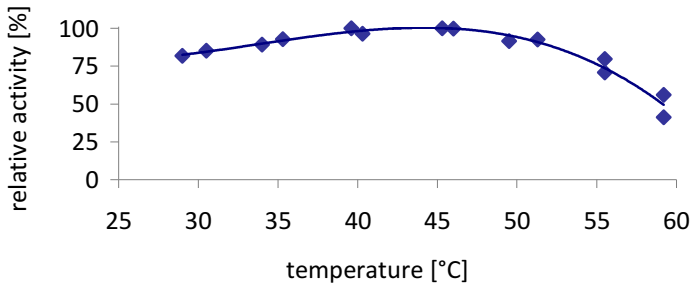

Figure 3.10: *Ba*Lac *wt* temperature optimum

3.4.3 *Ba*Lac stability

Temperature and pH dependency of enzyme stability

For the stability tests *Ba*Lac *wt* with protein concentration of 16.3 µg*ml^{-1} was used. Storage temperatures of 4, 21, 37, 45, 55 and 65℃ were tes ted and for the lower three temperatures the influence of storage buffer solutions from pH 4.5 to 7.5 was observed. Activity was measured in standard ABTS assays and a 3 variable hyperbolic decay function was chosen to describe the development of enzyme activity (Figure 3.11 and Figure 3.12). The stability rapidly decreased at a pH higher than 7.5. The highest enzyme stabilities were measured at pH 4.5 - 5.5. The $t_{1/2}$ in the most stable environment tested (4℃, pH 4.5) was 8 days. At a physiologic temperature no sample showed a $t_{1/2}$ longer than 5 hours and at higher temperatures $t_{1/2}$ was even less than half an hour.

In contrast to these results *Ba*Lac *wt* stored at stock concentrations of 25.4 mg*ml^{-1} in pH 5.5 citrate buffer (100 mM) with $(NH_4)_2SO_4$ (50 mM) at 4℃ had after 3 months still 2/3 of its initial activity left (standard ABTS assay). When stored in the same environment for the same time but at -80℃ only 12% of the initial activity was l ost.

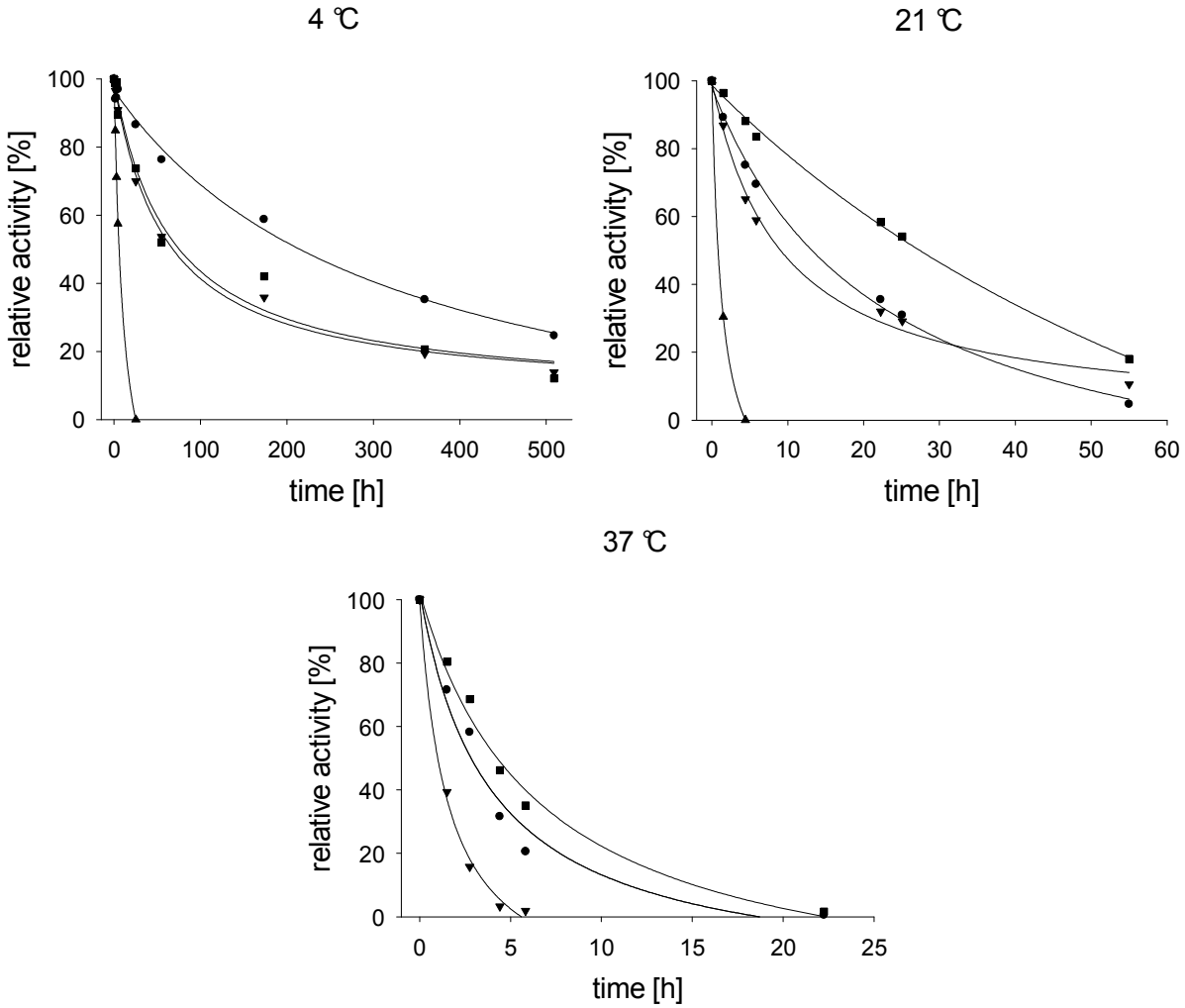

Figure 3.11: Enzyme stability with 100 mM citrate buffer at pH 4.5 (●), 5.5 (■), 100 mM citrate phosphate buffer at pH 6.5 (▼), 7.5 (▲) and storage temperatures of 4℃, 21℃ and 37℃.

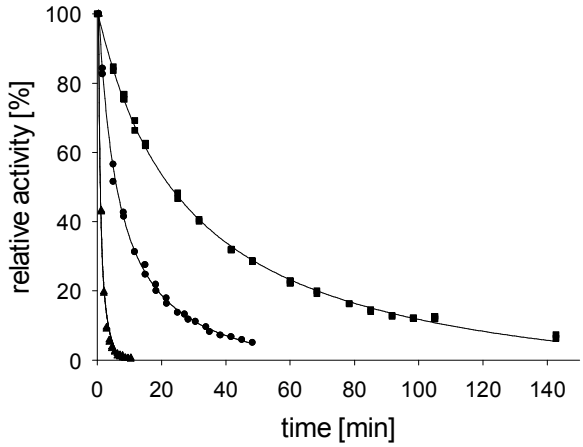

Figure 3.12: Enzyme stability at pH 4.0 (100 mM citrate buffer) and storage temperatures of 45℃ (■), 55℃ (●) and 65℃ (▲).

Inactivation by solvents

Solvent dependent enzyme inactivation assays were conducted with *Ba*Lac *wt* and 0 – 50% ethanol and methanol, respectively (Figure 3.13). After 20 h at 4℃ activity decreased significantly at ethanol concentrations higher than 10% and at methanol concentrations higher than 30%.

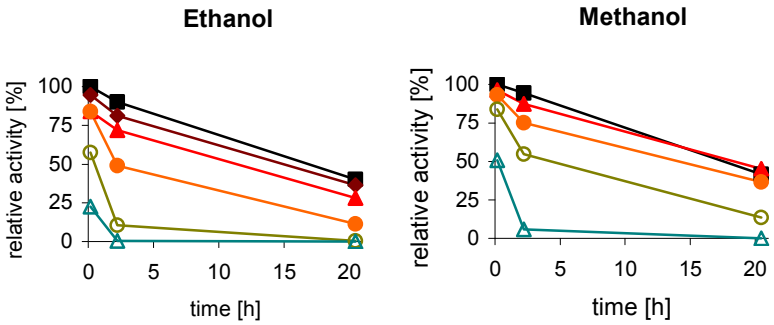

Figure 3.13: Inactivation of *Ba*Lac *wt* stored in ethanol and methanol (0% (■), 10% (♦), 20% (▲), 30% (●), 40% (○), 50% (Δ)) at pH 5 (100 mM citrate buffer).

Inactivation by redox polymers

In the initial enzyme inactivation assay *Ba*Lac *wt* was tested with two Os-modified anodic polymers, p009-p91 and p405. As can be seen in Figure 3.14 A activity rapidly declined. Within 90 minutes less than 10% of activity relative to the reference was left.

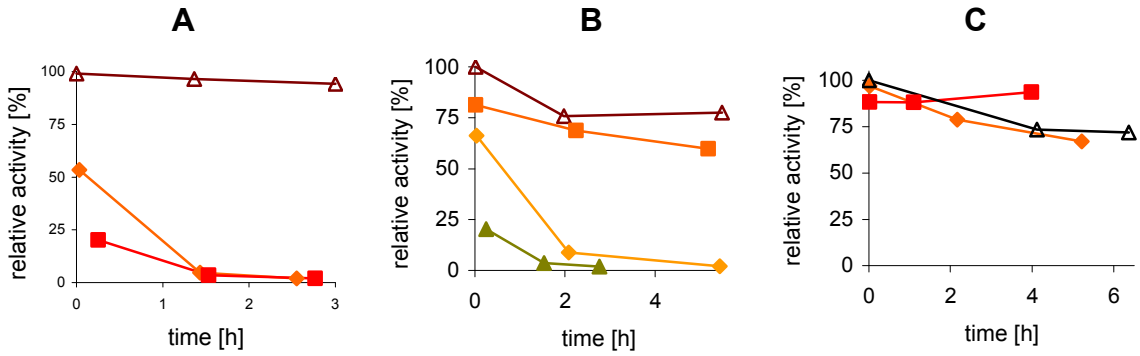

Figure 3.14: Enzyme stability in solution with Os-modified anodic redox polymers at pH 4 (citrate buffer 100 mM) and room temperature. Reference was enzyme in buffer only (Δ) and all activities are in relation to its initial activity (**A**) Inactivation of *Ba*Lac *wt* by Os-modified anodic polymers p009-p91 (♦) and p405-p91 (■). (**B**) Inactivation of *Ba*Lac *wt* by Os-complex p91 alone (■), non modified polymer backbone of p405 (♦) and Os-modified polymer p405 (▲) **(C)** Inactivation of *Th*Lac *wt* by Os-modified anodic polymers p009-p91 (♦) and p405 (■)

In order to investigate the reasons for this another inactivation assay with *Ba*Lac *wt* was conducted with non modified polymer backbone of p405 and the Os-complex p91 alone (Figure 3.14 B). Also the non modified polymer backbone led to a similar rapid inactivation as

the modified polymer. However Os-complex p91 alone did not cause activity to fall under ¾ of the reference within 5 hours. Another test was aimed at showing the effect of anodic polymers on other laccases. *Trametes hirsuta* laccase (*Th*Lac *wt*) was therefore incubated with p009-p91 and p405 (Figure 3.14 C) and the activity never fell below 90% of the reference over the entire observed time.

In order to acquire further information about the effect Os-modified anodic polymers have on *Botrytis aclada* laccase *wt* an inactivation assay was conducted with the Os-modified cathodic polymers p002b-p91 and p004b-p91 at pH 5. These caused a more moderate decrease in enzyme activity over time than the anodic ones (Figure 3.15). No immediate effect could be observed unlike in the assays with p009-p91 and p405-p91. After 5 hours still at least 1/3 of the activity was left relative to the remaining activity of the reference.

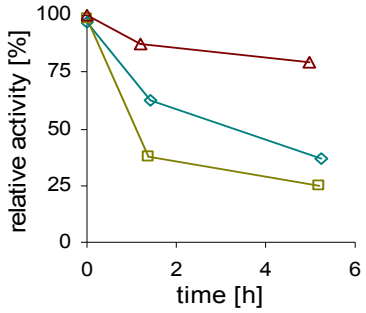

Figure 3.15: *Ba*Lac *wt* stability in solution at pH 5 (citrate buffer 100 mM) with Os-modified cathodic redox polymers p002b-p91 (◊) and p004b-p91 (□) at room temperature with reference of *Ba*Lac *wt* in buffer only (Δ)

As a consequence of the assays above a new Os-modified polymer, p011-p91, was synthesized which featured a non-charged backbone. In Figure 3.16 A the inactivation assay with *Ba*Lac *wt* and *Th*Lac *wt* with p011-p91 is shown. Unlike with the other Os-modified polymers, as an immediate effect a higher initial activity was measured with both enzymes relative to the reference. Within the tested time the activity of both enzymes developed similarly to the reference. As Os-modified polymers need covalent binding for film building on a glassy carbon electrode the impact of a potential crosslinker, 2,2′-(Ethylenedioxy) diethanthiol, on *Ba*Lac *wt* stability was observed as well (Figure 3.16 B). A concentration of 0.36% crosslinker was used in the assay. Furthermore a 1:40 dilution of the already mixed assay containing enzyme and crosslinker was created. This dilution had a final concentration of 0.009% and was measured immediately and after more than 5 hours. While the higher concentrated crosslinker caused an inactivation of about 50% in relation to the reference within 90 minutes, once further diluted the extend of the decrease in activity was comparable to the reference.

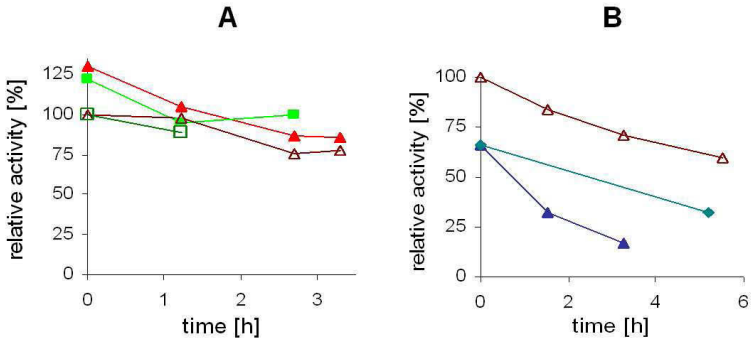

Figure 3.16: **(A)** Comparing *Ba*Lac *wt* (▲)and *Th*Lac *wt* (■) stability in solution at pH 4 (citrate buffer 100 mM) with Os-modified non-charged backbone redox polymers p011-p91. BaLac *wt* (Δ) respectively ThLac *wt* (□) with buffer only served as reference. **(B)** Effect of 2,2′-(Ethylenedioxy)diethanthiol (dithiol-crosslinker) on stability of *Ba*Lac *wt* at pH 4 (citrate buffer 100 mM). 0.36% (▲) and 0.009% dithiol-crosslinker (♦) were tested with BaLac *wt* (Δ) in buffer only as reference.

3.4.4 NaCl tolerance *Ba*Lac mutants

The two NaCl tolerance mutants *Ba*Lac R129F and *Ba*Lac R129H were tested together with *Ba*Lac *wt* in a NaCl inhibition assay with ABTS at standard conditions. NaCl concentrations ranged from 0 to 1 M. It was not possible to measure higher concentrations in this setup as ABTS started to precipitate at NaCl concentrations higher than 1 M. The relative activity curves (activity at 0 M NaCl being 100%) of the NaCl tolerance mutants and of the *Botrytis aclada* laccase *wt* are shown in Figure 3.17. The loss in relative activity of NaCl tolerance mutants and *Ba*Lac wt differed less than 10%.

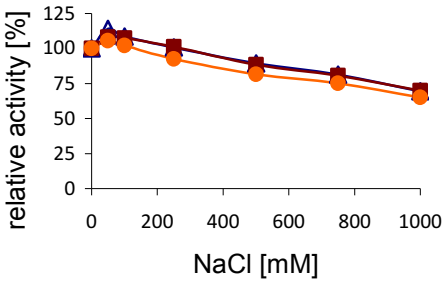

Figure 3.17: Cl- inihibition of *Ba*Lac *wt* (Δ), *Ba*Lac R129H (■) and *Ba*Lac R129F (●) at pH 4

3.4.5 NaCl / NaF inhibition assays

Preliminary conventional Cl^- inhibition assays with *Ba*Lac and 2,6-DMP as substrate showed that the inhibition curve at pH 3 differed substantially from the one at pH 4.5 (Figure 3.18). At pH 4.5 Cl^- had only little effect at standard conditions compared to pH 3.

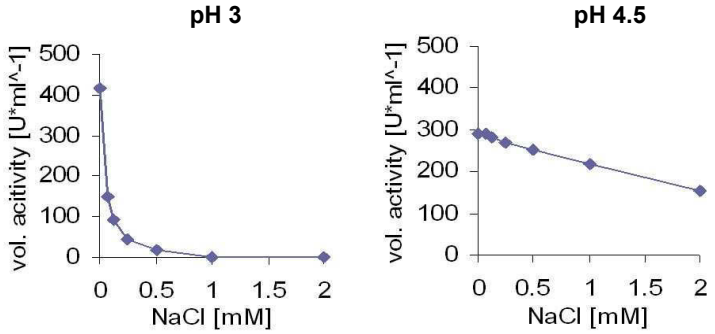

Figure 3.18: Conventional NaCl inhibition assay of *Ba*Lac *wt* with 2.6-DMP at pH 3 and pH 4.5 (citrate buffer 100 mM)

To investigate the pH dependency of inhibition of *Ba*Lac *wt* and *Tp*Lac more closely 96-well plate high throughput assays were conducted. Both enzymes were tested with NaF and NaCl in 96-well plate inhibition assays at pH 3, 4.5 and 6. Substrates used were ABTS, 2,6-DMP and guaiacol. The detailed results are subject of the following subchapters and the numeric raw results are found in the appendix. As Michaelis-Mendten kinetics was not properly describing the received curves the data is presented graphically and discussed as such together with the approximation of K_m values based on Michaelis-Mendten kinetics for a semi quantitative / qualitative assessment of substrate specifity.

Substrate: ABTS

Inhibitor: NaCl

The Cl^- inhibition assays of *Ba*Lac *wt* with ABTS at pH 3, 4.5 and 6 are shown in Figure 3.19 and selected apparent K_m values in Table 3.11. Substrate inhibition was only observed at pH 6 with ABTS concentrations of above 2 mM. Apparent K_m values increased with rising inhibitor concentration and decreased with rising OH^- concentration. v_{max} was dependent on inhibitor concentration at pH 3 but only to a small extend at pH 4.5 and higher. Consequently the inhibiting effect of NaCl was reduced by higher OH^- concentrations.

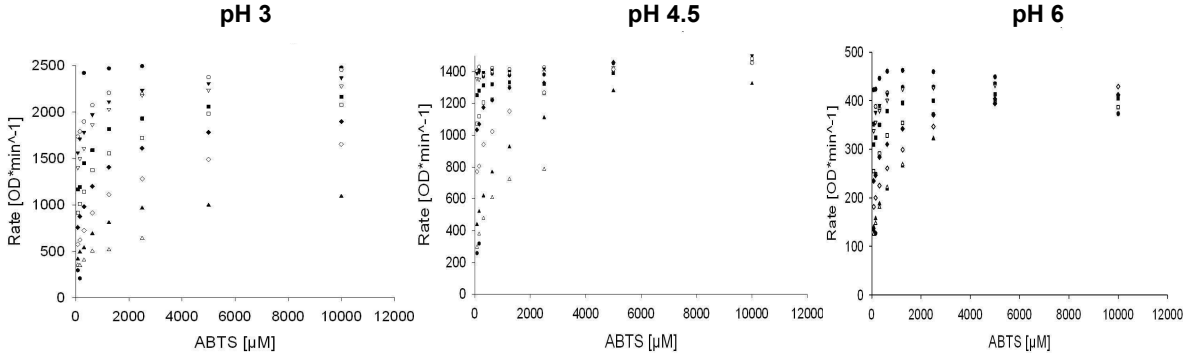

Figure 3.19: 96-well inhibition assay of *Ba*Lac *wt* with ABTS and inhibitor NaCl (0 mM (●), 3.9 mM (○), 7.8 mM (▼), 15.6 mM (▽), 31.3 mM (■), 62.5 mM (□), 125 mM (♦), 250 mM (◊), 500 mM (▲), 1 M (Δ), 2 M (●)) at pH 3, 4.5 and 6.

Table 3.11: Apparent K_m values determined by Michaelis-Mendten regression of individual data sets from 96-well inhibition assay of *Ba*Lac *wt* with NaCl and ABTS at pH 3 and 4.5.

***Ba*Lac *wt* - ABTS**		
NaCl [mM]	**K_m pH 3 [µM]**	**K_m pH 4.5 [µM]**
3.9	34	
250		94
500	206	297

The Cl^- inhibition assay with *Tp*Lac and the substrate ABTS (Figure 3.20 and Table 3.12) lead to similar results as with *Ba*Lac *wt*. However v_{max} was dependent on inhibitor concentration at pH 3-4.5. Furthermore about ten times smaller Cl^- concentrations lead to similar inhibition as with *Ba*Lac *wt*, also K_m values were generally higher and increased more. A slight substrate inhibition was observed at pH 3-6 above 2 mM ABTS.

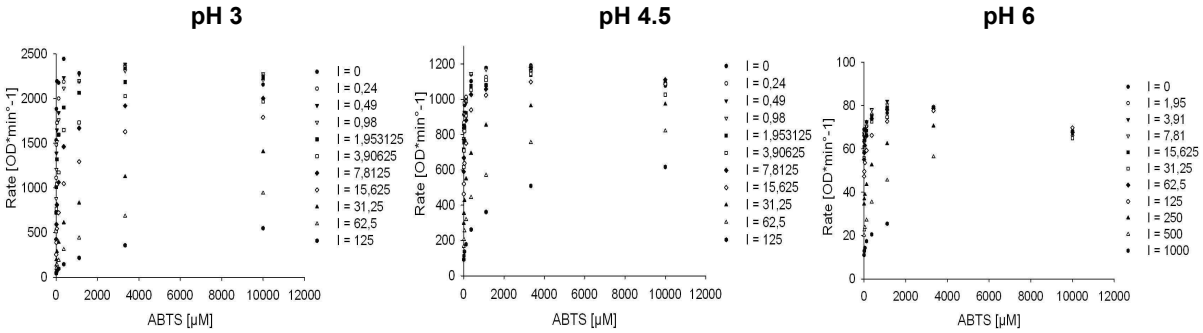

Figure 3.20: 96-well inhibition assay of *Tp*Lac with ABTS and inhibitor NaCl (concentrations given in graph in µM) at pH 3, 4.5 and 6.

Table 3.12: Apparent K_m values determined by Michaelis-Mendten regression of individual data sets from 96-well inhibition assay of *Tp*Lac with NaCl and ABTS at pH 3 and 4.5

***Tp*Lac - ABTS**		
NaCl [mM]	**K_m pH 3 [µM]**	**K_m pH 4.5 [µM]**
0.24	5.8	1.78
3.9	27.9	4.66
125	1764	393

Inhibitor: NaF

Substrate concentration showed no impact on F^- inhibition assays of *Ba*Lac *wt* at pH 3 and 4.5 but it did at pH 6 (Figure 3.21). As the tested ABTS concentrations were not low enough, only v_{max} could be calculated but not K_m which apparently increased however at rising pH. The recognizable v_{max} values varied according to inhibitor concentration. High OH^- concentrations reduced the inhibitory effect of F^-.

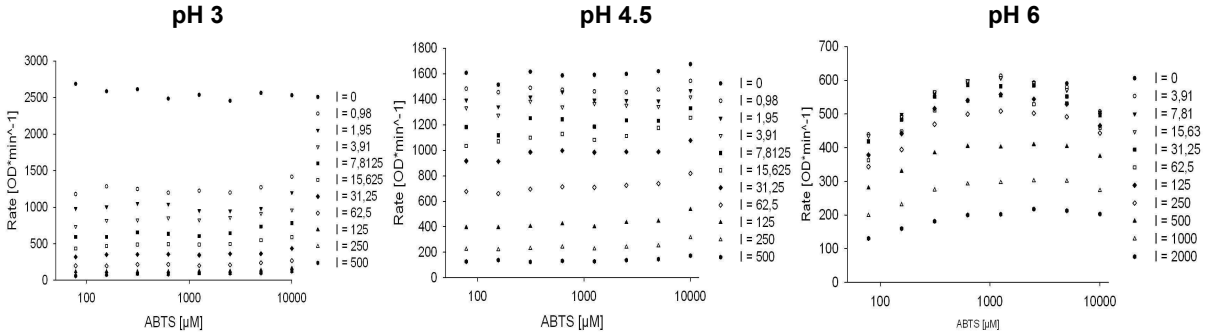

Figure 3.21: 96-well inhibition assay of *Ba*Lac with ABTS and inhibitor NaF (concentrations given in graph in µM) at pH 3, 4.5 and 6.

Substrate: 2,6-DMP and guaiacol

Inhibitor: NaCl

96-well Cl^- inhibition assays of *Ba*Lac *wt* using the substrate 2,6-DMP and guaiacol are depicted in Figure 3.22, Table 3.13, Figure 3.23 and Table 3.14. At pH 3 K_m values as well as v_{max} values depended on the NaCl concentration, whereas guaiacol featured approximately 100 times higher K_m values than 2,6-DMP. At higher pH levels however v_{max} values showed only small variations anymore and K_m values were generally lower and increased to a lesser extend with rising inhibitor concentration. Similar to Cl^- inhibition with ABTS the one with 2,6-DMP was weak from pH 4.5 onwards but differently from it apparent K_m values were lower and less dependent on Cl^- concentration at that pH. At pH 6 no Cl^- inhibition could be identified anymore. Cl^- inhibition with guaiacol was stronger than with 2,6-DMP or ABTS at all tested pH levels and v_{max} dependency on Cl^- concentration largely disappaered only at pH 6. No substrate inhibition was observed with guaiacol but 2,6-DMP concentrations above 2 mM showed some.

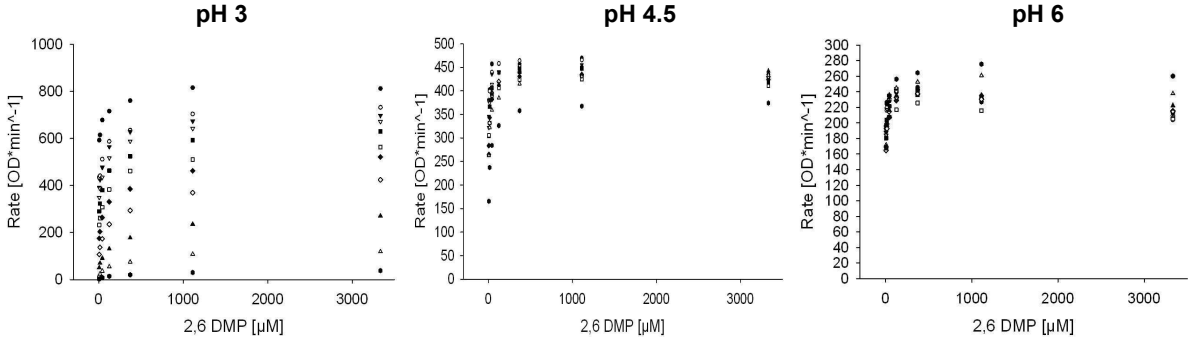

Figure 3.22: 96-well inhibition assay of *Ba*Lac *wt* with 2,6-DMP and inhibitor NaCl (0 mM (●), 3.9 mM (○), 7.8 mM (▼), 15.6 mM (▽), 31.3 mM (■), 62.5 mM (□), 125 mM (♦), 250 mM (◊), 500 mM (▲), 1 M (Δ), 2 M (●)) at pH 3, 4.5 and 6.

Table 3.13: Apparent K_m values determined by Michaelis-Mendten regression of individual data sets from 96-well inhibition assay of *Ba*Lac *wt* with NaCl and 2,6-DMP at pH 3 and 4.5

***Ba*Lac *wt* - 2,6-DMP**		
NaCl [mM]	**K_m pH 3 [µM]**	**K_m pH 4.5 [µM]**
0	1.5	0.6
500	91	3.2
2000	153	5.8

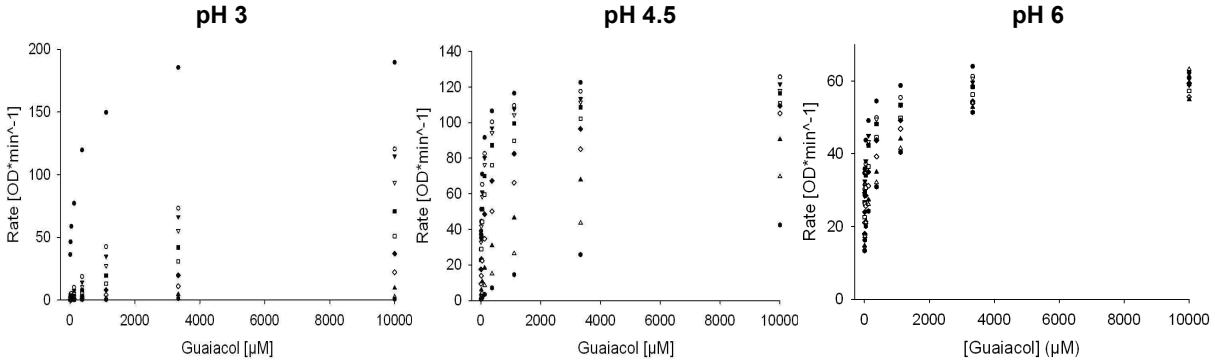

Figure 3.23: 96-well inhibition assay of *Ba*Lac *wt* with guaiacol and inhibitor NaCl (0 mM (●), 3.9 mM (○), 7.8 mM (▼), 15.6 mM (▽), 31.3 mM (■), 62.5 mM (□), 125 mM (♦), 250 mM (◊), 500 mM (▲), 1 M (Δ), 2 M (●)) at pH 3, 4.5 and 6.

Table 3.14: Apparent K_m values determined by Michaelis-Mendten regression of individual data sets from 96-well inhibition assay of *Ba*Lac *wt* with NaCl and guaiacol at pH 3 and 4.5.

***Ba*Lac *wt* – guaiacol**		
NaCl [mM]	**K_m pH 3 [µM]**	**K_m pH 4.5 [µM]**
0	131	19.5
3.9	3303	24.6
125	7693	104
500	13014	873

*Tp*Lac was not tested for Cl^- inhibition with guaiacol but with 2,6-DMP. The results are given in Figure 3.24 and Table 3.15. Compared to *Ba*Lac *wt* inhibition assays substrate inhibition with 2,6-DMP was stronger, especially at higher pH. Otherwise the differences in Cl^- inhibition between *Tp*Lac and *Ba*Lac were similar to those seen with ABTS as substrate. These were lower Cl^- tolerance of *Tp*Lac as well as higher OH^- concentrations that were needed to reduce the inhibiting effect of Cl^-. Like the Cl^- inhibition assay of *Ba*Lac *wt* with 2,6-DMP also the one of *Tp*Lac exhibited a dependency of v_{max} on inhibitor concentration but at all tested pH levels. At pH 6 this got overlayed by strong substrate inhibition however. The apparent K_m values were rising with increasing inhibitor concentration and falling at higher pH.

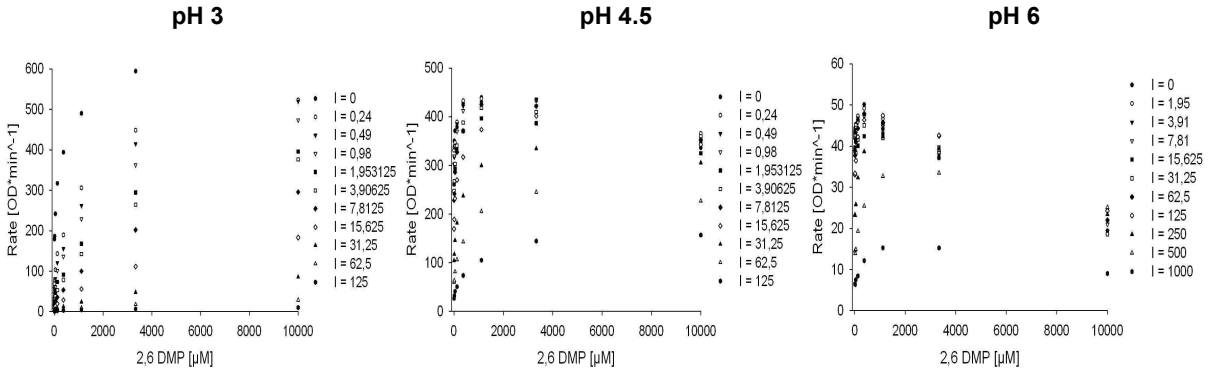

Figure 3.24: 96-well inhibition assay of *Tp*Lac with 2,6-DMP and inhibitor NaCl (concentrations given in graph in µM) at pH 3, 4.5 and 6.

Table 3.15: Apparent K_m values determined by Michaelis-Mendten regression of individual data sets from 96-well inhibition assay of *Tp*Lac with NaCl and 2,6-DMP at pH 3 and 4.5.

***Tp*Lac – 2,6-DMP**		
NaCl [mM]	**K_m pH 3 [µM]**	**K_m pH 4.5 [µM]**
0.24	562	1.9
3.9	2136	3.8
125	1424	196

Inhibitor: NaF

F^- inhibition assays with *Ba*Lac *wt* and 2,6-DMP lead to comparable results as with ABTS as can be seen in Figure 3.25. Differences were however the substrate inhibition and that the apparent K_m values were higher. They were however still too low to be calculated. The same assay but with guaiacol (Figure 3.26) resembled those of the other two substrates except that it showed even higher apparent K_m values which could be calculated (Table 3.16). The K_m values appeared not to change with inhbitor concentration but decreased with higher pH. One major exception was at pH 3 without F^- where the K_m value was three times lower than with F^-.

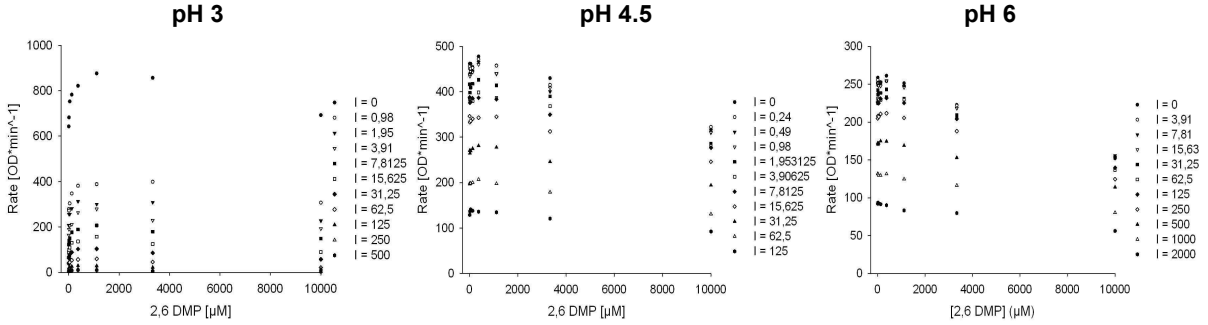

Figure 3.25: 96-well inhibition assay of *Ba*Lac with 2,6-DMP and inhibitor NaF (concentrations given in graph in µM) at pH 3, 4.5 and 6.

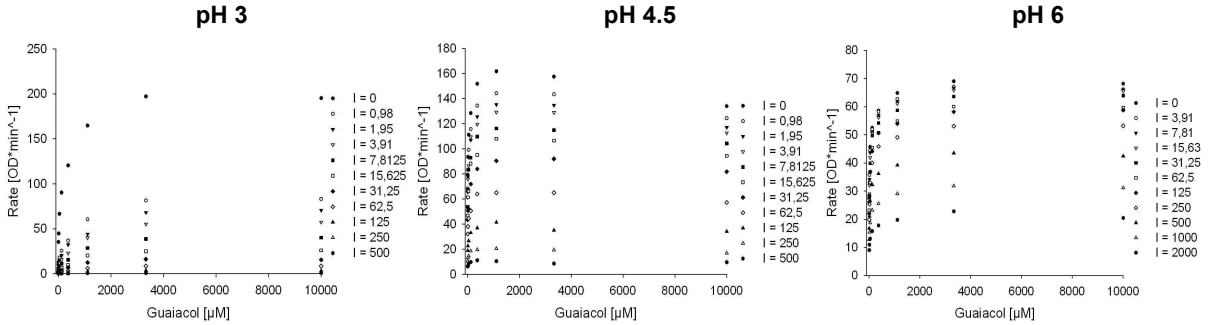

Figure 3.26: 96-well inhibition assay of *Ba*Lac *wt* with guaiacol and inhibitor NaF (concentrations given in graph in µM) at pH 3, 4.5 and 6.

Table 3.16: Apparent K_m values determined by Michaelis-Mendten regression of individual data sets from 96-well inhibition assay of *Ba*Lac *wt* with NaF as inhibitor and guaiacol as substrate at pH 3 and 4.5.

***Ba*Lac *wt* - guaiacol**		
NaF [µM]	**K_m pH 3 [µM]**	**K_m pH 4.5 [µM]**
0	**113**	6.48
1.0	362	7.02
3.9	454	7.04
125	370	6.72

3.5 Application of laccases on glassy carbon electrodes

The aim was to demonstrate reproducible catalytic current of *Botrytis aclada* laccase by mediated electron transfer via Os-modified polymers from a glassy carbon (GC) electrode surface, which was tested by circular voltammetry. The following two different modification strategies were used:

Laccase Os-modified anodic polymer glassy carbon electrode

*Ba*Lac *wt* and the Os-modified anodic polymer p009-p91 were deposited in acidic environment (pH 3) on GC electrodes as described in the method section. They were immediately used for circular voltammetry at standard conditions. An initial measurement was taken in oxygen atmosphere which was followed by one in argon and finally a third one in oxygen again (Figure 3.27). The reductive peak in an oxygen environment was compared to the one in anaerobic conditions. Between 1st and 2nd measurement the difference at 0 mV (E vs Ag/AgCl (3 M)) amounted to 13 µA cm^{-2}. The 3rd measurement however showed no change to the 2nd one anymore. No clear reductive or oxidative peaks around 400-500 mV (E vs Ag/AgCl (3 M)) could be identified in any of the three runs.

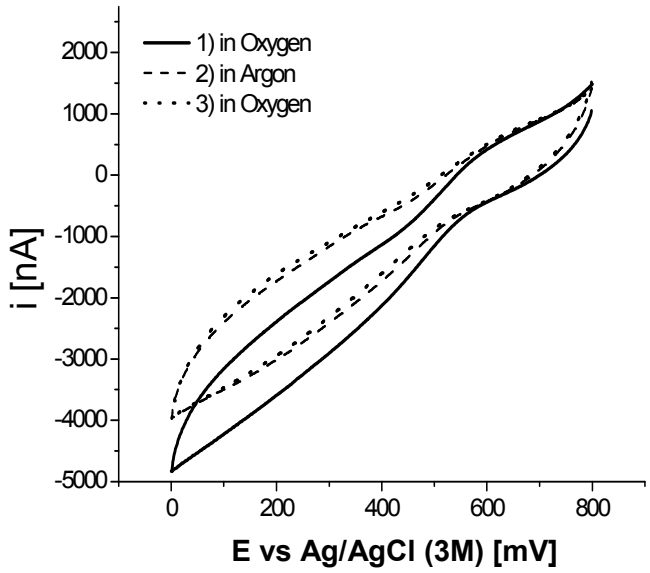

Figure 3.27: Circular Voltammetry of glassy carbon electrode modified with *Botrytis aclada* laccase *wt* and Os-modified polymer p009-p91, conducted at standard conditions in argon and oxygen (100 mM citrate buffer: pH 4, reference electrode: Ag/AgCl (3 M), scan rate: 0.005 $V*s^{-1}$)

Laccase Os-modified non-charged backbone polymer glassy carbon electrode

Due to the results gathered in the first approach, a novel strategy was applied for modification of GC electrodes. To create a proof of concept of this method *Th*Lac was used as laccase instead of *Ba*Lac *wt* as it was available at higher specific activity and also had shown better resilience against inactivation by polymers in experiments before. The Os-modified non-charged backbone polymer p011-p91 served as electron mediator and as enclosing and immobilization layer for the enzyme. Because of the non-charged nature of the polymer backbone covalent binding with 2,2′-(Ethylenedioxy)diethanthiol had to be used instead of acidic deposition on the electrode. The electrodes were modified according to the covalent binding procedure in the method section therefore. The following circular voltammetry in four runs (1st in oxygen, 2nd in argon, 3rd in oxygen and 4th in argon atmosphere) was conducted at standard conditions. As shown in Figure 3.28 the reductive peak at 0 mV (E vs Ag/AgCl (3 M)) of the 1st measurement in oxygen was 17 µA cm^{-2} lower than at the 2nd one in argon and the 3rd one still showed a 13 µA cm^{-2} lower value than the 4th one at the same potential. Over time all reductive currents were decreasing however. Initially a strong reductive peak was located around 400 mV (E vs Ag/AgCl (3 M)) and a strong oxidative peak around 500 mV (E vs Ag/AgCl (3 M)). Even though they were decreasing they remained visible until the last run.

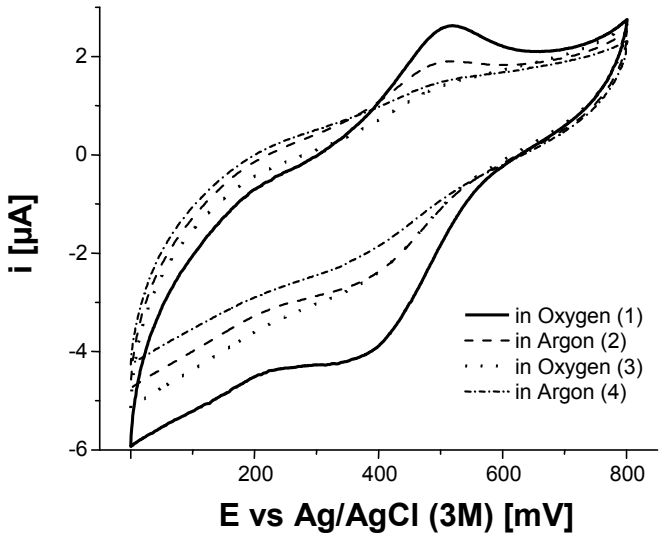

Figure 3.28: Circular Voltammetry of glassy carbon electrode modified with *Trametes hirsuta* laccase *wt* and Os-modified polymer p011-p91, conducted at standard conditions in argon and oxygen (100 mM citrate buffer: pH 4, reference electrode: Ag/AgCl (3 M), scan rate: 0.005 $V*s^{-1}$)

Because of time restraints this GC electrode modification approach could not be tested for *Botrytis aclada* laccase anymore.

4 Discussion

4.1 Creation and screening of single point BaLac mutants

In the following activity and pH optima tests and the NaCl tolerance mutation tests several new *Ba*Lac mutants were screened (Table 3.3 and Table 3.4). All new mutant sequences were successfully created and confirmed by sequencing. Also expression of the mutant enzymes in *Pichia pastoris* was confirmed on BMM plates with ABTS for all mutants but *Ba*Lac R129L. This mutation showed a very weak green halo after about 7 days which was interpreted as a successful transformation of *Pichia pastoris* but activity was too low for that mutant to be of interest for further study. Either *Pichia pastoris* could not express and/or secrete it properly or the mutation had a considerable negative impact on the enzyme's activity as it is close to the T2/T3 site where the reduction of O_2 to H_2O takes place (Xu, 2001).

The T1 redox potential mutants and direct electron transfer pathway mutants of *Ba*Lac listed in Table 3.5 were screened for activity with the substrates ABTS, 2,6-DMP and selected ones also with guaiacol and catechol. Also plate reader based pH profiles with ABTS and 2,6-DMP were established for all those mutants in order to select the most interesting ones in terms of activity and pH optima for heterologous expression in shaking flask cultures. The activity screening showed large standard variations of about one third of the determined relative activities. This was however expected as the 96-well fermentations were not seeded with the exactly same amount of biomass. The standard deviation furthermore did not show errors between the fermentations of different mutants but only within the quadruplets of the same mutant. For these reasons the method only allows for a first semi-quantitative screening for expressed enzymes with sufficient enzymatic activity. Of all the tested mutants many of the mutations of *Ba*Lac I505 and W373 showed activities of less than 10% of the wild type. Furthermore three of the BaLac I505 mutants namely M, S and W had comparable activities with ABTS (relative activities >50%) and except for *Ba*Lac I505W also with 2,6-DMP, but all three showed barely any activity with guaiacol (relative activities <10%) and even less with catechol. The mutation *Ba*Lac I505W therefore effected the metabolization of phenols far stronger than the one of non-phenols like ABTS. This could be caused by the different binding of phenolic substrates at the T1 site compared to ABTS which Kallio et al. (2009) described for *Melanocarpus albomyces* laccase. The three phenolic substrates differ regarding their redox potentials or more specifically in their different content of methoxy and hydroxyl groups which could explain the higher activity with 2,6-DMP. For confirmation of

these results and in order to elucidate the mechanisms these mutants would need to be heterologously expressed in shaking flask cultures and tested regarding their activities with these substrates to gain more credible data than one could get from these screening assays.

The pH profile assays revealed that some of the T1 redox potential mutants showed optima at a higher pH with 2,6-DMP than the wild type. *Ba*Lac I505D, I505S, I505M, I505N and *Ba*Lac L513M were the mutants with the most pronouncedly changed pH activity optimum. They had their optimum or activities close to it at pH 6 or higher. With ABTS however the profiles of all tested mutants where either very similar to the wild type or showed an even greater decrease in activity with rising pH. That was the case especially with *Ba*Lac I505 mutants. Two mechanisms were suggested by Xu (1997a) to explain the pH activity profiles of laccases with phenolic and non-phenolic substrates. One of them is an inhibition by OH^- at the T2/T3 site which reduces the rate of electron transfer from the T1 copper to the T2/T3 coppers. This would affect both substrates and lead to reduced activity at higher pH. The other mechanism is based on oxidative proton release of phenolic substrates at higher OH^- concentrations. This would reduce E° of the substrate and therefore increase the $\Delta E°$ between substrate and the T1 copper which would lead to higher enzyme activities at higher pH. ABTS is therefore expected to have a monotonically falling pH profile at rising pH while 2,6-DMP should have a bell shaped one. The ABTS pH profile of *Ba*Lac *wt* was well in line with the one described by Xu (1997a) with the high potential laccase *Trametes villosa*. However the 2,6-DMP pH activity profile differed from it. While *Trametes villosa* laccase had a bell shaped one, *Ba*Lac *wt* lacked the rising part in its 2,6-DMP profile which was therefore very similar to the one with ABTS. A separate pH profile of *Ba*Lac *wt* with 2,6-DMP at pH 2.5-8 showed an initial rise in activity either has to take place below pH 2.5 or does not exist at all.

Among the *Ba*Lac mutants with changed pH optima some further deviations could be observed. I505N and I505D exhibited a monotonically rising profile, whereas the latter had rapidly decreasing activities around pH 7 which is where *Ba*Lac starts to be rapidly inactivated. An OH^- inhibition of those two mutants was not recognizable with 2,6-DMP while it was with ABTS and even appeared there to be stronger than for *Ba*Lac *wt*. This phenomenon could be caused by a lowered T1 copper redox potential which could further slow down the already rate limiting step of the electron transfer from substrate to T1 copper and increase the amount of OH^- needed to lead to a recognizable inhibition of enzyme activity (Xu et al.,1998b). At the same time the possibility of a T1 copper redox potential dependency on the pH (Xu, 1997a) could play a role as well. If the T1 copper E° decreased

with rising pH this could lead to a stronger loss of activity with ABTS while it might be compensated in the case of 2,6-DMP by a decrease of the substrate's E°.

*Ba*Lac L513M differed from the wild type in its pH profile with 2,6-DMP as it showed similar activities (relative activities > 80%) at a broad pH range from 4 to 6.5. This result of the high throughput screening assay was later confirmed by separate measurements of the mutant at pH 2.5 - 8. The point mutation of L513M affects an axial ligand of the T1 copper. Mutation studies at the equivalent amino acid sequence position of the one copper oxidase azurine showed that methionine lead to 70-100 mV lower redox potentials than leucine (Farver et al., 1993; Karlsson et al., 1989). *Ba*Lac L513M had similar k_{cat} values compared to the wild type in this work unlike *Ba*Lac I505N. These numbers were only an estimation because of unknown impact of inactivation and different purification procedures but they suggested that a lowered T1 redox potential was not the reason for the deviant *Ba*Lac L513M pH profile. This is in contradiction however to those single point mutation studies which were shown to lower the T1 redox potential in some cases. To elucidate the mechanism which caused the deviant pH optima of *Ba*Lac I505 mutants and *Ba*Lac L513M detailed tests on the T1 redox potential also in dependence of pH and reliable quantification of catalytic rate would be necessary.

*Ba*Lac I505N and *Ba*Lac L513M were selected for heterologous expression in shaking flask cultures and additional characterization. The former was chosen because it showed one of the most deviant 2,6-DMP pH profiles, even though its volumetric activity was less than 10% of the wild type at standard conditions. The latter was picked because of the broad pH optimum plateau reaching up to pH 6.5 (relative activities > 80%) and because it had among the best volumetric and specific activities of mutants with deviant pH optimum.

4.2 Heterologous expression and purification of BaLac

Two salt tolerance mutants were heterologously expressed primarily to test for a potentially deviant Cl^- inhibition and the two T1 redox potential mutants were chosen for kinetic studies together with the *Ba*Lac *wt*. Of these four mutants *Ba*Lac L513M had the highest volumetric activity (more than 5 times higher than the others) and *Ba*Lac I505N the lowest. As the enzyme concentrations could not be determined in the supernatant it remains unclear if the low activity was due to less expressed or less active enzyme. Another reason for low total activity at harvest could be the stability of the enzyme at 30℃ because rapid inactivation of *Ba*Lac was shown to be caused by this temperature in this work. Possibly the I505N mutation also further destabilized the enzyme.

The purification led to very different results. The highest specific activity (58.8 U*mg^{-1}) could be achieved with *Ba*Lac R129F but *Ba*Lac R129H lost almost all its activity during HIC. Possibly the histidine in this position led to changes in the binding of either the T2 or T3 copper atoms and as a consequence destabilized the active enzyme. Generally speaking the largest activity losses during downstream processing were due to strict pooling at the HIC however especially destabilized mutants might have also lost copper and possibly were inactivated that way.

*Ba*Lac L513M expressed in a better controlled environment of a fermenter showed at harvest a higher specific activity and volumetric activity of 15 U*ml^{-1} which was about 6 times more than with expression in shaking flasks. The more sophisticated two step HIC ensured the highest achieved specific activity in this work of 88 U*mg^{-1} in the final enzyme solution. As standard protocols were used their optimization could further improve efficiency especially by preventing enzyme inactivation.

4.3 Characterization of BaLac

4.3.1 *General Ba*Lac kinetics

*Ba*Lac *wt* and *Ba*Lac I505N, L513M, R129F and R129H were characterized in regard to their K_m and k_{cat} values as well as pH dependency of activity. Due to the low storage stability of *Ba*Lac the determined k_{cat} values were lower than in fresh enzyme solutions as the wild type laccase was not tested immediately after heterologous expression and purification but after several months of storage at 4℃. For guaiacol this was even more the case than with the other substrates as the according assay was conducted at an even later point. K_m values were not affected by these aspects however and compared to median K_m values of fungal laccases in literature of 39, 405, 420 µM for ABTS, 2,6-DMP and guaiacol, respectively (Baldrian, 2006) those measured with *Ba*Lac *wt* were considerably lower with 3.6, 4.5 and 72.3 µM for ABTS, 2,6-DMP and guaiacol, respectively. For ABTS and 2,6-DMP the K_m values were even around or below the lowest values described by Baldrian. Compared to other fungal laccases studied so far *Botrytis aclada* laccase therefore exhibited very high affinities to these common substrates. The salt tolerance mutants showed little impact on binding of the substrate which was expected as the mutations were far away from the substrate binding pocket. The T1 redox potential mutants however featured increased K_m values, more than 100 times for *Ba*Lac I505N. *Ba*Lac L513M had about 10 times lower affinity for 2,6-DMP, guaiacol and catechol. K_m for ABTS (18.4 µM) was less increased than for phenolic substrates compared to the wild type however. Both tested mutations were

located next to the T1 copper and at the substrate binding pocket. Apparently they had an impact on the binding of the substrate. That affinity of *Ba*Lac L513M to phenolic substrates was more reduced than for ABTS is possibly caused by the different ways phenolic substrates and ABTS are bound there.

pH dependency of K_m values of *Ba*Lac *wt* with phenolic substrates (2,6-DMP, catechol and guaiacol) differed from the one with ABTS. Phenolic substrates showed a stronger specific binding to the enzyme with rising pH, ABTS had the opposite tendency. Xu (1997a) suggested such a difference exists because phenolic substrates feature a proton equilibrium and ABTS does not.

Activity profiles with 2,6-DMP from pH 2.5 to 8 for the four tested mutants and the wild type were determined. The results of the 96-well pH profile screening of the enzyme variants were confirmed and for *Ba*Lac L513M the first half of a bell shaped profile could be identified which was outside the pH range of the initial screening. Therefore *Ba*Lac L513M fitted into the two-phase pH profile scheme suggested by Xu (1997a). The wild type however did not show a bell shaped 2,6-DMP profile even in this assay. That means this 1st phase is either located below pH 2.5 or does not exist at all. With 2,6-DMP *Ba*Lac R129F was almost identical in its profile to the wild type while *Ba*Lac R129H showed a stronger inhibition already at lower OH^- concentrations. Possibly this is due to a slowing down of the electron transfer from T1 to T2/T3 copper due to the mutation. This could enable already lower OH^- concentrations to turn that electron transfer step into the rate limiting step.

The temperature optimum for *Ba*Lac *wt* activity was found to be 43℃. At physiological temperature still 92% of the maximum activity was left. Studies of 42 different fungal laccases revealed temperature optima covering a range as broad as from 25 to 80℃ with a median as well as mean optimum at 55℃ (Baldrian 20 06).

4.3.2 *Ba*Lac stability

Enzyme stability is of major importance for practical applications and good stability at physiological conditions is an essential criterion for medical applications of biosensors or fuel cells. In this work thermostability of *Ba*Lac *wt* at different pH environments and stability in presence of solvents and Os-modified polymers were studied.

Thermostability assays showed that at the tested low enzyme concentrations activity was lost rapidly at all investigated temperatures and pH environments. Even at the optimal conditions (4℃, pH 4.5) $t_{1/2}$ was only 8 days. At physiological temperature the highest $t_{1/2}$ was at pH 5.5 with only 5 hours. Higher pH than 5.5 led to increasingly rapid inactivation. Enzyme stock

solutions concentrated 1000 times higher and stored at close to optimal conditions (4℃, pH 5.5) were found to have a much larger $t_{1/2}$ of above 90 days. That means lower enzyme as well as higher OH^- concentrations reduced stability of BaLac *wt*. A molecular explanation for the temperature related loss in activity of laccases in general was suggested by Hildén et al. (2009). It was assumed that the loss of T2 copper was the major cause for the decreasing activity which was supported recently by yet unpublished *Ba*Lac crystal structures that showed T2 copper depletion. Additionally activity reducing conformation changes in T1 and T2 copper were shown to occur at higher temperatures. The reason why higher OH^- concentrations lead to more rapid activity loss remains unclear but the hydroxide molecules bind to the T2/T3 copper site. Possibly they increased the instability of the T2 copper and facilitated its loss. As long term stability, especially at physiological conditions, appeared to be a central weakness of *Botrytis aclada* laccase improving it is of a major concern for its practical application. It was not tested in this work if the mutations at the T1 site (T1 redox potential mutants) respectively those at the T3/T2 site changed the stability. Mutations there could be promising however as the coordination of the T2 copper and the confirmation of the according site could be of importance for maintaining enzymatic activity at higher temperatures and pH. As alternative to such a rational approach also directed evolution, with high throughput screening for thermostability mutants, is thinkable.

With foresight for application of *Ba*Lac in biofuel cells the enzyme's stability with common solvents as well as Os-modified polymers was tested. Methanol was found to be less harmful than ethanol. Concentrations of up to 30% showed little impact on the enzyme's activity. This is more than what was needed for bringing the polymers used in this work into solution. The use of methanol as solvent was considered unproblematic therefore and sufficed for preventing premature polymer precipitates.

Because of limited polymer supply all the assays with polymers were conducted with very small volumes resulting in larger errors, the following qualitative conclusions were however clearly visible and the results of the duplicates congruent. Os-modified anodic polymers proved to be problematic as they caused rapid irreversible inactivation of *Ba*Lac *wt*. Tests with Os-complex alone as well as anodic polymer alone revealed that mostly the latter is the cause for this inactivation. However *Trametes hirsuta* laccase which was tested with the same anodic polymers as the *Botrytis aclada* laccase did not show any inactivation caused by these polymers. Furthermore Os-modified cathodic polymers inactivated *Ba*Lac *wt* to a considerably lesser extend and Os-modified non-polar backbone polymers did so barely at all. The used anodic polymer backbones differed from the others as they had carboxylic group side chains and because the polymers which lacked these groups did not show that

strong inactivation of *Ba*Lac it appeared they were the cause for it. Chelating agents are known to be potential inhibitors of laccases (Lorenzo et al., 2005). Possibly carboxylic groups from the polymer backbone were forming complexes with coppers of the enzyme. This could have lead to loss of copper and laccase inactivation. If this was the case the copper complex binding of *Ba*Lac *wt* would have to be weaker than of *Trametes hirsuta* laccase because *Ba*Lac *wt* was strongly affected by those carboxylic groups while *Th*Lac was not.

Os-modified non-charged backbone polymers were identified as most promising choice for immobilization of *Ba*Lac on glassy carbon electrodes in terms of enzyme stability. Due to their non-charged nature however they can not be deposited by pH change but need a crosslinker which creates covalent binding between the epoxide groups of the polymer backbone. The effect of 2,2'-(Ethylenedioxy)diethanthiol on *Ba*Lac *wt* stability was tested therefore as well. While higher concentrations showed a $t_{1/2}$ of about 3 hours a final concentration of 0.009% which came closer to the one used for actual cross-linking on the electrode had no discernable effect on the enzyme activity. Therefore this crosslinker was considered suitable for *Botrytis aclada* laccase immobilization.

Long term stability of immobilized *Botrytis aclada* laccase was not studied in this work as an established method of immobilization would be a precondition for that. Especially for application in biosensors or biofuel cells this would be of great importance because stability of immobilized enzyme could differ largely from the one in solution.

4.3.3 NaCl tolerance *Ba*Lac mutants

The tested NaCl tolerance mutants showed no clear impact on enzyme activity, neither *Ba*Lac R129F nor R129H. Deviations from the *Ba*Lac *wt* activities over time never exceeded 10%. Of special interest in this regard was *Ba*Lac R129F as the high potential laccases *Th*Lac and *Tp*Lac also were found to have a phenylalanine in the equivalent amino acid sequence position (Frasconi et al., 2010; Galhaup et al., 2002). *Tp*Lac also showed a 10 times lower Cl^- tolerance than *Ba*Lac *wt*. Possibly Cl^- which could be next to these mutations according to Hakulinen et al. (2002) was not affected by the change of the neighboring amino acid from arginine to phenylalanine or histidine. It could also be the case that this chloride ion itself does not affect the Cl^- inhibition of the enzyme or that it was only an artifact in the X-ray crystallography normally not found there. The results of these tests suggested that this amino acid position was not the reason why basidiomycete high potential laccases like *Tp*Lac showed substantially lower Cl^- tolerance than *Ba*Lac *wt*.

4.3.4 NaCl / NaF inhibition assays

Substrate: ABTS

At pH 3 the changing apparent K_m values and varying v_{max} values at different NaCl concentrations (Figure 3.19, for *Ba*Lac *wt* and Figure 3.20, for *Tp*Lac) pointed towards non-competitive inhibition. The inhibition however weakened with increasing ABTS concentrations which was indicating a partly competitive inhibition. Therefore Cl^- showed mixed type inhibition characteristics whereas the non-competitive component was dominant. However for *Ba*Lac *wt* from pH 4.5 and for *Tp*Lac from pH 6 onwards it was the other way round and the competitive inhibition was dominant. As Figure 3.21 shows F^- inhibition assays had different v_{max} values at all tested F^- concentrations. This suggested a non-competitive F^- inhibition but also an uncompetitive inhibition could not be ruled out as apparent K_m values could not be calculated. Also at high pH no tendency towards competitive inhibition was visible with F^- unlike with Cl^-. Because the apparent K_m at pH 6 was higher than at pH 3 and because v_{max} differed depending on the pH as well, OH^- inhibition appeared to be non-competitive.

F^- did not show competitive inhibition characteristics therefore it seemed not to interact with the T1 copper center where the substrate binds. Because activities at high amounts of F^- increased if OH^- concentration was raised both inhibitors appeared to compete with each other. Xu (2001) suggested that halides as well as OH^- attack the O_2 reduction step to H_2O at the T2/T3 copper site. The results of the *Ba*Lac *wt* F^- inhibition assays with ABTS confirmed this in regards to F^-. Cl^- on the other side showed a more complex inhibition typology. Competition with ABTS became the dominant Cl^- inhibition component at high pH. Therefore Cl^- appeared not only to interact at the T2/T3 copper site like F^- but also at the T1 copper site where it can compete with ABTS. A competitive inhibition by Cl^- was described already by Naki and Varfolomeev (1981). Vaz-Dominguez et al. (2008) confirmed that and proposed that Cl^- interacts with the T1 copper site of laccases. A description for a combined mixed type Cl^- inhibition mechanism involving T1 and T2/T3 sites could not be found in literature however and is considered a novel concept therefore.

*Tp*Lac showed the same Cl^- inhibition typology as *Ba*Lac *wt* but higher pH was needed for the non-competitive inhibition to subside. This indicated that more OH^- was needed to compete with Cl^- for the T2/T3 site. *Ba*Lac *wt* proved in general to be superior to *Tp*Lac in apparent Cl^- tolerance. For similar inhibition effects as exhibited by *Tp*Lac it needed about 10 times higher Cl^- concentrations which confirmed the expected high Cl^- tolerance of *Ba*Lac wt compared to high potential laccases.

Substrate: 2,6-DMP and guaiacol

*Ba*Lac *wt* Cl^- inhibition characteristics with 2,6-DMP as well as guaiacol were similar to those with ABTS. That means it was also a complex mixed type inhibition. The non-competitive inhibition was dominant as well at low pH and subsiding at higher pH. But with the smaller phenolic substrates 2,6-DMP and guaiacol less competitive Cl^- inhibition of *Ba*Lac was observed than with the bigger non-phenolic substrate ABTS. This could have steric reasons or have to do with the different mechanisms of interaction of non-phenolic and phenolic substrates with the T1 copper site.

*Tp*Lac Cl^- inhibition with 2,6-DMP showed features already found with ABTS as well as those found in *Ba*Lac Cl^- inhibition assays with 2,6-DMP. That means the non competitive Cl^- inhibition was stronger at lower pH but little to no competitive inhibition could be observed at pH 6. These characteristics could be due to the same mechanisms which were already mentioned above. The reasons why competitive inhibition was seen with ABTS but not with 2,6-DMP were possibly in *Tp*Lac the same as in *Ba*Lac *wt*, that means steric ones or differences in the precise binding mechanism in the substrate pocket. The different binding mechanism would be supported by the findings of Kallio et al. (2009) who suggested in studies with *Melanocarpus albomyces* laccase that ABTS and phenolic substrate binding in the substrate pocket differ from each other.

F^- inhibition of *Ba*Lac with 2,6-DMP and guaiacol largely resembled the one with ABTS as it was also either a non-competitive or uncompetitive inhibition. The apparent K_m values with guaiacol showed very little variation which would suggest an uncompetitive inhibition. As the quality of these calculated K_m values is in doubt due to a suboptimal substrate range in the assays however further empirical data would be needed for confirmation. Doubts remain especially as the mechanism described by Xu (2001) was a non-competitive one.

Concluding remarks

The two halides Cl^- and F^- were tested in order to clarify the inhibition mechanisms of *Botrytis aclada* laccase. In Figure 4.1 the suggested sites of inhibition are summarized and visualized. As described above OH^-, F^- and Cl^- are apparently attacking at the T2/T3 site which causes non-competitive inhibition. Cl^- but not F^- was suggested to affect also the T1 site where it competes with the substrate causing a competitive inhibition. The non-competitive inhibition was proposed to be based on a reduction of the electron transfer rate from T1 to T2/T3 coppers (k_{et2}). In order to have a visible inhibitory impact this rate has to become slower than the electron transfer rate from the substrate to the T1 copper (k_{et1}) which

is normally the rate limiting step (Xu et al., 1998b). The competitive inhibition by Cl^- was only visible with ABTS as substrate but barely or not at all with tested phenolic substrates. ABTS is a considerably larger molecule and does not involve proton equilibriums in its oxidation. Possibly the observed competitive inhibition was therefore due to steric reasons or the different binding mechanisms.

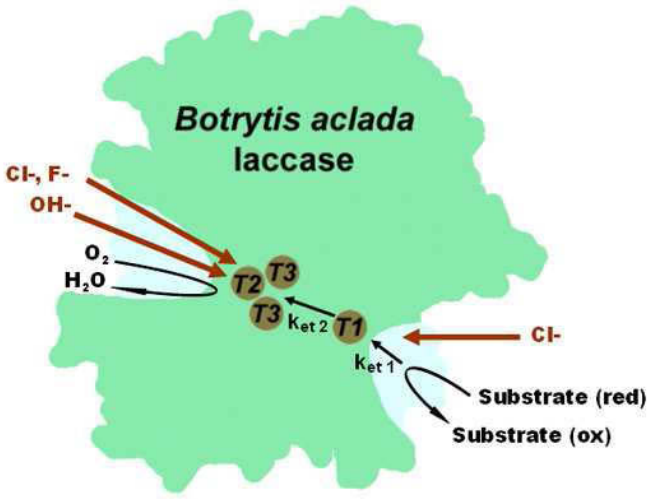

Figure 4.1: Suggested locations of inhibition at *Botrytis aclada* laccase

While Cl^-, F^- and the substrates ABTS, 2,6-DMP and guaiacol were subject of numerous inhibition assays, OH^- was tested in only three different concentrations and the reduction of oxygen to water was not observed at all. Further tests with OH^- as inhibitor at various concentrations versus substrate at various concentrations in 96-well plates should be conducted therefore to study the nature of OH^- inhibition which is according to Xu (1997a) one of two factors defining the pH optimum of the enzyme. These 96-well assays could be repeated in presence of different Cl^- concentrations. To test the influence of O_2, assays involving a Clark electrode and a controlled atmospheric environment would be necessary. Xu (2001) tested already how F^- inhibition affected O_2 binding and reduction rates in among others *Trametes* laccases and described a suitable analytical method. He suggested that inhibition of O_2 reduction by F^- is non-competitive and that not the binding of O_2 is affected but its reduction rate. Similar tests with Cl^- and *Ba*Lac could give insight if this is also the case there as well.

One problem which affects all these inhibition studies is the complex nature of laccase catalysis as well as inhibition. Simple Michaelis-Mendten kinetics did not appropriately describe the conducted inhibition assays. For quantitative tests other models would have to be chosen, for example a two site saturation inhibition with two K_m and k_{cat} values.

4.4 Application of laccases on glassy carbon electrodes

A possible use for laccases is in small bio fuel cells. The laccase's purpose there is to reduce oxygen to water at the cathode where it is immobilized. A thin 3D layer of Os-modified polymer enclosed and immobilized the laccase and also served as electron mediator between electrode surface and the T1 copper site of the enzyme. The first tests were based on pH dependent deposition of *Ba*Lac-Os-modified anodic polymers on glassy carbon electrodes. This method was already used by Ackermann et al. (2010) for *Th*Lac at a lower precipitation pH. The circular voltammetry of the *Ba*Lac-Os-modified polymer p009-p91 modified GC electrode showed in the 1st measurement in oxygen a stronger reductive current than in the 2nd measurement in argon. The 3rd measurement which was done in oxygen saturated atmosphere again was however almost identical to the 2nd one. Moreover no clear Os-complex caused peaks were recognizable around 400-500 mV (E vs AgCl (3M)). That means Os-complex was only present in low concentrations. The current differences could not be confirmed to be catalytic currents because they were not reproducible in the 3rd run in oxygen. The results showed however that the used polymer precipitation strategy was not suitable the way it was conducted. Other than washing away of laccase-Os-modified polymer, also an inactivation of *Ba*Lac by Os-modified polymers was considered a possible reason for the non reproducibility of the reductive current in oxygen saturated atmosphere. The conducted inactivation tests (see 4.3.2) discouraged the further use of Os-modified anodic polymers for *Ba*Lac because of rapid inactivation in solution. Therefore instead of aiming for an improvement of the precipitation of the laccase-Os-modified anodic polymers on GC electrodes, an entirely new approach was considered.

This novel approach relied on Os-modified non-polar backbone polymers which lacked the carboxylic acid side chains that were shown to cause rapid inactivation of *Ba*Lac in solution. The more complex GC modification procedure was tested for proof of concept with *Th*Lac which was known to work well with pH precipitated Os-modified anodic polymers yielding catalytic activities of up to -325 µA cm^{-2} (Ackermann et al., 2010). In circular voltammetry of a *Th*Lac-Os-modified polymer p011-p91 modified GC electrode a reductive and an oxidative peak were located at 400 mV and 500 mV (E vs AgCl (3M)), respectively. The reductive current in saturated oxygen atmosphere persisted to be higher than in argon also in the third measurement. The observed peaks as well as the reductive current decreased over time however nonetheless. These results suggest that the observed variation in current was catalytic current caused by active enzyme in presence of oxygen and that current amounted to -13 to -17 µA cm^{-2}. The diminishing of the two peaks over time indicated a loss of Os-complex rather than a loss of enzyme activity as not only the reductive but also the oxidative peak was affected. This does not necessarily mean that the modified polymer as a whole

was lost as the loss possibly was due to not properly covalently bound Os-complex that diffused out of the film. Due to time constraints this could not be investigated anymore nor could this approach be tested with *Ba*Lac *wt*. Additional tests could have included new Os-modified non-charged polymers with more stable binding of the Os-complex with *Th*Lac as well as *Ba*Lac.

5 Conclusion

In this thesis *Ba*Lac which was heterologously expressed by methanol induced *Pichia pastoris* cultures was studied. The aim was to characterize this ascomycete laccase and possibly improve it via rational approach techniques for potential application in bio fuel cells or sensors. Higher pH optimum closer to physiological pH and Cl^- tolerance were a focus because they are essential for laccase based bio fuel cells for medical applications.

The major strengths of *Ba*Lac are its high Cl^- tolerance and its easy heterologous expression in *Pichia pastoris* compared to other laccases. The precise nature of halide inhibition of laccases is still little understood. Cl^- inhibition of *Ba*Lac *wt* and *Tp*Lac was therefore studied and it was shown to be largely affected by changes in pH. Cl^- appeared to cause a complex mixed type inhibition by acting at the T2/T3 cluster but unlike F^- also at the T1 site. While the temperature optimum of *Ba*Lac *wt* at 43℃ suited a physiological environment the low enzyme stability ($t_{1/2}$ = 5 h at 37℃, pH 5.5; $t_{1/2}$ = 8 days at 4℃, pH 4.5) and pH optimum (pH 2.5 or below) of *Ba*Lac have to be addressed. *Ba*Lac L513M was identified in this work as mutant with an increased pH optimum with 2,6-DMP at pH 6 and could be produced with specific activities of up to 88 U mg^{-1}. An immobilization technique for *Ba*Lac *wt* on glassy carbon electrodes was tested for potential application in biofuel cells. Due to time constraints only a proof of concept with *Th*Lac could be conducted which yielded an apparent catalytic current of -13 to -17 µA cm^{-2}.

Of special interest for further research of *Ba*Lac *wt* are T1 redox potentials of the wild type enzyme and mutants like *Ba*Lac L513M and their possible pH dependency. This can be determined by redox titration. To improve enzyme stability a rational approach could focus on the T2 site as the T2 copper seems to play a major role there but also directed evolution could be used. For higher activity at pH 7 the T1 as well as T2/T3 sites seem to be of importance. A rational approach was already attempted in this work, but one that focused on the T1 site. Directed evolution could have more potential to create mutants with higher pH activity optimum. High throughput screening which could be used for selection was already used in this work.

In laccase inhibition assays conducted in this work, OH^- inhibition was not looked at in equal depth as halide inhibition and the reduction of oxygen to water was not investigated at all. Therefore additional high throughput assays with OH^- as inhibitor are of interest. Assays with controlled O_2 environment could elucidate the possible role of inhibition of O_2 reduction in

*Ba*Lac. Last but not least it should be ruled out that the results of Cl^- inhibition assays with ABTS are affected by precipitation of the substrate which takes visibly place at Cl^- concentrations of 1 M and higher.

In the development of *Ba*Lac based thin 3D film electrodes a possible loss of Os-complex and/or enzyme should be investigated. Also the preparation technique needs further optimization and a proof of concept with *Ba*Lac *wt* is still needed. Once a working immobilization method is established, the enzyme stability in that environment is of special interest.

A. Appendix

*Ba*Lac *wt* cDNA sequence:

```
....|....| ....|....| ....|....| ....|....| ....|....| ....|....|
     5         15         25         35         45         55
atgaagtatt tcacagtctt tactgccctc actgcattat ttgcacaggc ctctgcatca

....|....| ....|....| ....|....| ....|....| ....|....| ....|....|
    65         75         85         95        105        115
gctattccag ctgttcgttc aacactcact cctcgtcaaa ataccactgc ctcttgtgca

....|....| ....|....| ....|....| ....|....| ....|....| ....|....|
   125        135        145        155        165        175
aactcagcta cttccagatc ttgctgggga gagtattcca ttgataccaa ctggtatgat

....|....| ....|....| ....|....| ....|....| ....|....| ....|....|
   185        195        205        215        225        235
gttactccta caggagtcac cagagaatac tggctttcag ttgagaattc taccatcaca

....|....| ....|....| ....|....| ....|....| ....|....| ....|....|
   245        255        265        275        285        295
cctgatggtt atactcgctc agccatgact ttcaatggaa ctgttccggg accagcaatt

....|....| ....|....| ....|....| ....|....| ....|....| ....|....|
   305        315        325        335        345        355
atagcagact ggggtgacaa tcttataatc cacgttacca acaatcttga acacaacggt

....|....| ....|....| ....|....| ....|....| ....|....| ....|....|
   365        375        385        395        405        415
acatctattc actggcatgg aattcgtcaa ctaggaagtc tcgaatacga cggtgtaccc

....|....| ....|....| ....|....| ....|....| ....|....| ....|....|
   425        435        445        455        465        475
ggtgtaacgc aatgtcccat cgctcctgga gataccttga cctacaagtt ccaagttact

....|....| ....|....| ....|....| ....|....| ....|....| ....|....|
   485        495        505        515        525        535
caatatggaa ccacttggta tcattctcac ttctctcttc aatacggtga tggactcttt

....|....| ....|....| ....|....| ....|....| ....|....| ....|....|
   545        555        565        575        585        595
ggacccttga tcattaacgg tcctgctact gcggactatg atgaagacgt tggtgtaatt

....|....| ....|....| ....|....| ....|....| ....|....| ....|....|
   605        615        625        635        645        655
ttcctccaag attgggcaca tgaatccgtt ttcgaaattt gggacaccgc tagactcggc

....|....| ....|....| ....|....| ....|....| ....|....| ....|....|
   665        675        685        695        705        715
gctcccccag cacttgagaa cactttgatg aatggaacca acacctttga ctgctcagct

....|....| ....|....| ....|....| ....|....| ....|....| ....|....|
   725        735        745        755        765        775
tctaccgatc ctaactgcgt tgggggtggt aagaaatttg agttgacttt cgtcgaaggt

....|....| ....|....| ....|....| ....|....| ....|....| ....|....|
   785        795        805        815        825        835
accaaatata gattgagatt gatcaatgtc ggaattgaca gtcacttcga attcgccatt

....|....| ....|....| ....|....| ....|....| ....|....| ....|....|
   845        855        865        875        885        895
gataaccaca cacttactgt cattgccaac gatcttgttc caattgtacc ctacactacc
```

```
....|....| ....|....| ....|....| ....|....| ....|....| ....|....|
   905        915        925        935        945        955
gacacacttc tcattggcat tggtcaaaga tacgatgtca ttgttgaagc caatgcggca

....|....| ....|....| ....|....| ....|....| ....|....| ....|....|
   965        975        985        995        1005       1015
gcagacaact actggattag aggtaattgg ggaaccacct gctcaaccaa caatgaagca

....|....| ....|....| ....|....| ....|....| ....|....| ....|....|
   1025       1035       1045       1055       1065       1075
gcaaatgcta caggtatcct ccgatacgat agctccagca tcgcaaatcc tacctctgtt

....|....| ....|....| ....|....| ....|....| ....|....| ....|....|
   1085       1095       1105       1115       1125       1135
ggcaccacgc cccgcggtac ttgcgaggat gagccggttg ccagtcttgt cccacacttg

....|....| ....|....| ....|....| ....|....| ....|....| ....|....|
   1145       1155       1165       1175       1185       1195
gcattggacg ttggtggata ctctctcgtc gatgaacagg tgtcctccgc attcaccaac

....|....| ....|....| ....|....| ....|....| ....|....| ....|....|
   1205       1215       1225       1235       1245       1255
tacttcacat ggaccatcaa ctcaagcagt ttactcctcg attggagctc cccaaccact

....|....| ....|....| ....|....| ....|....| ....|....| ....|....|
   1265       1275       1285       1295       1305       1315
ctcaaaattt tcaataatga gacaatcttc ccaactgaat acaacgttgt cgctctcgag

....|....| ....|....| ....|....| ....|....| ....|....| ....|....|
   1325       1335       1345       1355       1365       1375
caaaccaacg ctaacgaaga gtgggtcgta tatgtcatcg aagatctcac cggcttcggc

....|....| ....|....| ....|....| ....|....| ....|....| ....|....|
   1385       1395       1405       1415       1425       1435
atttggcatc ctatccatct ccacggccac gatttcttca tcgtagctca agaaactgat

....|....| ....|....| ....|....| ....|....| ....|....| ....|....|
   1445       1455       1465       1475       1485       1495
gtgttcaatt ccgacgagtc gccagccaag ttcaaccttg tcaatcctcc acgtcgtgac

....|....| ....|....| ....|....| ....|....| ....|....| ....|....|
   1505       1515       1525       1535       1545       1555
gtcgcggcac ttcccggaaa cggttatctt gccattgcat tcaagcttga caatcctggt

....|....| ....|....| ....|....| ....|....| ....|....| ....|....|
   1565       1575       1585       1595       1605       1615
tcatggcttc ttcattgtca tatcgcatgg cacgcatctg aggggttggc aatgcaattt

....|....| ....|....| ....|....| ....|....| ....|....| ....|....|
   1625       1635       1645       1655       1665       1675
gtggagtctc aaagctcaat tgcggtcaag atgaccgaca ctgctatatt tgaggatact

....|....| ....|....| ....|....| ....|....| ....|....| ....|....|
   1685       1695       1705       1715       1725       1735
tgtgcaaact ggaatgctta tactcctact caattgtttg ctgaggacga ttctggaatt

...

taa
```

Figure A.1: Nucleotide sequence of *Ba*Lac wt cDNA.

*Ba*Lac *wt* amino acid sequence:

```
....|....| ....|....| ....|....| ....|....| ....|....|
    5          15         25         35         45
mknftvftal talfaqasas aipavrstlt prqnttasca nsatsrscwg

....|....| ....|....| ....|....| ....|....| ....|....|
   55         65         75         85         95
eysidtnwyd vtptgvtrey wlsvenstit pdgytrsamt fngtvpgpai

....|....| ....|....| ....|....| ....|....| ....|....|
  105        115        125        135        145
iadwgdnlii hvtnnlehng tsihwhgirq lgsleydgvp gvtqcpiapg

....|....| ....|....| ....|....| ....|....| ....|....|
  155        165        175        185        195
dtltykfqvt qygttwyhsh fslqygdglf gpliingpat adydedvgvi

....|....| ....|....| ....|....| ....|....| ....|....|
  205        215        225        235        245
flqdwahesv feiwdtarlg appalentlm ngtntfdcsa stdpncvggg

....|....| ....|....| ....|....| ....|....| ....|....|
  255        265        275        285        295
kkfeltfveg tkyrlrlinv gidshfefai dnhtltvian dlvpivpytt

....|....| ....|....| ....|....| ....|....| ....|....|
  305        315        325        335        345
dtlligigqr ydviveanaa adnywirgnw gttcstnnea anatgilryd

....|....| ....|....| ....|....| ....|....| ....|....|
  355        365        375        385        395
sssianptsv gttprgtced epvaslvphl aldvggyslv deqvssaftn

....|....| ....|....| ....|....| ....|....| ....|....|
  405        415        425        435        445
yftwtinsss llldwssptt lkifnnetif pteynvvale qtnaneewvv

....|....| ....|....| ....|....| ....|....| ....|....|
  455        465        475        485        495
yviedltgfg iwhpihlhgh dffivaqetd vfnsdespak fnlvnpprrd

....|....| ....|....| ....|....| ....|....| ....|....|
  505        515        525        535        545
vaalpgngyl aiafkldnpg swllhchiaw haseglamqf vesqssiavk

....|....| ....|....| ....|....|
  555        565        575
mtdtaifedt canwnaytpt qlfaeddsgi
```

Figure A.2: Amino acid sequence derived from *Ba*Lac wt cDNA. The positions of the salt tolerance mutants (green) and T1 copper redox potential mutants (yellow) created in this work are marked. Single point mutations of other mutants used in this work are highlighted in blue (T1 copper redox potential mutants) and in grey (direct electron pathway mutants)

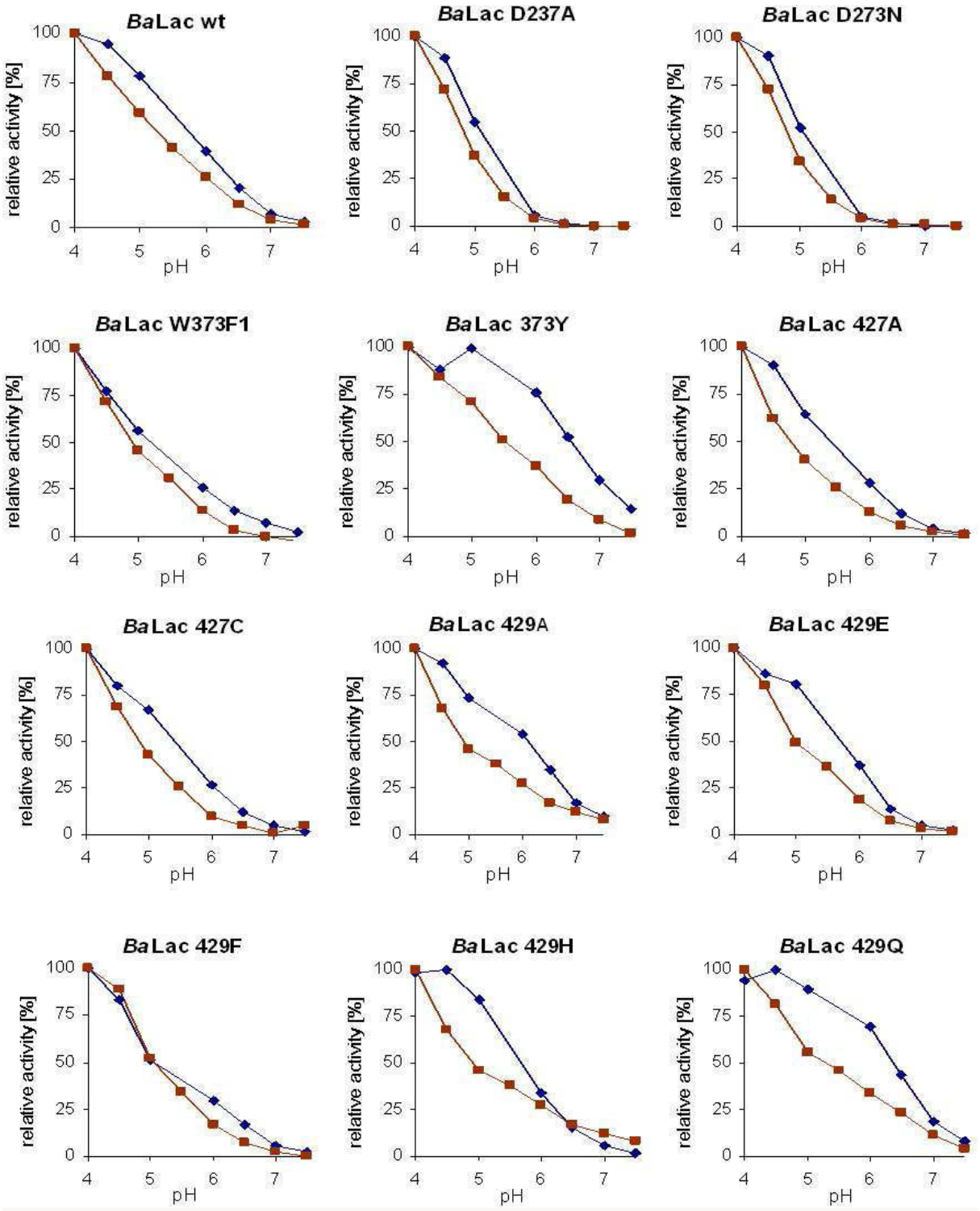

Figure A.3: pH profiles of *Ba*Lac 273, 373, 429 mutants and wild type. Standard high throughput assays with 0.5 mM ABTS (■) and 0.2 mM 2,6-DMP (♦) in citrate buffer (pH 4-5.5, 100 mM) respectively citrate-phosphate buffer (pH 6-7.5, 100 mM).

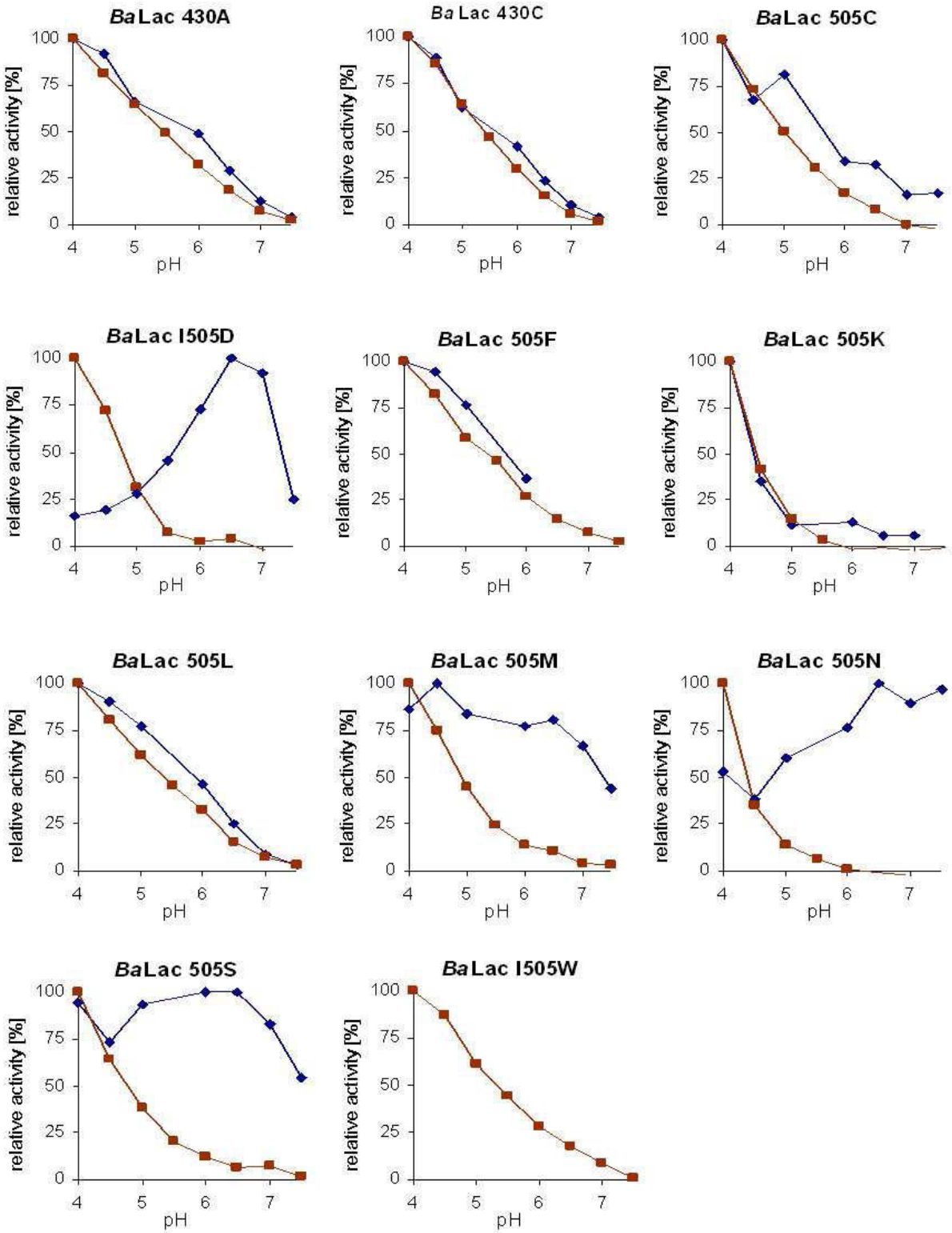

Figure A.4: pH profiles of *Ba*Lac 430 and 505 mutants. Standard high throughput assays with 0.5 mM ABTS (■) and 0.2 mM 2,6-DMP (♦) in citrate buffer (pH 4-5.5, 100 mM) respectively citrate-phosphate buffer (pH 6-7.5, 100 mM). *Ba*Lac I505D with 2,6-DMP was measured in a conventional standard pH profile assay.

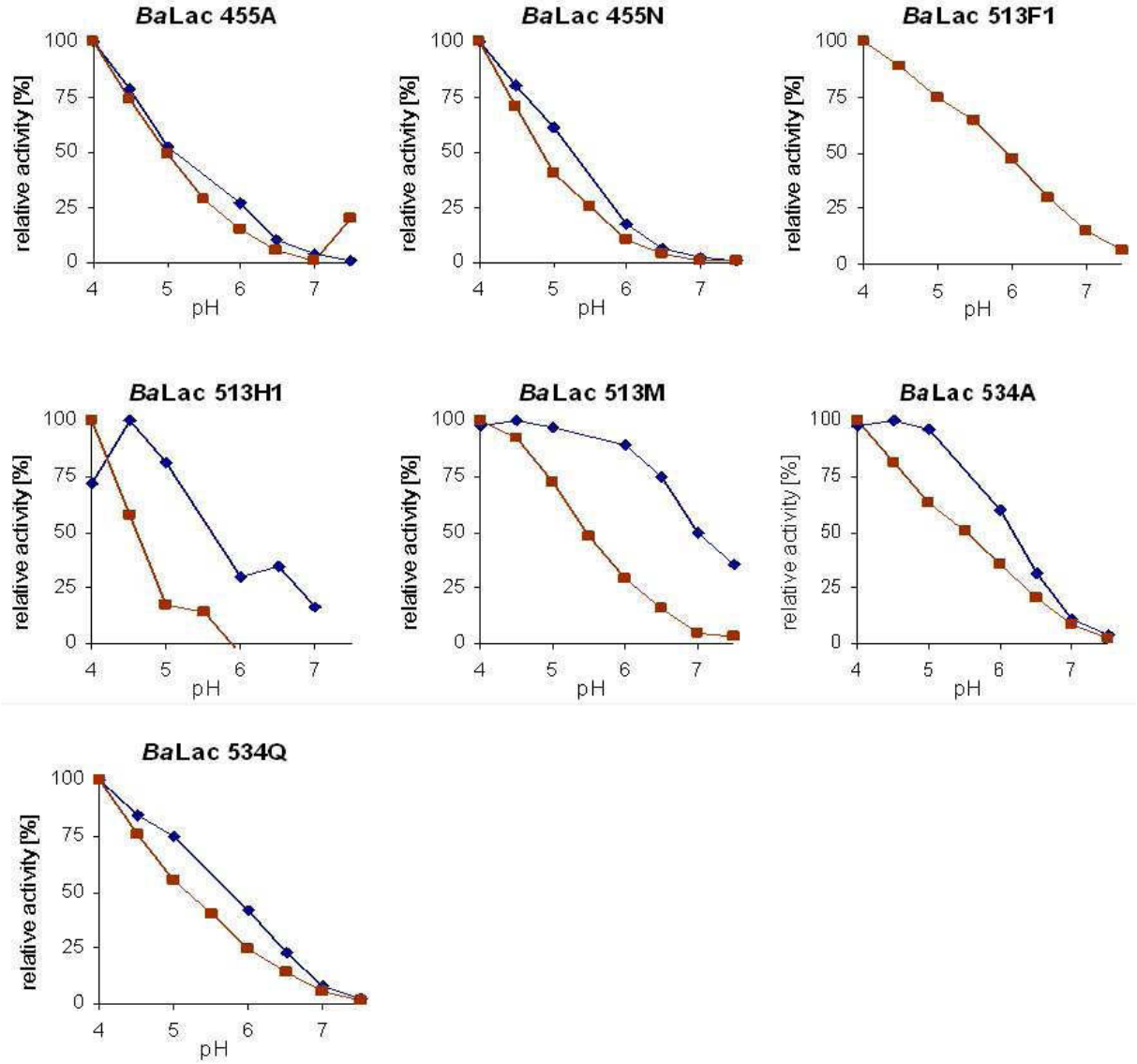

Figure A.5: pH profiles of *Ba*Lac 455, 513 and 534 mutants. Standard high throughput assays with 0.5 mM ABTS (■) and 0.2 mM 2,6-DMP (♦) in citrate buffer (pH 4-5.5, 100 mM) respectively citrate-phosphate buffer (pH 6-7.5, 100 mM).

Table A.1: 96-well inhibition assay of *Ba*Lac with ABTS and inhibitor NaCl at pH 3, 4.5 (citrate buffer, 100 mM) and pH 6 (citrate-phosphate buffer, 100 mM)

BaL - NaCl - ABTS

undiluted

Average OD/min **pH3, ABTS Stock 80 mM** **NaCl [mM]**

	2000	1000	500	250	125	62.5	31.25	15.63	7.81	3.91	0.00
10000.0			1090.4	1650.7	1894.8	2074.7	2162.1	2276.7	2366.9	2453.2	2477.4
5000.0			995.6	1489.7	1780.6	1980.1	2058.2	2234.4	2306.1	2373.3	2506.2
2500.0		639.6	965.2	1279.3	1609.1	1719.6	1928.6	2180.3	2231.8	2188.5	2493.1
1250.0		516.1	808.0	1109.9	1405.1	1553.2	1813.3	2028.9	2109.9	2204.6	2466.8
625.0		500.7	689.8	912.6	1198.0	1374.2	1588.2	1861.0	1969.5	2072.0	2557.8
312.5		404.8	538.2	722.2	978.7	1139.6	1448.5	1606.3	1780.0	1895.3	2418.5
156.3	209.4	346.3	492.2	621.1	875.9	1011.5	1192.2	1496.8	1708.7	1787.8	2542.8
78.1	296.6	351.3	417.1	574.9	755.4	914.7	1165.2	1400.7	1560.4	1732.9	2677.9

ABTS [µM]

undiluted

Average OD/min **pH4,5, ABTS Stock 80 mM** **NaCl [mM]**

	2000	1000	500	250	125	62.5	31.25	15.63	7.81	3.91	0.00
10000.0			1324.1	1455.6	1538.0	1479.7	1477.9	1509.3	1499.9	1523.9	1453.8
5000.0			1280.8	1415.0	1457.8	1414.1	1390.3	1424.4	1423.4	1453.7	1451.4
2500.0		785.1	1110.9	1268.2	1328.2	1263.9	1323.7	1400.0	1416.4	1425.4	1380.9
1250.0		723.0	926.4	1151.0	1298.0	1301.8	1331.8	1391.3	1401.8	1415.2	1376.6
625.0		608.0	767.4	1023.8	1221.5	1224.5	1320.8	1397.5	1409.9	1421.5	1386.9
312.5		477.0	618.7	941.4	1174.3	1206.2	1312.7	1379.1	1394.2	1386.8	1368.5
156.3	319.1	377.6	520.0	805.1	1070.2	1119.5	1279.7	1350.9	1395.8	1429.0	1408.7
78.1	258.7	296.7	438.3	771.5	1033.9	1072.6	1251.4	1355.3	1388.3	1403.5	1532.2

ABTS [µM]

undiluted

Average OD/min **pH6, ABTS Stock 80 mM** **NaCl [mM]**

	2000	1000	500	250	125	62.5	31.25	15.63	7.81	3.91	0.00
10000.0			592.7	429.0	412.0	386.8	404.5	407.7	407.5	410.9	373.1
5000.0			395.1	394.2	403.8	400.7	413.3	431.5	435.0	434.7	448.9
2500.0		504.5	321.8	346.6	371.0	371.7	400.1	426.6	428.5	427.9	459.6
1250.0		268.4	265.8	299.1	342.0	354.7	395.3	423.8	427.6	427.4	462.3
625.0		221.5	218.5	260.7	310.2	328.4	379.0	400.6	413.0	415.8	460.5
312.5		180.9	187.8	225.1	283.9	290.9	350.2	379.2	389.9	384.0	446.0
156.3	127.1	147.8	157.4	200.1	246.2	248.6	323.8	355.3	376.0	387.9	423.7
78.1	134.7	125.1	139.9	181.5	234.8	255.1	309.9	337.8	353.1	351.3	422.2

ABTS [µM]

Table A.2 96-well inhibition assay of *Ba*Lac with ABTS and inhibitor NaF at pH 3, 4.5 (citrate buffer, 100 mM) and pH 6 (citrate-phosphate buffer, 100 mM)

BaL - NaF - ABTS

undiluted

Average OD/min **pH3, ABTS Stock 80 mM** **NaF [µM]**

ABTS [µM]	500	250	125	62.5	31.25	15.625	7.8125	3.91	1.95	0.98	0.00
10000.0	122.4	125.3	165.0	268.4	434.0	590.4	782.7	961.9	1200.2	1415.1	2530.6
5000.0	99.0	103.6	137.1	238.5	363.0	547.9	735.1	914.8	982.9	1270.7	2563.7
2500.0	94.6	96.0	124.3	210.3	361.6	497.5	643.5	860.1	949.9	1198.3	2454.1
1250.0	101.3	88.6	123.2	200.7	345.1	488.8	605.5	826.2	953.5	1224.6	2536.6
625.0	81.5	86.6	117.9	216.9	356.4	495.0	635.6	851.8	1042.1	1197.5	2484.7
312.5	91.6	85.4	116.9	215.1	351.5	488.5	654.9	823.9	1051.9	1247.7	2611.9
156.3	75.5	85.7	118.1	196.4	349.5	467.9	593.4	817.3	1004.0	1283.2	2585.7
78.1	58.8	74.9	116.5	197.2	319.8	434.3	593.9	736.0	981.4	1178.7	2686.1

undiluted

Average OD/min **pH4,5, ABTS Stock 80 mM** **NaF [µM]**

ABTS [µM]	500	250	125	62.5	31.25	15.625	7.8125	3.91	1.95	0.98	0.00
10000.0	173.6	314.6	535.1	818.0	1076.7	1255.2	1329.7	1418.5	1468.2	1543.9	1674.1
5000.0	146.8	250.4	443.3	738.6	987.7	1175.7	1231.2	1342.8	1386.2	1475.9	1619.3
2500.0	138.0	241.0	433.7	725.2	988.1	1113.0	1234.2	1352.1	1389.4	1454.1	1597.9
1250.0	128.9	226.5	400.4	708.3	983.8	1082.6	1184.4	1365.5	1392.5	1460.9	1590.4
625.0	133.0	241.5	422.8	712.9	997.1	1127.9	1242.9	1338.4	1456.8	1474.2	1586.6
312.5	124.3	229.9	404.3	695.9	985.1	1098.6	1251.0	1384.0	1415.9	1488.9	1615.1
156.3	138.4	221.6	395.0	659.5	912.2	1070.4	1116.7	1273.8	1341.2	1454.2	1513.1
78.1	126.8	223.3	395.1	677.0	916.1	1033.4	1181.3	1333.2	1393.9	1482.4	1606.8

undiluted

Average OD/min **pH6, ABTS Stock 80 mM** **NaF [µM]**

ABTS [µM]	2000	1000	500	250	125	62.5	31.25	15.63	7.81	3.91	0.00
10000.0	203.0	273.0	374.4	443.2	465.1	459.9	495.5	498.2	504.5	507.2	506.1
5000.0	212.9	300.4	403.3	491.6	529.3	531.3	551.9	571.9	570.2	579.8	590.4
2500.0	217.8	302.0	409.4	502.3	544.1	529.0	584.9	592.7	593.2	591.6	592.9
1250.0	202.2	296.7	401.9	508.3	558.1	555.7	582.6	607.9	606.1	613.1	608.5
625.0	200.1	292.1	404.1	499.5	540.2	539.3	586.2	596.8	598.7	595.8	591.3
312.5	181.5	274.7	384.6	469.3	516.2	510.8	551.5	566.0	563.5	562.4	561.9
156.3	159.8	230.5	330.0	394.0	441.9	447.7	483.1	492.5	498.2	487.3	493.6
78.1	130.6	198.7	280.7	343.5	378.2	362.4	418.5	435.1	434.5	439.1	438.4

Table A.3: 96-well inhibition assay of *Tp*Lac with ABTS and inhibitor NaCl at pH 3, 4.5 (citrate buffer, 100 mM) and pH 6 (citrate-phosphate buffer, 100 mM)

TpL - NaCl - ABTS

undiluted

Average OD/min **pH3, ABTS Stock 80 mM**

NaCl [mM]

	125	62.5	31.25	15.625	7.8125	3.9063	1.9531	0.98	0.49	0.24	0.00
10000.0	549.1	940.6	1405.8	1790.1	2003.9	1968.5	2231.6	2278.6	2255.1	2212.3	2155.8
3333.3	357.8	685.0	1125.5	1628.9	1919.0	2027.3	2184.6	2309.5	2384.1	2365.4	2340.2
1111.1	217.2	439.7	831.1	1294.6	1669.2	1730.9	2063.3	2202.6	2272.0	2190.7	2283.7
370.4	146.3	311.6	610.2	1048.2	1461.1	1647.6	1899.9	2114.6	2234.9	2187.7	2444.3
123.5	95.7	189.2	391.2	722.4	1061.6	1173.4	1595.1	1761.5	1840.7	2000.4	2176.5
41.2	74.4	142.7	286.8	545.0	811.1	1043.0	1320.3	1516.2	1649.1	1728.3	2193.4
13.7	56.6	100.5	197.4	389.3	591.8	765.9	1008.0	1207.2	1388.7	1484.4	1883.6
4.6	42.9	65.8	134.4	255.0	423.9	514.0	724.0	880.3	1007.2	1113.5	1532.0

ABTS [µM]

undiluted

Average OD/min **pH4,5, ABTS Stock 80 mM** **NaCl [mM]**

	125	62.5	31.25	15.625	7.8125	3.9063	1.9531	0.98	0.49	0.24	0.00
10000.0	616.5	820.3	972.1	1086.5	1110.8	1025.9	1092.9	1103.9	1087.0	1088.9	1076.2
3333.3	509.1	755.5	962.4	1098.4	1178.4	1143.9	1139.0	1161.5	1154.1	1185.5	1191.1
1111.1	361.5	569.6	853.8	1022.8	1057.1	1108.5	1079.7	1169.3	1176.1	1125.8	1176.4
370.4	261.7	444.1	693.6	939.0	1027.0	1052.5	1075.3	1144.5	1145.5	1140.3	1102.4
123.5	178.5	318.6	549.5	749.8	880.6	907.2	921.0	990.0	978.4	1012.9	1008.5
41.2	137.1	254.4	427.5	637.2	768.9	820.3	842.2	915.8	925.8	980.0	965.9
13.7	113.2	205.3	353.8	521.0	668.2	710.0	754.5	850.0	815.5	868.3	912.3
4.6	92.4	166.4	297.2	463.1	590.4	616.0	714.7	777.1	766.3	853.2	835.8

ABTS [µM]

undiluted

Average OD/min **pH6, ABTS Stock 80 mM** **NaCl [mM]**

	1000	500	250	125	62.5	31.25	15.625	7.81	3.91	1.95	0.00
10000.0			66.7	69.7	67.7	65.0	67.9	67.2	67.9	68.2	67.7
3333.3		56.4	70.6	77.7	78.7	77.9	79.0	79.1	79.1	79.4	79.0
1111.1	25.5	45.5	62.4	72.7	78.1	74.6	78.9	80.3	82.0	79.3	76.6
370.4	20.6	35.5	52.7	66.3	73.9	72.6	75.2	78.0	78.3	75.9	75.4
123.5	17.4	27.2	43.5	59.3	66.0	66.3	68.5	70.6	72.7	72.4	70.4
41.2	14.4	23.8	39.0	53.7	61.7	60.8	64.1	66.9	66.0	66.6	69.0
13.7	12.9	22.6	36.9	49.6	58.2	58.5	61.0	63.5	63.9	65.8	66.5
4.6	11.0	20.2	34.6	47.3	55.1	55.8	58.5	63.0	65.8	67.3	69.0

ABTS [µM]

Table A.4: 96-well inhibition assay of *Ba*Lac with 2,6-DMP and inhibitor NaCl at pH 3, 4.5 (citrate buffer, 100 mM) and pH 6 (citrate-phosphate buffer, 100 mM)

BaL - NaCl - 2,6-DMP

undiluted

Average OD/min **pH3, 2,6-DMP Stock 80 mM** **NaCl [mM]**

2,6-DMP [µM]	2000	1000	500	250	125	62.5	31.25	15.63	7.81	3.91	0.00
10000.0	27.4	101.8	259.0	415.7	496.2	510.0	591.5	619.8	620.5	627.9	641.5
3333.3	37.9	118.8	271.0	424.3	521.0	563.5	630.3	671.7	698.0	732.1	812.2
1111.1	30.2	108.0	235.8	369.3	463.0	510.1	593.1	642.1	673.5	703.9	815.7
370.4	20.4	74.8	177.4	293.7	385.7	461.8	524.6	588.6	628.1	634.7	760.8
123.5	14.2	54.4	130.6	235.5	330.7	382.7	463.3	517.8	565.0	587.3	715.8
41.2	8.7	36.1	90.8	173.3	264.1	307.8	380.4	434.8	477.3	511.6	678.4
13.7	4.6	23.7	69.9	137.2	204.0	261.1	323.8	387.5	424.2	441.3	614.8
4.6	2.1	16.1	50.4	107.1	175.1	232.2	290.4	349.6	392.0	434.5	592.9

undiluted

Average OD/min **pH4,5, 2,6-DMP Stock 80 mM** **NaCl [mM]**

2,6-DMP [µM]	2000	1000	500	250	125	62.5	31.25	15.63	7.81	3.91	0.00
10000.0	300.4	351.3	388.1	370.7	364.4	329.6	348.5	348.3	338.7	329.8	319.4
3333.3	374.2	433.6	442.4	430.7	424.2	410.7	418.3	422.6	426.6	429.0	434.7
1111.1	367.6	430.6	446.3	432.0	435.3	424.9	448.7	448.5	455.7	465.9	469.7
370.4	358.1	415.1	439.1	439.9	431.1	424.0	447.0	453.2	456.6	464.3	451.8
123.5	326.3	384.9	414.0	420.1	419.8	405.9	439.2	440.1	439.4	458.3	458.1
41.2	284.2	359.2	393.3	395.7	382.2	390.2	406.4	413.7	435.8	439.9	457.2
13.7	237.3	322.4	323.1	331.7	343.3	331.9	366.7	374.6	379.2	399.7	402.6
4.6	165.6	262.4	264.3	265.2	283.8	305.4	304.2	322.2	345.7	380.1	380.0

undiluted

Average OD/min **pH6 2,6-DMP Stock 80 mM** **NaCl [mM]**

2,6-DMP [µM]	2000	1000	500	250	125	62.5	31.25	15.63	7.81	3.91	0.00
10000.0	184.2	175.5	171.5	159.7	145.1	148.0	156.3	151.1	149.7	148.0	130.5
3333.3	260.1	237.6	222.2	214.5	215.4	205.0	205.7	212.3	211.7	209.4	204.2
1111.1	275.6	260.9	235.8	230.4	230.7	215.6	231.7	233.9	233.4	234.3	227.0
370.4	264.4	252.6	241.3	237.6	237.0	225.6	236.0	241.9	240.6	242.5	245.5
123.5	256.2	244.8	235.0	232.8	228.6	216.9	232.5	240.4	244.0	239.8	239.8
41.2	235.3	235.6	216.2	214.6	207.1	207.6	221.6	234.4	232.5	230.9	228.4
13.7	226.5	220.3	197.1	192.7	198.6	197.7	203.8	218.2	223.2	216.2	224.2
4.6	169.3	171.7	166.9	164.8	169.1	167.5	180.6	184.3	187.6	193.0	195.9

Table A.5: 96-well inhibition assay of *Ba*Lac with 2,6-DMP and inhibitor NaF at pH 3, 4.5 (citrate buffer, 100 mM) and pH 6 (citrate-phosphate buffer, 100 mM)

BaL - NaF - 2,6-DMP

undiluted

Average OD/min **pH3, 2,6-DMP Stock 80 mM**

NaF [µM]

2,6-DMP [µM]	500	250	125	62.5	31.25	15.625	7.8125	3.91	1.95	0.98	0.00
10000.0	3.3	5.5	14.7	21.8	57.9	89.6	149.2	192.7	227.7	307.1	693.0
3333.3	6.2	9.9	21.9	46.0	86.1	125.2	179.4	229.6	308.8	399.4	856.9
1111.1	10.0	14.6	29.0	59.8	104.1	157.7	206.9	279.5	300.5	388.7	876.3
370.4	10.7	15.0	29.6	57.0	103.2	136.8	188.9	263.7	312.9	381.8	821.9
123.5	8.7	13.6	26.5	54.4	88.8	130.7	177.1	211.5	281.8	347.4	782.8
41.2	7.0	11.3	21.5	44.7	80.1	110.2	150.2	206.1	256.9	304.3	753.1
13.7	6.8	9.6	20.6	42.2	70.6	99.9	140.3	190.0	256.9	272.1	682.7
4.6	6.0	9.4	18.5	37.7	63.6	88.1	123.0	164.5	207.5	279.0	642.8

undiluted

Average OD/min **pH4,5, 2,6-DMP Stock 80 mM** **NaF [µM]**

2,6-DMP [µM]	125	62.5	31.25	15.625	7.8125	3.9063	1.9531	0.98	0.49	0.24	0.00
10000.0	92.5	130.9	194.3	246.0	276.8	280.9	285.5	310.8	309.7	322.6	316.8
3333.3	121.0	179.1	245.8	312.6	349.6	368.2	389.7	408.3	400.2	415.0	429.9
1111.1	134.8	197.6	277.6	344.9	383.3	386.5	413.8	440.3	439.1	457.1	457.5
370.4	136.0	207.1	281.1	343.0	386.6	398.6	426.4	459.7	465.2	471.8	477.8
123.5	138.3	200.3	275.0	340.4	385.6	379.7	417.4	443.1	445.6	452.3	454.1
41.2	141.2	199.0	270.1	335.8	378.3	384.2	409.3	444.3	439.7	450.8	461.4
13.7	136.9	196.6	264.5	333.0	375.5	382.7	398.0	434.1	436.7	439.6	450.6
4.6	129.2	198.2	270.8	346.2	387.9	386.8	416.5	437.5	436.7	455.5	461.6

undiluted

Average OD/min **pH6 2,6-DMP Stock 80 mM** **NaF [µM]**

2,6-DMP [µM]	2000	1000	500	250	125	62.5	31.25	15.63	7.81	3.91	0.00
10000.0	56.2	80.4	114.1	124.6	139.7	136.8	155.3	155.9	153.2	153.2	152.0
3333.3	79.8	116.4	153.1	188.1	204.2	205.1	209.1	218.3	218.1	221.8	222.6
1111.1	83.4	124.8	168.9	205.4	225.3	229.7	231.0	245.6	247.4	247.5	251.3
370.4	90.1	131.4	174.6	211.7	231.8	232.8	243.1	254.5	254.7	254.0	261.2
123.5	91.5	129.6	174.8	210.9	231.0	229.4	238.6	247.6	253.0	252.7	251.7
41.2	92.7	129.7	171.8	207.0	224.9	229.0	238.5	248.1	249.7	252.1	252.7
13.7	93.6	131.5	170.6	208.0	225.0	224.6	236.4	249.4	252.7	251.8	248.6
4.6	92.2	131.9	172.3	204.9	226.6	230.8	242.3	251.2	249.7	255.6	258.7

Table A.6: 96-well inhibition assay of *Tp*Lac with 2,6-DMP and inhibitor NaCl at pH 3, 4.5 (citrate buffer, 100 mM) and pH 6 (citrate-phosphate buffer, 100 mM)

TpL - NaCl - 2,6-DMP

undiluted

Average OD/min **pH3, 2,6-DMP Stock 80 mM** **NaCl [mM]**

	125	62.5	31.25	15.625	7.8125	3.9063	1.9531	0.98	0.49	0.24	0.00
10000.0	10.0	28.8	85.5	183.2	295.6	376.1	395.6	473.2	519.8	523.3	628.1
3333.3	6.6	17.5	47.7	111.3	202.1	264.4	294.6	362.6	414.7	448.1	594.3
1111.1	4.1	9.1	23.7	55.7	100.0	142.2	167.6	229.0	262.0	306.1	490.2
370.4	2.9	4.9	12.1	28.9	53.3	78.5	91.4	136.0	155.7	189.6	393.9
123.5	2.0	3.5	8.6	19.2	35.7	52.9	73.3	101.2	120.9	143.2	316.9
41.2	1.7	2.8	6.1	13.8	27.2	38.3	48.3	61.2	81.4	103.6	241.8
13.7	1.1	2.4	5.0	11.1	20.3	29.8	36.0	50.6	62.2	78.0	186.3
4.6	0.9	2.1	4.5	8.1	16.5	23.1	31.5	44.5	56.9	68.4	179.3

2,6-DMP [µM]

undiluted

Average OD/min **pH4,5, 2,6-DMP Stock 80 mM** **NaCl [mM]**

	125	62.5	31.25	15.625	7.8125	3.9063	1.9531	0.98	0.49	0.24	0.00
10000.0	156.9	226.8	305.4	343.1	352.0	359.5	325.0	345.3	351.1	365.7	336.2
3333.3	144.5	244.9	334.6	401.5	421.6	409.7	386.5	422.3	435.5	433.4	433.3
1111.1	105.3	205.3	299.6	373.5	425.3	418.0	396.5	424.7	429.4	437.3	439.5
370.4	73.9	142.9	237.2	317.2	370.7	387.9	370.4	412.1	421.9	432.8	427.3
123.5	50.9	106.5	181.7	270.1	326.9	340.7	334.0	369.6	384.8	389.1	378.9
41.2	41.2	81.5	145.8	231.7	286.3	303.1	293.5	340.1	336.9	347.1	370.9
13.7	32.3	63.4	117.5	189.1	241.6	267.4	267.2	319.4	316.9	337.7	350.2
4.6	26.8	60.2	104.3	169.6	228.4	247.4	261.3	301.8	317.7	331.0	331.4

2,6-DMP [µM]

undiluted

Average OD/min **pH6, ABTS Stock 80 mM** **NaCl [mM]**

	1000	500	250	125	62.5	31.25	15.625	7.81	3.91	1.95	0.00
10000.0	9.0	25.1	23.4	24.3	22.0	18.6	24.5	21.0	19.3	18.6	19.4
3333.3	15.2	33.5	39.4	42.6	42.5	39.7	37.2	38.4	37.9	38.7	37.1
1111.1	15.3	32.6	42.3	47.4	45.7	42.0	43.0	45.1	44.8	46.6	44.2
370.4	12.2	25.5	38.7	46.4	47.9	45.0	42.4	47.2	47.6	49.2	50.1
123.5	8.4	19.3	32.3	42.2	44.3	41.6	40.1	45.8	46.8	47.3	46.4
41.2	7.5	14.9	25.8	36.5	41.0	38.3	41.1	44.5	43.1	45.1	45.3
13.7	6.4	13.9	23.1	33.4	37.7	38.0	38.2	42.6	41.7	43.1	44.4
4.6	6.5	14.6	23.3	33.1	39.0	38.9	39.6	42.8	41.6	42.4	43.6

2,6-DMP [µM]

Table A.7: 96-well inhibition assay of *Ba*Lac with guaiacol and inhibitor NaCl at pH 3, 4.5 (citrate buffer, 100 mM) and pH 6 (citrate-phosphate buffer, 100 mM)

BaL - NaCl - Guaiacol

undiluted

Average OD/min **pH3, Guaiacol Stock 80 mM** **NaCl [mM]**

Guaiacol [µM]	2000	1000	500	250	125	62.5	31.25	15.63	7.81	3.91	0.00
10000.0	0.8	2.6	9.6	22.2	37.0	51.0	70.8	93.7	114.9	120.5	189.6
3333.3	1.3	1.3	4.6	11.0	19.7	30.9	42.0	55.3	66.4	73.2	185.5
1111.1	0.5	0.8	1.5	4.1	8.1	13.0	19.6	27.4	35.1	42.6	149.6
370.4	0.5	0.3	0.7	1.5	3.2	5.1	7.8	10.6	14.4	18.8	119.7
123.5	0.4	0.1	0.3	0.5	1.4	2.2	3.4	5.3	7.3	10.1	77.2
41.2	0.3	0.2	0.4	0.2	0.7	1.1	1.8	2.8	3.7	5.3	58.8
13.7	0.4	0.2	0.2	0.2	0.5	0.8	1.5	2.3	4.0	4.7	46.4
4.6	0.4	-0.2	0.3	0.3	0.5	0.4	0.9	1.3	1.6	2.6	36.3

undiluted

Average OD/min **pH4,5 Guaiacol Stock 80 mM** **NaCl [mM]**

Guaiacol [µM]	2000	1000	500	250	125	62.5	31.25	15.63	7.81	3.91	0.00
10000.0	42.5	69.7	90.6	105.2	109.4	110.9	116.5	118.1	121.6	125.6	125.8
3333.3	25.8	43.6	67.9	85.1	96.4	102.2	108.6	111.5	113.4	117.6	122.6
1111.1	14.5	26.5	46.5	66.2	82.5	89.8	99.5	104.3	107.6	109.7	116.5
370.4	7.1	15.0	30.8	50.2	67.2	76.0	87.2	94.1	97.0	100.4	106.5
123.5	3.5	8.5	18.3	34.7	48.6	59.5	70.0	76.3	80.2	82.6	91.6
41.2	1.6	4.3	10.6	22.3	35.2	44.2	51.3	58.4	61.0	65.2	71.0
13.7	0.8	2.3	6.0	13.9	23.3	28.9	36.5	41.6	43.5	44.5	51.3
4.6	0.7	1.3	3.6	9.4	17.5	22.7	28.8	32.8	34.7	37.1	39.0

undiluted

Average OD/min **pH6 Guaiacol Stock 80 mM** **NaCl [mM]**

Guaiacol [µM]	2000	1000	500	250	125	62.5	31.25	15.63	7.81	3.91	0.00
10000.0	60.9	63.2	54.9	55.7	59.4	57.3	59.2	58.9	60.6	61.0	62.3
3333.3	51.4	54.0	52.8	53.9	54.4	56.3	58.4	60.7	59.7	61.3	64.0
1111.1	40.4	41.5	44.1	46.9	49.2	49.9	53.3	53.4	53.6	55.4	58.7
370.4	30.9	32.1	34.9	39.2	43.7	44.5	48.2	49.4	48.4	49.9	54.5
123.5	24.2	26.1	27.4	31.2	35.0	36.5	42.3	43.3	45.0	42.4	49.1
41.2	20.1	21.1	21.6	25.6	28.5	30.7	34.0	34.6	38.0	37.2	43.7
13.7	16.3	17.3	17.9	21.1	24.0	26.3	29.5	31.1	32.4	31.5	35.9
4.6	13.3	13.8	14.7	17.9	21.1	22.5	26.7	28.4	29.0	30.1	34.7

Table A.8: 96-well inhibition assay of *Ba*Lac with guaiacol and inhibitor NaF at pH 3, 4.5 (citrate buffer, 100 mM) and pH 6 (citrate-phosphate buffer, 100 mM)

BaL - NaF - Guaiacol

undiluted

Average OD/min **pH3, Guaiacol Stock 80 mM**

NaF [µM]

	500	250	125	62.5	31.25	15.625	7.8125	3.91	1.95	0.98	0.00
10000.0	1.1	1.6	3.4	8.6	15.5	26.0	40.2	57.5	70.7	83.2	195.2
3333.3	0.9	1.8	3.8	8.5	16.3	25.1	38.7	55.3	68.2	81.4	197.0
1111.1	0.8	1.5	2.7	6.1	12.5	20.4	28.7	40.2	44.3	60.5	164.8
370.4	0.5	0.6	1.5	3.3	6.9	9.7	15.5	23.1	32.4	36.8	120.4
123.5	0.4	0.6	0.8	2.3	3.9	6.6	11.3	15.6	20.4	25.7	90.3
41.2	0.9	0.1	0.9	1.9	3.4	4.7	6.8	11.7	15.3	17.9	66.6
13.7	-0.5	0.4	0.2	0.5	1.9	3.2	5.4	8.1	10.7	12.1	44.8
4.6	0.3	0.1	0.0	1.0	2.2	2.9	4.5	6.0	9.2	12.8	35.4

Guaiacol [µM]

undiluted

Average OD/min **pH4,5, Guaiacol Stock 80 mM** **NaF [µM]**

	500	250	125	62.5	31.25	15.625	7.8125	3.91	1.95	0.98	0.00
10000.0	9.8	16.9	34.2	57.3	81.8	94.5	104.2	112.7	117.0	124.3	133.9
3333.3	8.7	19.4	35.2	65.1	92.0	106.4	114.8	128.8	134.6	143.3	157.4
1111.1	10.6	20.6	41.4	65.1	90.4	108.1	116.2	129.1	135.3	144.1	161.6
370.4	11.3	19.7	37.0	64.0	84.0	95.2	109.7	119.5	125.6	134.3	151.7
123.5	9.9	18.7	33.2	50.6	71.9	88.2	92.9	109.5	107.0	115.7	128.4
41.2	8.8	14.7	26.7	44.6	52.1	66.3	83.3	86.6	93.4	99.2	111.2
13.7	6.7	13.3	22.6	38.1	50.7	61.4	67.3	75.9	77.9	83.3	93.5
4.6	6.5	10.7	18.9	32.3	43.5	46.9	53.9	61.4	65.5	68.4	79.4

Guaiacol [µM]

undiluted

Average OD/min **pH6 Guaiacol Stock 80 mM** **NaF [µM]**

	2000	1000	500	250	125	62.5	31.25	15.63	7.81	3.91	0.00
10000.0	20.4	31.1	42.5	53.2	58.7	59.6	63.9	65.5	66.0	66.1	68.1
3333.3	22.8	31.8	43.5	53.1	58.2	60.0	63.6	65.9	66.6	67.1	69.0
1111.1	19.8	29.1	39.3	49.1	53.9	54.8	58.7	61.1	61.9	62.7	64.9
370.4	17.8	25.5	36.2	45.9	50.7	50.8	54.2	56.2	57.0	58.2	58.6
123.5	15.8	23.3	32.2	40.1	44.2	45.5	49.8	50.6	51.1	52.0	52.5
41.2	13.1	18.7	26.6	33.0	36.9	36.9	39.9	41.9	43.6	44.5	45.7
13.7	11.0	15.3	21.1	25.3	28.3	28.9	33.0	32.1	34.2	35.7	35.9
4.6	9.0	12.8	16.8	19.8	22.0	23.1	26.0	26.9	25.7	28.4	27.8

Guaiacol [µM]

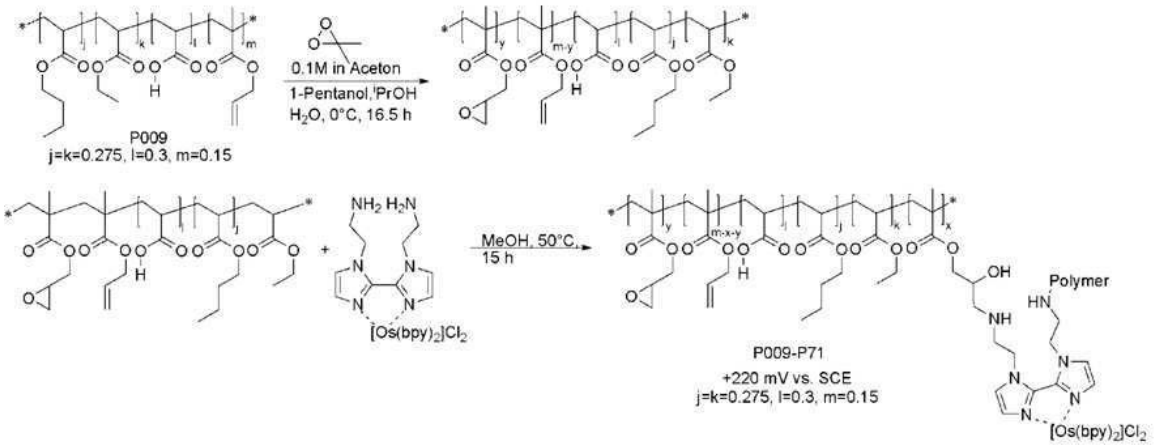

Figure A.6: Alternative scheme for creating Os-modified polymers

B. Abbreviations

2,6-DMP	2,6-Dimethoxyphenol, synonym: Syringol
ABTS	2,2'-azino-bis(3-ethylbenzthiazoline-6-sulphonic acid)
*Ba*Lac	*Botrytis aclada* laccase
catechol	1,2-dihydroxybenzene
GC	glassy carbon
guaiacol	2-methoxyphenol
HIC	Hydrophobic Interaction Chromatography
PCR	Polymerase Chain Reaction
*Th*Lac	*Trametes hirsuta* laccase
*Tp*Lac	*Trametes pubescens* laccase

C. Bibliography

Ackermann, Yvonne, Dmitrii A. Guschin, Kathrin Eckhard, Sergey Shleev, and Wolfgang Schuhmann. 2010. „Design of a bioelectrocatalytic electrode interface for oxygen reduction in biofuel cells based on a specifically adapted Os-complex containing redox polymer with entrapped Trametes hirsuta laccase“. *Electrochemistry Communications* 12 (5) (Mai): 640-643. doi:doi: DOI: 10.1016/j.elecom.2010.02.019.

Antorini, Matteo, Isabelle Herpoel-Gimbert, Thomas Choinowski, Jean-Claude Sigoillot, Marcel Asther, Kaspar Winterhalter, and Klaus Piontek. 2002. „Purification, crystallisation and X-ray diffraction study of fully functional laccases from two ligninolytic fungi“. *Biochimica et Biophysica Acta (BBA) - Protein Structure and Molecular Enzymology* 1594 (1) (Januar 31): 109-114. doi:doi: DOI: 10.1016/S0167-4838(01)00289-8.

Baldrian, Petr. 2006. „Fungal laccases – occurrence and properties“. *FEMS Microbiology Reviews* 30 (2): 215-242.

Barrière, Frédéric, Paul Kavanagh, and Dónal Leech. 2006. „A laccase-glucose oxidase biofuel cell prototype operating in a physiological buffer“. *Electrochimica Acta* 51 (24) (Juli 15): 5187-5192. doi:doi: DOI: 10.1016/j.electacta.2006.03.050.

Bisswanger, Hans. 2000. *Enzymkinetik - Theorie und Methoden*. 3rd Aufl. D-69469 Weinheim (Germany): Wiley-VCH.

Bourbonnais, Robert, Dónal Leech, and Michael G. Paice. 1998. „Electrochemical analysis of the interactions of laccase mediators with lignin model compounds“. *Biochimica et Biophysica Acta (BBA) - General Subjects* 1379 (3) (März 2): 381-390. doi:doi: DOI: 10.1016/S0304-4165(97)00117-7.

Bradford, M.M. 1976. „A rapid and sensitive method for the quantitation of microgram quantities of protein utilizing the principle of protein dye binding“. *Analytical Biochemistry* 72 (1-2): 248-254.

Breton, T., and D. Bélanger. 2008. „Modification of carbon electrode with aryl groups having an aliphatic amine by electrochemical reduction of in situ generated diazonium cations“. *Langmuir* 24 (16): 8711-8718.

Chen, Ting, Scott Calabrese Barton, Gary Binyamin, Zhiqiang Gao, Yongchao Zhang, Hyug-Han Kim, and Adam Heller. 2001. „A Miniature Biofuel Cell“. *Journal of the American Chemical Society* 123 (35): 8630-8631. doi:doi: 10.1021/ja0163164.

Christenson, Andreas, Nina Dimcheva, Elena E. Ferapontova, Lo Gorton, Tautgirdas Ruzgas, Leonard Stoica, Sergey Shleev, et al., 2004. „Direct Electron Transfer Between Ligninolytic Redox Enzymes and Electrodes“. *Electroanalysis* 16 (13-14): 1074-1092.

Farver, Ole, Lars K. Skov, Torbjoern Pascher, B. Goeran Karlsson, Margareta Nordling, Lennart G. Lundberg, Tore Vaenngaard, and Israel Pecht. 1993. „Intramolecular electron transfer in single-site-mutated azurins“. *Biochemistry* 32 (28): 7317-7322. doi:doi: 10.1021/bi00079a031.

Frasconi, Marco, Gabriele Favero, Harry Boer, Anu Koivula, and Franco Mazzei. 2010. „Kinetic and biochemical properties of high and low redox potential laccases from fungal and plant origin“. *Biochimica et Biophysica Acta (BBA) - Proteins & Proteomics* 1804 (4) (April): 899-908. doi:doi: DOI: 10.1016/j.bbapap.2009.12.018.

Galhaup, Christiane, Sabine Goller, Clemens K Peterbauer, Josef Strauss, and Dietmar Haltrich. 2002. „Characterization of the major laccase isoenzyme from Trametes pubescens and regulation of its synthesis by metal ions“. *Microbiology* 148 (7): 2159-2169.

Garzillo, A. M. V., M. C. Colao, C. Caruso, C. Caporale, D. Celletti, and V. Buonocore. 1998. „Laccase from the white-rot fungus *Trametes trogii*“. *Applied Microbiology and Biotechnology* 49 (5) (Mai 16): 545-551.

Gianfreda, Liliana, Feng Xu, and Jean-Marc Bollag. 1999. „Laccases: A Useful Group of Oxidoreductive Enzymes“. *Bioremediation Journal* 3 (1): 1-26.

Giardina, Paola, Vincenza Faraco, Cinzia Pezzella, Alessandra Piscitelli, Sophie Vanhulle, and Giovanni Sannia. 2010. „Laccases: a never-ending story“. *Cellular and Molecular Life Sciences* 67 (3) (Februar 1): 369-385.

Hakulinen, N., M. Andberg, J Kallio, A. Koivula, K. Kruus, and J. Rouvinen. 2008. „A near atomic resolution structure of a Melanocarpus albomyces laccase“. *Journal of Structural Biology* 162 (1) (April): 29-39. doi:doi: DOI: 10.1016/j.jsb.2007.12.003.

Hakulinen, Nina, Laura-Leena Kiiskinen, Kristiina Kruus, Markku Saloheimo, Arja Paananen, Anu Koivula, and Juha Rouvinen. 2002. „Crystal structure of a laccase from Melanocarpus albomyces with an intact trinuclear copper site“. *Nat Struct Mol Biol* 9 (8): 601-605. doi:10.1038/nsb823.

Hildén, Kristiina, Terhi Hakala, and Taina Lundell. 2009. „Thermotolerant and thermostable laccases“. *Biotechnology Letters* 31 (8) (August 1): 1117-1128.

Kallio, JP, S. Auer, J. Jänis, M. Andberg, K. Kruus, J. Rouvinen, A. Koivula, and N. Hakulinen. 2009. „Structure-Function Studies of a Melanocarpus albomyces Laccase Suggest a Pathway for Oxidation of Phenolic Compounds“. *Journal of Molecular Biology* 392 (4) (Oktober 2): 895-909. doi:doi: DOI: 10.1016/j.jmb.2009.06.053.

Karlsson, B. G., R. Aasa, B. G. Malmström, and L. G. Lundberg. 1989. „Rack-induced bonding in blue copper proteins: Spectroscopic properties and reduction potential of the azurin mutant Met-121 --> Leu“. *FEBS Letters* 253 (1-2) (August 14): 99-102. doi:doi: DOI: 10.1016/0014-5793(89)80938-X.

Katz, Eugenii, Itamar Willner, and Alexander B Kotlyar. 1999. „A non-compartmentalized glucose | O2 biofuel cell by bioengineered electrode surfaces“. *Journal of Electroanalytical Chemistry* 479 (1) (Dezember 15): 64-68. doi:doi: DOI: 10.1016/S0022-0728(99)00425-8.

Koroleva, Olga V., Elena V. Stepanova, Vladimir I. Binukov, Vladimir P. Timofeev, and Wolfgang Pfeil. 2001. „Temperature-induced changes in copper centers and protein conformation of two fungal laccases from Coriolus hirsutus and Coriolus zonatus“. *Biochimica et Biophysica Acta (BBA) - Protein Structure and Molecular Enzymology* 1547 (2) (Juni 11): 397-407. doi:doi: DOI: 10.1016/S0167-4838(01)00209-6.

Kudanga, Tukayi, Gibson S. Nyanhongo, Georg M. Guebitz, and Stephanie Burton. 2011. „Potential applications of laccase-mediated coupling and grafting reactions: A review“. *Enzyme and Microbial Technology* 48 (3) (März 7): 195-208. doi:doi: DOI: 10.1016/j.enzmictec.2010.11.007.

Kunamneni, Adinarayana, Susana Camarero, Carlos Garcia-Burgos, Francisco Plou, Antonio Ballesteros, and Miguel Alcalde. 2008. „Engineering and Applications of fungal laccases for organic synthesis“. *Microbial Cell Factories* 7 (1): 32.

Lorenzo, M., D. Moldes, S. Rodriguez Couto, and MA. Sanromán. 2005. „Inhibition of laccase activity from Trametes versicolor by heavy metals and organic compounds“. *Chemosphere* 60 (8) (August): 1124-1128. doi:doi: DOI: 10.1016/j.chemosphere.2004.12.051.

Madzak, C., M.C. Mimmi, E. Caminade, A. Brault, S. Baumberger, P. Briozzo, C. Mougin, and C. Jolivalt. 2006. „Shifting the optimal pH of activity for a laccase from the fungus Trametes versicolor by structure-based mutagenesis“. *Protein Engineering Design and Selection* 19 (2) (Februar): 77 -84. doi:10.1093/protein/gzj004.

Mueangtoom, K., R. Kittl, O. Mann, D. Haltrich, and R. Ludwig. 2010. „Low pH dye decolorization with ascomycete Lamprospora wrightii laccase“. *Biotechnology Journal* 5 (8): 857-870.

Naki, A., and S. D. Varfolomeev. 1981. „Inhibition mechanism of Polyporus versicolor laccase by halide ions [Mekhanizm ingibirovaniia aktivnosti lakkazy iz Polyporus versicolor ionami galogenov.]“. *Biokhimiya* 46 (9): pp. 1694-1702.

Piontek, Klaus, Matteo Antorini, and Thomas Choinowski. 2002. „Crystal Structure of a Laccase from the FungusTrametes versicolor at 1.90-Å Resolution Containing a Full Complement of Coppers“. *Journal of Biological Chemistry* 277 (40) (Oktober 4): 37663 -37669. doi:10.1074/jbc.M204571200.

Rodgers, Caroline J., Christopher F. Blanford, Stephen R. Giddens, Pari Skamnioti, Fraser A. Armstrong, and Sarah J. Gurr. 2010. „Designer laccases: a vogue for high-potential fungal enzymes?“ *Trends in Biotechnology* 28 (2) (Februar): 63-72. doi:doi: DOI: 10.1016/j.tibtech.2009.11.001.

Solomon, Edward I., Uma M. Sundaram, and Timothy E. Machonkin. 1996. „Multicopper Oxidases and Oxygenases“. *Chemical Reviews* 96 (7) (Januar 1): 2563-2606. doi:doi: 10.1021/cr950046o.

Stoica, L., N. Dimcheva, Y. Ackermann, K. Karnicka, D.A. Guschin, P.J. Kulesza, J. Rogalski, et al., 2009. „Membrane-Less Biofuel Cell Based on Cellobiose Dehydrogenase (Anode)/Laccase (Cathode) Wired via Specific Os-Redox Polymers“. *Fuel Cells* 9 (1): 53-62.

Vaz-Dominguez, C., S. Campuzo, Olaf Rudiger, M. Pita, M. Gorbacheva, Sergey Shleev, V. M. Fernandez, and A. De Lacey. 2008. „Laccase electrode for direct electrocatalytic reduction of O2 to H2O with high-operational stability and resistance to chloride inhibition“. *Biosensors and Bioelectronics* 24 (4): pp. 531-537.

Wariishi, H., K. Valli, and M. H. Gold. 1992. „Manganese(II) oxidation by manganese peroxidase from the basidiomycete Phanerochaete chrysosporium. Kinetic mechanism and role of chelators“. *Journal of Biological Chemistry* 267 (33): pp. 23688-23695.

Xu, F. 1996. „Oxidation of phenols, anilines, and benzenethiols by fungal laccases: Correlation between activity and redox potentials as well as halide inhibition“. *Biochemistry* 35 (23): pp. 7608-7614.

Xu, F. 1997. „Effects of redox potential and hydroxide inhibition on the pH activity profile of fungal laccases“. *Journal of Biological Chemistry* 272 (2): pp. 924-928.

Xu, F. 2001. „Dioxygen reactivity of laccase: Dependence on laccase source, pH, and anion inhibition“. *Applied Biochemistry and Biotechnology - Part A Enzyme Engineering and Biotechnology* 95 (2): pp. 125-133.

Xu, F., R. M. Berka, B. A. Nelson, J. R. Shuster, S. H. Brown, A. E. Palmer, and E. I. Solomon. 1998. „Site-directed mutations in fungal laccase: Effect on redox potential, activity and pH profile“. *Biochemical Journal* 334 (1): pp. 63-70.

Xu, F., A. E. Palmer, D. S. Yaver, R. M. Berka, G. A. Gambetta, S. H. Brown, and E. I. Solomon. 1999. „Targeted mutations in a Trametes villosa laccase: Axial perturbations of the T1 copper“. *Journal of Biological Chemistry* 274 (18): pp. 12372-12375.

Yoshida, H. 1883. „Chemistry of Lacquer (Urushi) part 1“. *J Chem Soc* 43: pp. 472-486.